Differential Regulation of Cyclic Nucleotide Phosphodiesterases in Anterior Pituitary Cells

KOK LONG ANG

Thesis for the Degree of

Doctor of Philosophy

University of Edinburgh

1999

To my parents

DECLARATION

This study was carried out under the guidance of Dr. Ferenc A. Antoni at the MRC Brain Metabolism Unit, Department of Pharmacology, University of Edinburgh between October 1995 and October 1998.

The experimental work presented in this thesis is my own and this thesis has been composed by myself. Where contributions from others have been presented these are acknowledged in the text.

KOK LONG ANG

MRC Brain Metabolism Unit

Department of Pharmacology

University of Edinburgh

1 George Square

Edinburgh EH8 9JZ

Aug 1999

ABSTRACT

Cyclic nucleotide hydrolysis by phosphodiesterases (PDEs) is an important process determining the amplitude and duration of the responses to cyclic nucleotide generating agonists. In adenohypophysial corticotrophs and mouse pituitary corticotroph tumour AtT20 cells, ACTH secretion is known to be mediated by the cyclic adenosine-3,5-monophosphate (cAMP) pathway. The aim of this thesis is to identify the cAMP-hydrolysing phosphodiesterase isozymes expressed in rat adenohypophysis and AtT20 cells. In addition, the regulation of their activities by cAMP-dependent pathway in AtT20 cells will be studied.

Combination of biochemical, pharmacological and molecular biological methods of analysis showed that Ca^{2+}/calmodulin (CaM)-stimulated (PDE1) and cAMP-specific, rolipram-inhibitable (PDE4) PDE isotypes are expressed in AtT20 cells as well as rat adenohypophysis. Kinetic studies indicated that both rat adenohypophysis and AtT20 cells contain low- and high-K_m PDE1 activities. RT-PCR analysis revealed the expression of mRNAs from the PDE1B, PDE1C, PDE4A, PDE4B and PDE4D subfamilies in AtT20 cells and PDE1C, PDE4B and PDE4D in rat adenohypophysis.

Stimulation of the cAMP pathway in AtT20 cells was found to increase the PDE4 activity and reduce that of PDE1. Calyculin A, an inhibitor of protein phosphatase 1 and 2A, had an additive effect on PDE4 activation by CPT-cAMP and synergistically enhanced the inhibition of PDE1 by CPT-cAMP. Incubation of AtT20 cytosol with the catalytic subunit of PKA produced the same changes of PDE1 and PDE4

activities as the activation of PKA in intact cells. The reduction of PDE1 activity was associated with a markedly diminished response to stimulation by Ca^{2+}/CaM.

Immunoprecipitation studies with isozyme-specific antibodies showed that PDE4D isozymes accounted for more than half of the control as well as CPT-cAMP and/or calyculin A activated PDE4 activity in AtT20 cells. Immunoblot analysis of the immunoprecipitate showed two distinct bands which, on the basis of their respective molecular weights, corresponded to splice variants, PDE4D3 and PDE4D5. The migration of both bands in SDS-PAGE was retarded upon CPT-cAMP and/or calyculin A treatments, indicative of covalent modification by phosphorylation.

In sum, these data indicate that 1) Splice variants derived from multiple PDE1 and PDE4 genes are expressed in rat adenohypophysis as well as AtT20 cells 2) Low K_m PDE1, plausibly PDE1C, is found in rat adenohypophysis and AtT20 cells 3) The rapid and differential regulation of PDE1 and PDE4 by cAMP-dependent phosphorylation and dephosphorylation in AtT20 cells may provide a mechanism for fine tuning the Ca^{2+}/CaM-dependency and the extent of cAMP hydrolysis in relation to the momentary status of cAMP and Ca^{2+}/CaM signalling.

ACKNOWLEDGEMENTS

I would like to express my sincere gratitude to my supervisor, Dr. Ferenc A. Antoni, for the opportunity to work with him on this project. I am indebted to his unfailing patience and guidance, which has undoubtedly helped the development of my foundation and skills to carry out independent research. Furthermore, his research fervour has been my constant source of encouragement and inspiration.

I would also like to thank all the people who have helped me in many ways and made my life in Edinburgh most enjoyable. My colleagues in the MRC Brain Metabolism Unit, in particular, Janet Dalitz, Diane Crook, Marianne Eastwood and John Mitchell for all the administrative works, and Jim Simpson for technical assistance. Prof. Miles Houslay (Glasgow University), Prof. Marco Conti (Stanford University) and their colleagues (in particular, Dr. Elaine Huston, Glasgow University, and Linda Lan, Stanford University), who have generously provided reagents and advice for the PDE4 studies.

Finally and most importantly, I am grateful to my parents for both financial and moral support, without which all these would not be possible. I am also grateful to my wife who has shared with me the ups and downs all along.

CONTENTS

2 MATERIALS AND METHODS

3 RESULTS

ABBREVIATIONS

AC	Adenylyl cyclase
ACTH	Adrenocorticotrophic hormone
5'-AMP	Adenosine-5'-monophosphate
AtT20	Mouse clonal corticotroph cell line D16:16
ATP	Adenosine triphosphate
AVP	Arginine vasopressin
bp	Base pair
BSA	Bovine serum albumin
Ca^{2+}	Calcium
CaM	Calmodulin
CaMK	CaM regulated kinase
cAMP	Cyclic adenosine-3',5'-monophosphate
cGMP	Cyclic guanosine-3',5'-monophosphate
CPT-cAMP	8-(4-chlorophenylthio)adenosine-3',5'-monophosphate
CRF	Corticotropin-releasing factor
DG	Diacylglycerol
DMEM	Dulbecco's modified Eagle's medium
DMSO	Dimethylsulphoxide
dNTP	Deoxy(nucleotide)triphosphate
dpm	Disintegrations per minute
DTT	Dithiothreitol
EDTA	Ethylenediamine-tetraacetic acid
EGTA	Ethylene glycol-bis(β-amino ethyl ether)N,N'-tetraacetic acid
EHNA	Erythro-9-(2-hydroxy-3-nonyl)adenine
ERK	Extracellular receptor stimulated kinase
FCS	Foetal calf serum
h	Hour
H-89	*N*-[2-[[3-(4-bromophenyl)-2-propenyl]amino]ethyl]-5-isoquinoline sulfonamide
HBSS	Hank's balanced salt solution
HPA	Hypothalamic-pituitary-adrenal
IBMX	3-isobutyl-1-methylxanthine
IP_3	Inositol 1,4,5-triphosphate
kDa	Kilodalton
8-MIX	8-methoxymethyl-IBMX
min	Minute
PBS	Phosphate buffered saline
PCR	Polymerase chain reaction
PDE	Cyclic nucleotide phosphodiesterase
PKA	Protein kinase A
PKC	Protein kinase C
PKG	Protein kinase G
PKI	Protein kinase A inhibitor peptide
PMSF	Phenylmethylsulphonylfluoride
PP1	Protein phosphatase 1

PP2A	Protein phosphatase 2A
PP2B	Calcineurin
RT-PCR	Reverse transcription-PCR
SDS	Sodium dodecylsuphate
SDS-PAGE	SDS polyacrylamide gel electrophoresis
S.D.	Standard deviation
S.E.M.	Standard error of the mean

LIST OF FIGURES

LIST OF TABLES

LIST OF PUBLICATIONS

1. K. L. Ang & F. A. Antoni (1996) Rolipram-inhibitable cyclic nucleotide phosphodiesterase (PDE) in rat adenohypophysis: Potential functional role in corticotrophs and somatotrophs. British Journal of Pharmacology 119: 361P

2. A. Antaraki, K. L. Ang & F. A. Antoni (1997) Involvement of calyculin A inhibitable protein phosphatases in the cyclic AMP signal transduction pathway of mouse corticotroph tumour (AtT20) cells. British Journal of Pharmacology 121: 991-999

3. K. L. Ang & F. A. Antoni (1997) Characterization of cyclic nucleotide phosphodiesterase mRNA expression in corticotroph tumour (AtT20) cells: Coexpression of PDE1C and PDE4. British Journal of Pharmacology 122: 424P

1 INTRODUCTION

1.1 Intracellular Signal Transduction

The integrity and survival of an organism in a changing environment depend on the ability of the cells to perceive and respond to the changes, which can be either physical (e.g. light, electricity, pressure and temperature) or chemical (food, hormones and neurotransmitters). Extracellular signals are perceived through proteins known as receptors that are usually located on the cell surface but are also found within the cell. Upon perception of extracellular signals by their respective specific receptors, a diverse range of intracellular signalling components is involved to transduce these signals into and within the cell to produce the appropriate response through the modulation of intracellular protein functions and gene expression. The involvement of different signalling components and their sequence in the signal transduction cascades induced by different extracellular stimuli were found to constitute distinct signal transduction pathways. In addition to protein phosphorylation and dephosphorylation on serine, threonine or tyrosine residues, which are among the most common and important regulatory mechanisms in signal transduction [1, 2], many signalling pathways involved the generation of an intracellular second messenger (in response to the extracellular stimulus or the first messenger), such as the cyclic nucleotides (cAMP and cGMP), Ca^{2+}, and inositol 1,4,5-trisphosphate (IP_3), that apart from initiating the respective phosphorylation cascade, also modulate other protein functions and enzyme activity. Thus the second messenger system provides both an amplification function, where many readily diffusible molecules of the second messenger can be generated in response to a single molecule of the extracellular stimulus, and an additional regulatory and

integrative junction where both the synthesis and degradation of the signal transducing molecule can be modulated. It has been increasingly clear that extensive crosstalk can occur between many signalling pathways to integrate intracellular signalling and responses to the environmental stimuli [3-5]. Therefore, understanding the signal transduction mechanism underlying a physiological process and its interaction with other signalling pathways is fundamental to our understanding of its various modes including those that lead to malfunction/diseases.

1.1.1 The cAMP pathway: in the era of multiple isozymes/splice variants and signal integration

Adenosine 3',5'-cyclic monophosphate (cAMP) was first isolated and characterised more than four decades ago [6, 7], closely followed by reports of the enzymes responsible for its formation [8] and degradation [9], the adenylyl cyclase (AC) and cyclic nucleotide phosphodiesterase (PDE) respectively. Importantly, the existence of these enzymes capable of regulating the intracellular level of cAMP serves to fulfil the criteria for cAMP to function as an intracellular second messenger. Many hormones and neurotransmitters have since been shown to activate cAMP synthesis by AC via transmembrane signalling through agonist-specific G-protein coupled receptors (GPCRs). The level of intracellular cAMP is then a balance of the AC and PDE activities, which will determine the extent of activation of its intracellular effector, the cAMP-dependent protein kinase (PKA). PKA can then elicit both short-term (within min) and long-term (from h to days) regulation via phosphorylation of functional proteins that mediate the agonist actions [10]. The discovery of new signalling components, new interactions with other signalling pathways, and novel regulatory mechanisms (such as spatial and temporal factors) have revealed further the complexity and versatility of the cAMP signal transduction. In addition to PKA, cAMP is now known to directly regulate other intracellular effectors including the cyclic nucleotide-gated ion channels (reviewed in [11, 12]) and a newly described family of cAMP-binding proteins with guanine nucleotide exchange factor activity (cAMP-GEFs) that directly activate the Ras superfamily guanine nucleotide binding protein Rap1 [13, 14]. PKA is also found to be negatively regulated directly by a family of endogenous inhibitors, PKIα [15], PKIβ [16], and PKIγ [17], that exhibit tissue- and developmental-specific expression [18] and are themselves regulated by

hormone stimulation [19], synaptic stimulation [20], and cell cycle [21]. The cross-activation of cGMP-dependent protein kinase (PKG) by cAMP and PKA by cGMP have been documented [22, 23]. PKA-phosphorylated targets can be rapidly and selectively dephosphorylated by a growing superfamily of protein phosphatases [24], providing means for reversing the PKA action and for additional specificity in the regulation by this covalent modification [1]. Furthermore, there is an increasing appreciation of the importance of architectural organisation of signalling components in signal transduction, and the idea of the cell as a membrane-enclosed solution of proteins to which stochastic enzymatic theories apply is now replaced by a picture of a highly organised space in which most enzymes and proteins are linked in complexes by scaffolding and anchoring proteins through specific interacting domains [25-28]. The resulting architectural network of signalling components is thought to facilitate and to enable both versatility and specificity of intracellular signal transduction. Extensive molecular cloning has revealed further complexity within each component of the cAMP pathway, many of which, such as the protein kinases [2], protein phosphatases [24], ACs [29, 30], and PDEs [31, 32], are now known to each consists of a superfamily of isozymes encoded by distinct genes. Multiple isozymes of these components are found to co-exist in a single cell type. This diversity provides the mean for intricate and co-ordinated regulation of intercellular and intracellular events as these isozymes can be regulated differentially and have different kinetic properties. The challenge now is to elucidate and understand their integrative roles in mediating the cellular response to environmental signals.

1.1.2 Implications for studying the molecular mechanism of physiological processes

The multiplicity of signalling components, with both unique and overlapping functions has made it necessary to identify the exact components/isozymes/splice variants involved in a physiological process in order to understand their integrative role. The importance of crosstalk between signalling pathways and architectural organisation of signalling components in cell functions has cautioned interpretation of our experimental findings. Results obtained from *in vitro* systems or from studies looking at only a subset of the components known to be involved in a physiological process may not reflect the physiological relevance or significance. The dynamics of molecular events and their co-regulation by multiple factors, which will determine their functionality, may not be the same under different environments. Furthermore, the immense capacity of endogenous compensatory mechanisms in the cells can mask important functional roles of the protein under investigation. For example, it is commonly observed that conditions leading to an increase in cAMP synthesis by AC, such as constitutively active $G_{s\alpha}$ mutation [33, 34], are accompanied by an increased in PDE activity, such that the intracellular cAMP levels were only slightly elevated. Studies from transgenic mice have also shown increased expression of other proteins that compensate for the function of the gene that has been deleted [35-37]. Nevertheless, determination of the different isozymes of signalling components expressed in a system and their regulatory potential is crucial for hypothesising and finding out their exact physiological functions.

1.2 Cyclic Nucleotide Phosphodiesterases

The only route of enzymatic inactivation of cAMP and cGMP known to date is through the cyclic nucleotide phosphodiesterases (PDEs). Concepts on the role of cyclic nucleotide hydrolysis in signal transduction have evolved from viewing PDEs as passive terminators of the cyclic nucleotide signalling to the present level of understanding where PDEs are regarded as targets of complex regulation by various intracellular signalling pathways [31, 32, 38, 39]. Up to 10 different gene families of PDEs (coding for more than 30 different isozymes) have now been identified in mammals based on their distinct kinetic and substrate characteristics, inhibitor profiles, allosteric activators and inhibitors, and amino acid sequence (Table 1) [31, 32, 38, 40-45]. A general nomenclature for naming PDEs has been adopted [46]: 1. The first 2 letters represent the species, for example, HS for human, MM for mouse, and RN for rat. 2. The next 3 letters plus an Arabic numeral represent the PDE gene family. 3. The next letter represents individual gene product within the family. 4. The final Arabic numeral represents the splice variant. Multiple isozymes and splice variants within a family are known to exist, particularly in the PDE1 (Ca^{2+}/CaM-stimulated) and PDE4 (cAMP-specific, rolipram-inhibitable) families. These isozymes are expressed in distinct tissue- and cell-specific fashions, with discrete subcellular localisations, and exhibit distinct, but functionally concerted modes of regulation at the levels of mRNA transcription and post-translational modification [31, 38, 39]. Species-specific expression of the PDE isozymes in some tissues has also been reported [47-49]. These highlight the remarkable versatility of this superfamily of enzymes in the regulation of cAMP hydrolysis.

Table 1

PDE superfamily

PDE gene family	gene (splice variants)	Relative K_m[a]	Regulation[b]		Inhibitor[c]
			+	-	
PDE1 Ca^{2+}/CaM-stimulated	1A (3) 1B 1C (5)	cAMP >> cGMP cAMP > cGMP cAMP ≅ cGMP	Ca^{2+}/CaM Ca^{2+}/CaM Ca^{2+}/CaM	PKA CaMK II	8-MIX
PDE2 cGMP-stimulated	2A (3)	cAMP > cGMP	cGMP		EHNA
PDE3 cGMP-inhibited	3A 3B	cAMP ≅ cGMP	PKA PKA, PKB	cGMP	Cilostamide Milrinone
PDE4 cAMP-specific	4A (3) 4B (3) 4C 4D (5)	cAMP << cGMP	p70S6K PKA	 ERK2	Rolipram
PDE5 cGMP-specific	5A (2)	cAMP >> cGMP	PKG/PKA cGMP		Zaprinast
PDE6 photoreceptor	6A 6B 6C	cAMP >> cGMP	cGMP	PKC	Zaprinast
PDE7 cAMP-specific rolipram-insensitive	7A (2)	cAMP << cGMP	n.a.	n.a.	n.a.
PDE8 cAMP-specific IBMX-insensitive	8A 8B	cAMP << cGMP	n.a.	n.a.	n.a.
PDE9 cGMP-specific IBMX-insensitive	9A (2)	cAMP >> cGMP	n.a.	n.a.	n.a.
PDE10 dual-substrate	10A (2)	cAMP ≅ cGMP	n.a.	n.a.	n.a.

[a] > , less than 10-fold difference
>> or <<, more than 100-fold difference
≅, similar

[b] Acute regulation resulting in activation (+) or reduction (-) of enzyme activity

[c] Only selected examples are shown
IBMX = 3-isobutyl-1-methylxanthine
8-MIX = 8-methoxymethyl-IBMX
EHNA = Erythro-9-(2-hydroxy-3-nonyl)adenine

n.a., not available

1.2.1 Structure and Function of PDEs

Peptide mapping and mutagenesis studies have revealed a core catalytic domain of about 250 amino acids near the carboxyl-terminal half that is conserved among all PDEs [50-53]. This region is much more similar within an individual PDE family (>80% identity) than between different PDE families (25-40% identity) [53], and is thought to contain common structural elements important for hydrolysis of the cyclic nucleotides, as well as family-specific determinants responsible for differences in substrate affinities and inhibitor sensitivities among the different PDE gene families [54].

The widely divergent N-terminal domain of PDEs contains determinants that confer regulatory properties specific to the different gene families and splice variants [31, 32, 38]. For example, CaM-binding in PDE1; non-catalytic cGMP-binding in PDE2, 5 and 6; subcellular-targeting and protein-protein interaction in PDE4; hydrophobic membrane-association in PDE3 and 4; and phosphorylation in PDE1, 3, 4 and 5 [31, 32, 38, 55]. In general, part of the amino-terminal domain of several isozymes is thought to cause intramolecular inhibition of the catalytic activity, and the activation of these isozymes appeared to involve the removal of this self-inhibition albeit by different mechanisms. For example, CaM binding in PDE1 [56], PKA phosphorylation in PDE4D3 [57], activation of the long forms of PDE4 isozymes (PDE4A5,PDE4B1, and PDE4D3) by phosphatidic acid [58, 59], and proteolytic cleavage separating the amino-terminal fragment from the catalytic domain in PDE1 [60, 61] and PDE4 [50].

1.2.2 The PDE1 Family: the second checkpoint of cAMP pathway by Ca^{2+}/CaM

Since the first report in the rat brain [62], the Ca^{2+}/CaM-stimulated PDE1 activity has been detected and characterised in other mammalian tissues (for a recent review, refer to [63]). To date, three different genes (PDE1A, PDE1B, and PDE1C) have been identified in the PDE1 family [63-67]. Two splice variants from the bovine PDE1A gene, PDE1A1 and PDE1A2 have been isolated, which differ only in a short amino-terminal segment (PDE1A1 = 18 residues; PDE1A2 = 34) that constitutes part of a putative CaM-binding site [56]. This difference is likely to account for the observation that PDE1A1 has about 10-fold higher affinity for Ca^{2+}/CaM compared to PDE1A2 [56, 67-69]. So far only one mRNA product has been isolated from the PDE1B gene coding for PDE1B1, although RNase protection assays have also detected structurally related PDE1B variants in brain, kidney, and adrenal medulla [66]. Both PDE1A and PDE1B isozymes hydrolyse preferentially cGMP to cAMP at micromolar substrate concentrations, but their maximum rate of cAMP hydrolysis is higher than or equal to that of cGMP [31]. As the tissue level of cAMP is generally an order of magnitude or more higher than cGMP, it has been postulated that these enzymes serve to hydrolyse both cyclic nucleotides *in vivo* [70-72]. Although PDE1 activity showing high affinity for cAMP has been observed for a long time by many investigators [73-82], it was only recently characterised as a new PDE1 gene and named PDE1C [83]. To date, the PDE1C gene has been shown to generate up to five different splice variants (PDE1C1-5) that are expressed in a tissue-specific manner and showed differences in inhibition by some PDE1 inhibitors and sensitivity towards stimulation by Ca^{2+}/CaM [49, 84]. The fact that PDE1C isozymes hydrolyse both cAMP and cGMP with high affinity (about 1 μM) and

similar capacity, together with its activation by cellular levels of Ca^{2+} and calmodulin, strongly implicate their important role in regulating intracellular cyclic nucleotide levels with respect to the Ca^{2+}/CaM status of the cell.

PDE1s are unique among other PDEs in that their activities can be dramatically stimulated by Ca^{2+}/CaM, and thus serve as the second checkpoint (after Ca^{2+}/CaM-regulated ACs) of the cAMP pathway by Ca^{2+}/CaM. Several lines of evidence have supported the regulation of intracellular cAMP level by PDE1 activity in response to changes in intracellular Ca^{2+} [85, 86]. The functional significance of such a regulatory role has been implicated in the central nervous system, the olfactory neurons, the cardiovascular system and the testis (reviewed in [63]). In addition, PDE1s have also been found to be involved in many cell functions such as insulin action [87], leukemic cell survival [88], cell proliferation [33, 48, 89, 90], and cell development [75, 91].

In addition to regulation by Ca^{2+}/CaM, both PDE1A and PDE1B have been shown to be phosphorylated *in vitro* by PKA [69, 92] and CaMK II [93] respectively. In both cases, phosphorylation was found to decrease the sensitivity of the enzymes towards Ca^{2+}/CaM stimulation. This effect is highly significant as the dynamic range of Ca^{2+}/CaM-stimulated PDE1 activity is very wide (10-fold or more). However, the *in vivo* regulation of these PDE1s by phosphorylation has not been demonstrated yet. In the *in vitro* system, the main PKA phosphorylated residues in BTPDE1A2 have been mapped to Ser120 and Ser138, of which only PKA phosphorylation of Ser120 was found to reduce sensitivity toward CaM stimulation [92]. Interestingly,

sequence analysis has indicated that both PKA phosphorylation sites in PDE1A were also present in PDE1C isozymes [84], but there is no report yet regarding this potential regulation *in vitro* or *in vivo*. More recently, limited proteolysis through a Ca^{2+}-dependent cysteine protease, m-calpain, whose cleavage site is found in all PDE1 isozymes described so far, has been suggested as an additional mechanism for activating PDE1s [61]. Several studies have also demonstrated 'long-term' regulation of PDE1s through altered gene expression [33, 48, 89, 90, 94]. For example, the Chinese hamster ovary (CHO) cells, which normally do not express detectable PDE1 activity, were found to transiently express PDE1B isozyme with the characteristics of an immediate early gene upon receptor-mediated elevation of DAG levels [89, 94]. Thus, PDE1 isozymes can be regulated by multiple mechanisms, supporting that they probably serve an important role in integrating cAMP and Ca^{2+} signalling.

1.2.3 The PDE4 Family: diverse and versatile regulation of cAMP hydrolysis

Of all the PDE families, that of PDE4 has received the most attention and perhaps consequently is the best studied PDE family so far. There are various reasons why this is so: 1. PDE4s are the mammalian homologues of the *Drosophila* dunce gene that was the first and best characterised mutant shown to be critical for learning and memory [95-97]. Remarkably, a rat cDNA homologue of *dunce*, RD1 [96] (known now as PDE4A1), was able to rescue the phenotypes (defects in learning and memory, and female sterility) caused by mutations in *Drosophila* dunce gene [98]. 2. PDE4s are selectively inhibited by the antidepressant rolipram {4-[3-(cyclopentoxyl)-4-methoxyphenyl]-2-pyrrolidone} and structurally related compounds, and thus implicated in the control of mood [97]. 3. PDE4s are involved in the regulation of a wide range of processes including desensitization to hormonal stimulation [99], cell survival [100], tumour growth [101], reproduction [102, 103] and activation of the immune response [104].

Evidence for the presence of at least four different PDE4 genes was first demonstrated in rat [96, 105, 106], and was subsequently shown in mouse [107] and human [108]. The four genes code for the PDE4A, PDE4B, PDE4C and PDE4D subfamily of isozymes. Multiple alternative splice variants from each of these genes (with the exception of PDE4C) have been cloned and characterised (reviewed in [55]). For example, up to 5 distinct splice variants produced from the PDE4D gene has been shown to exist in man [109] and rat [110] at the level of both mRNA and protein expression. The 2 short (PDE4D1, 2) and 3 long (PDE4D3, 4, 5) forms of PDE4D are generated by alternate N-terminal splicing. Similarly, at least 3 splice

variants of PDE4A and PDE4B are known to exist [55]. Importantly, these splice variants have been shown to be differentially regulated by activation of the cAMP pathway in many cell types. In human promonocytic cell line, U937, short-term (2-20 min) treatment with prostaglandin E_2 produced a rapid activation of PDE4D3 activity by PKA phosphorylation [111], while prolonged (2-4 hr) exposure to prostaglandin E2, salbutamol, and 8-bromo-cAMP resulted in an increased expression of PDE4A (125 kDa) and PDE4B (70 kDa) isozymes [112, 113]. In rat FRTL-5 thyroid cell, thyroid stimulating hormone induced both a rapid (within min) activation/phosphorylation of PDE4D3 activity as well as an increased in gene expression of PDE4D1/PDE4D2 splice variants after prolonged stimulation [110, 114]. Many studies have suggested that the unique N-terminal regions of the various PDE4 splice variants may govern protein-protein interaction, intracellular targeting, as well as regulation by phosphorylation (reviewed in [55]).

1.2.4 Role of PDEs in cAMP signal transduction

A common feature of the hormone-dependent cAMP regulation is the transient nature of the increase in intracellular cAMP, that after an initial increase, the cAMP concentration returns toward basal levels. This phenomenon is thought to be associated with the refractoriness of the target cell that follows hormone stimulation, a crucial factor that determines cell responsiveness to hormones. There are multiple mechanisms involved in cell desensitization, including changes in the components of the signal transduction machinery at the plasma membrane as well as the expression of intracellular mechanisms terminating or limiting the effect of hormonal stimulation [115, 116]. These homeostatic mechanisms enable the cells to generate appropriate response and to adapt to acute and chronic hormone stimulation.

The significance of PDE activity in limiting basal and agonist-stimulated intracellular cAMP levels was evident for a long time, mainly through observations of the dramatic increase and prolonged agonist-induced cAMP accumulation in the presence of PDE inhibitors that was often translated to an increase in hormone secretion. Furthermore, an induction of PDE activity upon stimulation by cAMP-generating hormone/agonist has been well documented in many systems and appears to be a ubiquitous phenomenon, where an increase in cAMP breakdown by PDEs contributes to the termination of the agonist signal and to the development of desensitization [110, 112, 117-129]. In both Sertoli and FRTL-5 thyroid cells, prolonged stimulation with FSH and TSH respectively (or with PDE-resistant cAMP analogues), leads to an induction of PDE4D2 mRNA and protein expression. In addition, there is a rapid activation of PDE4D3 activity by PKA phosphorylation in

FRTL-5 cell. These findings demonstrate that intracellular feedback loops linking cAMP concentration and PDEs are operative in the cell and involve both rapid (short-term) post-translational modifications as well as long-term changes in PDE gene expression. A pathological model where an increase in cAMP-hydrolysing activity was found to cause hormone insensitively is present in a strain of nephrogenic (vasopressin-resistent) diabetes insipidus (NDI) mice [130, 131]. Cultured cells from the inner medullary duct from the kidneys of these mice do not respond to vasopressin in spite of an apparently normal complement of receptors and the normal ability of vasopressin to stimulate adenylyl cyclase in a cell-free system [132, 133]. Application of a PDE4-specific inhibitor, rolipram, either *in vitro* or *in vivo* restored the responsiveness to vasopressin-stimulated cAMP accumulation and water permeability of the renal collecting system in these mice [131, 134]. These findings indicate that PDE activity has a major impact on cell responsiveness to hormones and suggest the possibility that other syndromes of cell insensitivity or hormone resistance might be due to an alteration of PDE activity.

In addition to mediating feedback function, cAMP-hydrolysing PDEs which are regulated by other second messengers, such as Ca^{2+}/CaM (activating PDE1) and cGMP (inhibiting PDE2 and activating PDE3), may function as targets for crosstalk between stimulatory and inhibitory signals regulating cellular activity. Agonist-induced intracellular Ca^{2+} elevation has been shown to increase cAMP degradation via the activation of PDE1 activity in dog thyroid slices [135], rat cardiomyocytes [136] and cultured human astrocytoma cells [118]. In bovine glomerulosa cells of the adrenal cortex, atrial natriuretic peptide (ANP), which increases cGMP level, was

found to reduce ACTH-stimulated cAMP accumulation and aldosterone secretion via the activation of PDE2 [137]. Similar effects of ANP on agonist-stimulated cAMP levels in fibroblasts [138] and in PC-12 cells [139] have also been reported. On the other hand, in tissues where cAMP and cGMP have similar physiological effects, PDE3 serves as a target for cGMP to act synergistically with cAMP signalling [140, 141]. Thus, in addition to their general function as negative modulators of cyclic nucleotide signalling, PDEs serve as targets for integrating other intracellular signals.

Recent imaging studies using a cAMP fluorescent probe, FlCRhR [142], have demonstrated that as with Ca^{2+} signals [143, 144], there is also spatiotemporal dimension in cAMP signals [145, 146]. The FICRhR consists of the PKA holoenzyme complex, R2C2, in which the catalytic (C) and regulatory (R) subunits are labelled with fluorescein and rhodamine respectively. The dissociation of the C subunits upon cAMP binding to the R subunits disrupts the fluorescence resonance energy transfer (FRET) present in the holoenzyme complex, and results in a change in the fluorescence emission spectrum that can be visualised in living cells [142]. Using this approach, different neuromodulators were found to generate unique pattern of cAMP transients in different neurons of the lobster stomatogastric ganglion [146]. Furthermore, in an elegant study using whole cell patch-clamp technique on cardiac myocytes, cAMP was shown to diffuse minimally from the site of synthesis under normal conditions of agonist stimulation resulting in local activation of Ca^{2+} channels, while inhibition of PDEs causes a rapid diffusion of cAMP throughout the cell leading to increased activation of distant Ca^{2+} channels [147]. This provides supporting evidence to the postulation that PDEs may play an

important role in limiting cAMP diffusion [148], which together with other mechanisms, contribute to the specificity of cAMP signalling. This function is likely to be enhanced by the localisation of PDE isozymes in different subcellular sites. To this end, even though it has been known for a long time that a portion of the cellular PDE activity is recovered in the particulate fraction [149], the underlying molecular basis is only recently under intense investigation. This is probably due to both the identification of multiple PDE isozymes/splice variants with distinct sequences outside the conserved catalytic domain that contain targeting/interacting motifs and the emerging theme of targeting in signal transduction. While some PDE isozymes (PDE3B, PDE4A1, PDE7A2) possess a hydrophobic membrane targeting sequence [150-153], examples of specific interaction of PDE4 isozymes/splice variants with adaptor/scaffold proteins are emerging. For example, the amino-terminal proline-arginine motifs (PxxPx-R) of PDE4A5 enable interaction with selective SH3 domains, particularly those from Src family tyrosyl kinases, Lyn and Fyn [154, 155]. More recently, an unique amino-terminal region of PDE4D5 was shown to confer high affinity interaction with RACK1 *in vitro* and in intact cells [156]. Immunofluorescence studies have also shown differential subcellular localization of PDE4D splice variants in the cell that correlated well with observations by differential centrifugation [114]. Collectively, the accumulating evidence demonstrating that specific PDE isozymes/splice variants are differentially regulated and targeted to different subcellular locations strongly support the hypothesis that different PDE isozymes serve non-redundant functions in the regulation of cyclic nucleotide signal transduction.

1.2.5 Methods for determining the PDE profile

Several approaches have been used to characterise the PDE activities in a cell system (reviewed in [157]). There are family-specific PDE inhibitors and modulators (see Table 1) that can be used to differentiate PDE activities contributed by different isozymes [46]. Substrate saturation studies with cAMP and cGMP can also distinguish between PDE families (in the case of PDE1 family, may even differentiate PDE1C from PDE1A and PDE1B based on its low K_m for cAMP). Anion-exchange chromatography has proved to be an effective mean of separating some PDE families from each other and in some cases from their modulators present in cell extracts (for example, PDE1 and CaM). The fractions containing partially purified isozymes can then be used for more detailed kinetic analysis or for further purification. The reverse transcription-polymerase chain reaction (RT-PCR) has proven to be a powerful method that allows identification to the level of splice variants. More importantly, the development of antibodies against different PDE isozymes in many laboratories have provided definitive evidence to the identification and confirmation of expression at the protein level. These antibodies have also been used to isolate specific isozymes by immunoprecipitation, which when coupled with other methods (such as PDE activity measurement and SDS-PAGE) provide a very powerful mean in attributing regulation to specific isozymes. Using these methods one could have an idea of the involvement of specific PDE isozymes in the system of interest, and further detailed analysis can then be carried out if necessary.

1.3 Regulation of ACTH secretion in anterior pituitary corticotrophs

The secretion of adrenocorticotrophic hormone (ACTH) by the anterior pituitary corticotrophs is a crucial process in the activation of hypothalamic-pituitary-adrenocortical (HPA) axis in response to stress and to maintain homeostasis. Thus it is not surprising that ACTH secretion is tightly regulated by multiple factors. Although the principal physiological ACTH secretagogue is the hypothalamic neuropeptide, corticotropin-releasing factor (CRF), it is clear that interactions with other regulators including arginine vasopressin (AVP), angiotensin II (AII) and catecholamines, are necessary for the sustained increases of ACTH secretion in conditions such as stress [158-161]. The main inhibitory factor is the end product of HPA axis activation, the adrenalcortical glucocorticoid, which exerts a powerful negative feedback inhibition at several levels along the HPA axis including the anterior pituitary corticotrophs [162].

It is well established that CRF signals primarily through the cAMP pathway to stimulate ACTH secretion [162]. The role of Ca^{2+} in ACTH secretion, and other hormone secretion for that matter, is more complicated, as it serves both facilitatory and inhibitory actions [162, 163]. This is not surprising considering in addition to the unique spatiotemporal dynamics of intracellular Ca^{2+}, there is a diverse range of functional proteins that are regulated by Ca^{2+} alone or in combination with CaM [164]. Indeed, CRF stimulation is known to trigger oscillations of intracellular Ca^{2+} concentration that are essential for ACTH release [165, 166]. These oscillations may be the result of intracellular Ca^{2+} negative feedback loops [162]. Notably, the early glucocorticoid inhibition (within 2 h) of CRF-stimulated ACTH release appears to

act through this Ca^{2+} feedback loop and requires the induction of new proteins [166, 167]. Importantly, in the presence of AVP, which potentiates CRF-induced cAMP accumulation and ACTH secretion, the resulting ACTH secretion is resistant to glucocorticoid inhibition [168-170]. As AVP action is mediated primarily by a different signalling pathway, acting through the inositol 1,4,5-triphosphate (IP3)/protein kinase C (PKC) pathway [171, 172] and may utilise a different ACTH [169, 173] and Ca^{2+} [174, 175] pools, the escape of ACTH secretion from glucocorticoid inhibition could be due to a switch in the components regulating cAMP synthesis and degradation such that they are not longer susceptible to the Ca^{2+}-feedback [162]. Importantly, when corticotrophs were stimulated with CRF or cAMP analogue before and during subsequent glucocorticoid treatment, the early glucocorticoid feedback can be inactivated [176]. Thus it appears that glucocorticoid feedback inhibition is operative to maintain homeostasis, but is blocked under certain stressful situations where the signalling of ACTH secretagogues overwhelmed. Therefore in the physiological context, the interaction of CRF with other ACTH secretagogues and glucocorticoid signalling in corticotrophs is likely to be dynamic and the response to a new external signal may depend on the pre-existing state of this dynamism.

1.4 The AtT20 cell as a model for studying anterior pituitary corticotroph function

The low proportion of corticotrophs in the adenohypophysis and the ubiquitous expression of many proteins make the biochemical characterisation of functional proteins regulating ACTH secretion in corticotropes extremely difficult. The mouse pituitary tumour cell line AtT20 was established from pituitary tumour found to retain the major characteristics of corticotrophs [177] and thus provides a nominally homogeneous population of cells for the characterisation and study of factors involved in the regulation of ACTH secretion. In these cells, the early glucocorticoid inhibition has similar properties as in normal corticotrophs [178, 179]. The hallmarks of early glucocorticoid: onset within 2 h, mediation by type-2 glucocorticoid receptor, requirement for mRNA and protein synthesis, could be demonstrated in AtT20 D16:D16 cells [179]. To this end, AtT20 cells have been used extensively to study the molecular mechanism underlying the regulation of ACTH secretion [180-193].

Previous studies in this laboratory using AtT20 cells have shown that, as in normal rat corticotrophs, there is a pronounced feedback inhibitory effect of intracellular Ca^{2+} on agonist-induced cAMP accumulation (summarised in [162]). Importantly, this inhibitory Ca^{2+} effect is found to be mediated through calcineurin, a Ca^{2+}/CaM-stimulated protein phosphatase (PP2B) [181]. In addition, two targets of Ca^{2+} feedback in AtT20 cells have been identified, a novel isotype of AC that is inhibited by Ca^{2+}, AC9 [181], and the Ca^{2+}-activated BK-type K^+ channels [180]. In addition, glucocorticoid-induced calmodulin [182] may also directly interact with these and other cellular targets (such as PDE1) to mediate the feedback inhibition of agonist-

induced ACTH secretion. These findings indicated that the glucocorticoid feedback inhibition of ACTH secretion is multifactorial and involved the co-ordinated regulation of multiple intracellular signalling components.

1.5 Role of PDEs in the regulation of ACTH secretion

Corticotroph cells exhibit spontaneous as well as agonist-induced action potentials [194] and intracellular Ca^{2+} transients [165, 166, 195]. In this system cAMP-dependent phosphorylation has a prominent role in the control of the membrane potential through regulation of L-type Ca^{2+} channels [196, 197] and BK-type potassium channels [180]. Alterations in the rate of cAMP hydrolysis are therefore bound to be critically important in regulating various aspects of intracellular Ca^{2+} transients such as amplitude, duration, rate of increment and decrement, all of which may contribute to the decoding of the intracellular Ca^{2+} and cAMP signals by various intracellular target proteins [198].

Early studies have indicated the presence of multiple PDE activities in the rat and bovine anterior pituitary [199, 200]. Ca^{2+}/CaM-stimulated PDE activity and both low (about 1 μM) and high (10-20 μM) K_m cAMP-PDE activities were observed [199, 200]. These kinetic characteristics, together with their chromatographic profiles, clearly indicated the presence of PDE1 and plausibly PDE4 activities. Several studies have shown that PDE activity in anterior pituitary cells is regulated by hormone stimulation. AVP treatment was found to inhibit a high-K_m phosphodiesterase activity in rat anterior pituitary cells [168]. Somatostatin, which inhibits ACTH secretion, has been shown to stimulate PDE activity in rat anterior pituitary [201]. Studies using PDE inhibitors have shown that CRF-induced ACTH secretion was equally enhanced by rolipram and IBMX, whereas IBMX was more effective than rolipram in enhancing AVP-induced ACTH secretion [202]. This suggests that PDE4 contributes the main cAMP-hydrolysing activity during CRF

stimulation, while other PDEs in addition to PDE4 are involved in AVP stimulation. More recently, *in vivo* and *in vitro* pharmacological studies have shown the stimulation of HPA axis by PDE4 inhibitors [203], implicating a critical role for PDE4 in the control of corticotroph cell function. Previous studies in this laboratory have observed that inhibition of protein phosphatase 1/2A (PP1/2A) in AtT20 cells leads to a dramatic decrease of CRF-induced cAMP accumulation which appears to involve a reduction of G_s activation of AC and is also partly mediated by an activation of PDE activity [204]. Importantly, the inhibitory effects of Ca^{2+}/calcineurin on cAMP accumulation could not be observed in the presence of calyculin A, suggesting that PP1/2A function is permissive for the Ca^{2+} feedback regulation [181, 204]. These results undoubtedly indicated an important role of PDEs in the regulation of ACTH secretion at the level of anterior pituitary corticotrophs.

The PDE profile of adenohypophysis and AtT20 cells have not been examined in detail with respect to the expression of specific isozymes. Furthermore, while the inhibitory action of Ca^{2+} on cAMP synthesis in these systems is well documented (summarised in [162]), it has not been explored with respect to cAMP degradation by PDEs. With the current knowledge of the PDE superfamily, it is important to identity and to study the regulation of specific PDE isozymes that are involved in these processes to further our understanding of the molecular mechanism governing the regulation of ACTH secretion.

1.6 Aims and objectives of this thesis

This thesis has two fundamental objectives that were designed to compliment ongoing functional studies of the regulation of ACTH secretion in adenohypophysis in this laboratory:

1. To identify the cAMP-hydrolysing PDEs in anterior pituitary cells, primarily that of the experimental model, AtT20 cells. This would be accomplished by multi-faceted analysis using biochemical (kinetic studies, chromatographic separation), pharmacological (subfamily-selective PDE inhibitors), molecular (RT-PCR), and immunological (immunoprecipitation and immunoblot) methods.

2. To examine the potential regulation of PDEs in AtT20 cells by the cAMP-dependent pathway. Intact cells studies looking at the effects of CRF and a cell-permeable cAMP analogue on PDE activity will be carried out. In addition, *in vitro* treatment of cell extracts with PKA catalytic subunit will be performed.

2 MATERIALS AND METHODS

2.1 Biochemicals

All reagents were of the highest grade available and obtained from Sigma-Aldrich (Poole, Dorset, UK) unless otherwise stated. The following compounds were generously provided by the manufacturers: rolipram (Schering A.G., Berlin, F.R.G.), Zaprinast (Rhône Poulenc Rhorer Ltd, Dagenham, UK), and vinpocetine (Gedeon Richter Ltd, Budapest, Hungary). Dulbecco's modified Eagle's medium (DMEM), Hank's balanced salt solution (HBSS) and Geneticin® (G418 sulphate) were purchased from GIBCO BRL, Paisley, Strathclyde, UK. Foetal calf serum (FCS) was from Seralab, Crawley Down, Sussex, UK. [2,8,5-^{3}H]adenosine, [2-^{3}H]5'-AMP, and [2,8-^{3}H]3',5'-cAMP were from Dupont, Stevenage, UK or Amersham, Little Chalfont, UK. GF/C filter was from Whatman, Maidstone, Kent. SDS-electrophoresis calibration kit was from Pharmacia, St Alban, Herts, UK. Immobilon membrane was from Millipore. Acrylamide/bis-acrylamide was from Bio-Rad, Herfordshire, UK. HRP-anti-rabbit IgG was from SAPU, Lanarkshire, Scotland, UK. CRF and protein kinase A inhibitor peptide (TTYADFIASGRTGRRNAIHD) were from Bachem, UK. CPT-cAMP was from BIOLOG, Bremen, Germany. Calyculin A was from Alexis, Nottingham, UK. H-89 {*N*-[2-[[3-(4-bromophenyl)-2-propenyl]amino]ethyl]-5-isoquinoline sulfonamide} was from Calbiochem, Nottingham, UK or Biolog, Bremen, Germany. PKA catalytic subunit (purified from bovine heart) was from Promega, Southampton, UK. Recombinant PKA catalytic subunit was a generous gift from Dr. R. Clegg, Hannah Institute, Ayr, UK (recombinantly expressed murine C_α, purified from *E. coli* [205]).

2.2 Preparation and storage of stock solutions

PDE inhibitors were dissolved in dimethylsulphoxide (DMSO) to 0.1-0.5 M, aliquoted and stored at –20 C. 0.1 mM CRF was prepared in 1 mM ascorbic acid and 10 mM HCl, aliquoted and stored at –70 C. CPT-cAMP was dissolved in distilled water to a 50 mM stock solution, aliquoted and stored at –40 C. Calyculin A was dissolved in ethanol to a 100 μM stock solution and stored at –40 C. H-89 was dissolved in DMSO to a 10 mM stock solution and stored at 4 C. 10 μM calmodulin was prepared in 0.1% BSA, aliquoted and stored at –40 C. Phenylmethylsulphonylfluoride (PMSF) was prepared fresh in ethanol to 100 mM. Dithiothreitol was dissolved in distilled water to a 100 mM solution, aliquoted and stored at –20 C. 17.5 mM $Ba(OH)_2$ was prepared fresh for each PDE assay.

2.3 Cell lines

AtT20 D16:16 mouse anterior pituitary tumour cells were kindly provided by Dr S. L. Sabol, National Institute of Health, Bethesda, MD, USA [177]. Human embryonic kidney (HEK293) cells were kindly provided by Dr. L. Anderson, Medical Research Council Reproductive Biology Unit, Edinburgh, Scotland, UK.

2.4 Cell culture

AtT20 cells were maintained as monolayer culture in DMEM with 2.5g/L glucose, supplemented with 10% FCS and in an atmosphere of 5% CO_2/95% air at 37 C [179]. AtT20 cells were passaged every 7 days. All experiments were performed on cells between passage 10 to 30. HEK293 cells were maintained as AtT20 cells except that they were passaged every 4 days. HEK293 cells stably transfected with

pCI-HSPDE4D3-VSV plasmid (HEK293-4D3-VSV) were maintained as HEK293 cells except that 0.6 mg/ml Geneticin® was included in the growth medium to maintain selection pressure.

2.5 Cell treatment

Cells were detached from the tissue culture flasks with HBSS supplemented with 0.1% EDTA, pelleted at 200g for 5 min, resuspended at approximately 10^6 cells/ml (counted with a haemocytometer), aliquoted (0.5-2 ml per treatment) and preincubated in the incubation buffer (HBSS containing 25 mM HEPES, pH 7.3-7.4, 2 mM $CaCl_2$, 1 mM $MgSO_4$ and 0.25% (w/v) BSA) for 30 min at 37 C with gentle shaking or end-on-end turning. Vehicles or drugs were then applied and incubated at 37 C for the indicated times. Treatments were terminated by transferring the cells to an ice-bath for 5 min. The experiments with CRF were performed with AtT20 cells plated in 24-well tissue culture trays [179].

2.6 Preparation of cell extracts

After termination of the treatment, cells were pelleted at 200g for 5 min at 4 C and washed twice with ice-cold incubation buffer without BSA. The cell pellets were then resuspended (2-10x10^6 cells/ml) in a homogenisation buffer (HB) containing 20 mM Tris-HCl, pH 7.5, 1 mM EDTA, 0.2 mM EGTA, 50 mM NaF, 10 mM sodium pyrophosphate, 50 mM benzamidine, 0.5 μg/ml leupeptin, 0.7 μg/ml pepstatin, 4 μg/ml aprotinin, 10 μg/ml soybean trypsin inhibitor, 2 mM PMSF and 1 mM DTT, and lysed by freeze-thawing (liquid N_2 and 30 C until just thawed and then kept on ice). The homogenate was centrifuged at 200g for 10 min, 4 C, and the resultant

supernatant was spun at 30,000g for 20 min, 4 C, to obtain the cytosolic fraction (i.e. supernatant of 30000g). Protein content was quantitated using Coomassie Protein Assay Reagent (Pierce, Chester, UK) with BSA as standard [206].

2.7 Preparation of extracts from anterior pituitary glands and rat brain

Male Wistar rats (150-200g body weight; Harlan-Olac, Bicester, UK) were housed in individual cages for 24-48 h under controlled lighting and air conditioning, with free access to tap water and food pellets. Animals were killed by decapitation between 8:30 and 9:00 AM, taking precautions to avoid stressful stimulation. Adult balb/c mice were similarly treated. The anterior pituitary glands were excised and immediately processed for RNA extraction (detailed below) or homogenised with a Teflon-glass homogenizer (3 × 20 s) in 10 volumes of the same homogenization buffer used for AtT20 cells. The rat brains were removed and homogenised as above, and aliquots of the homogenate were kept at –70 C.

2.8 PDE assay

2.8.1 $ZnSO_4$-$Ba(OH)_2$ precipitation method

PDE activity was measured by minor modifications of a radiometric assay [207] based on the precipitation of the cAMP hydrolysis product, 5'-AMP, with $ZnSO_4$-$Ba(OH)_2$ treatment [208]. The PDE assay buffer contained 100 mM Tris-HCl, pH 7.5, 5 mM $MgSO_4$, 10-20 µl of cell extract (1-10 µg protein), and other additions for defining different PDE activities (detailed below), in a total volume of 150 µl. After preincubation at 30 C for 5 min, the reaction was initiated by the addition of 50 µl substrate mixture to give a final concentration of 1 µM cAMP and 0.2 µCi/ml [2,8-^{3}H]cAMP. The PDE assay was then incubated at 30°C for 5-30 min. The reaction was terminated by the addition of 100 µl of 21.5 mM $ZnSO_4$ followed by 100 µl of 17.5 mM $Ba(OH)_2$ to precipitate the 5'-AMP formed. The suspension was filtered over Whatman GF/C filters on a vacuum manifold, and washed twice with 3 ml of 1 mM NaOH/100 mM NaCl. Radioactivity retained on the filters was measured by liquid scintillation counting with 10 ml of Emulsifier-SAFE™ scintillation cocktail (Packard Bioscience, Pangbourne, Berkshire, UK). The % recovery (68 ± 2%, mean±S.E.M., n=18) of the counts (precipitates) was monitored with ^{3}H-AMP in place of ^{3}H-cAMP. Blanks were either with homogenisation buffer in place of cell extracts or with heat-inactivated (90 C, 5 min) cell extracts which gave similar results and were less than 2% of the total ^{3}H-cAMP added. PDE assay of each sample was performed in duplicate or triplicate. The coefficient of variation between the PDE assay triplicates was usually below 3%. To ensure cAMP hydrolysis was linear with respect to the incubation time and the amount of cytosolic proteins added, PDE activities were measured with less than 30% of the total cAMP hydrolysed

(Figure 1). For kinetic studies, total cAMP hydrolysed was kept below 15%. PDE activity is expressed as nanomoles of cAMP hydrolysed per min per mg cellular protein (nmol/min/mg).

Figure 1

Time-course and protein-dependence of the PDE activity in AtT20 cells

Figure 1: PDE activity in AtT20 cytosol were measured with 1 μM cAMP as substrate and in the presence of 100 μM Ca^{2+} and 100 nM CaM using the $ZnSO_4$-$Ba(OH)_2$ precipitation PDE assay. (A) For the time-course, aliquots of 10 μg AtT20 cytosol were incubated for 5 to 45 min at 30 C. (B) For the protein-dependence assessment, 2 to 32 μg AtT20 cytosol were incubated for 10 min at 30 . The PDE activity measured are expressed as a percentage of total cAMP (1 μM) hydrolysed. Data from one experiment representative of two performed are shown. The data plotted are mean±S.D. of PDE assay triplicates.

2.8.2 QAE-Sephadex column method

The $ZnSO_4$-$Ba(OH)_2$ precipitation method for PDE assay was compared to another PDE assay method which employs chromatographic separation of cyclic nucleotides and nucleosides on a column of an anion exchange resin, diethyl[2-hydroxypropyl]aminoethyl (QAE) A-25 Sephadex. In the QAE-Sephadex column method, ^{3}H-5'-nucleotides generated by PDE are further converted to ^{3}H-nucleosides by excess 5'-nucleotidase present in snake venom. The unreacted cyclic nucleotides are bound to the QAE-Sephadex resin, while the nucleosides and their catabolites are collected in the eluate for scintillation counting. The QAE A-25 Sephadex column method was carried out according to a published protocol [209]. Briefly, QAE-Sephadex A-25 (Sigma Q-25-120) in the chloride form was converted to the formate form before being packed into the Bio-Spin chromatography column (6 × 15 mm, Bio-Rad). The PDE assay buffer and the initiation of reaction were as for the $ZnSO_4$-$Ba(OH)_2$ precipitation method. The PDE reaction was terminated by the addition of 50 µl normalised 0.2 N HCl. After neutralisation with 50 µl normalised 0.2 N NaOH, 50 µl of 1 mg/ml snake venom (Sigma V7000) was added and the mixture incubated at 30 C for 10 min. The nucleotidase reaction was terminated with a stop buffer containing 120 mM EDTA, pH 7.0, and 0.8 mM adenosine. 350 µl of the PDE assay mixture was then applied to the QAE-Sephadex column previously equilibrated with 3 ml of 30 mM ammonium formate, pH 6.0. The eluate together with that from two additional 1 ml washes with 30 mM ammonium formate, pH 6.0, were collected in the same scintillation vial and counted with 15 ml of Emulsifier-SAFE™ scintillation cocktail. The QAE-Sephadex column was regenerated with 2 × 1 ml 0.2 N HCl, followed by 3 × 1 ml 30 mM ammonium

formate, pH 6.0. The blank was less than 3 % of the total ^{3}H-cAMP added. The radioactivity of ^{3}H-cAMP added was completely recovered in the eluate when excess PDE activity from rat brain cytosol was used to completely hydrolyse cAMP.

2.8.3 Assay conditions for measuring the activity of different PDE isozymes

The total PDE activity was taken as the activity measured in the presence of 100 μM Ca^{2+} and 100 nM CaM (Sigma P2277). No further increase in PDE activity was measured with up to 500 μM Ca^{2+} and 500 nM CaM. Ca^{2+}/CaM-independent activity was assayed in the presence of 0.5 mM EGTA. Ca^{2+}/CaM-dependent (PDE1) activity was taken as the difference between the total and Ca^{2+}/CaM-independent PDE activities. PDE4 activity is defined as the activity measured with 0.5 mM EGTA that was inhibited by 10 μM rolipram. For the CaM dose response studies of AtT20 cytosolic PDE1 activity, the endogenous CaM content in the cell extracts was determined using activator-deficient bovine brain PDE1 (Sigma P9529). Using 10 μM cAMP as substrate, the PDE activity of the activator-deficient PDE1 was measured in the presence of 0.1 - 100 nM CaM to obtain a CaM standard curve and with aliquots of heat-inactivated (10 min in a boiling water bath) AtT20 cell extracts. The endogenous CaM content in the cell extracts were then extrapolated from the CaM standard curve based on the extent of stimulation of the activator-deficient PDE1 activity by the heat-inactivated cell extracts.

2.8.4 Verification of the $ZnSO_4$-$Ba(OH)_2$ precipitation PDE assay

Under the conditions of the $ZnSO_4$-$Ba(OH)_2$ precipitation method described above, 97±0.1% of ^{3}H-AMP (n=24), 0.6±0.01% of ^{3}H-cAMP (n=12) and 1.7±0.01% of ^{3}H-adenosine (n=8) were precipitated in the presence of up to 3 μM of the respective unlabelled nucleotides (data are mean±S.E.M. of n separate determinations), indicating highly selective separation cAMP from 5'-AMP. As reported previously [208, 210, 211], adenosine was not precipitated with $BaSO_4$. Because 5'-AMP can be further converted to adenosine by nucleotidase and/or phosphatase activities present in cell extracts [212], the extent of this interference which may lead to an underestimation of PDE activity was assessed. Firstly, PDE activity in AtT20 cytosol measured by the $ZnSO_4$-$Ba(OH)_2$ precipitation assay or with the QAE-Sephadex column method [209] (which allows separation of both 5'-AMP and adenosine from cAMP) was near identical (Table 2). Secondly, PDE activity in AtT20 cytosol measured with the $ZnSO_4$-$Ba(OH)_2$ precipitation assay with or without 1 mM AMP supplement (that have been used to minimise nucleotidase interference [212-214]) was not significantly different, whereas 1 mM AMP markedly reduced nucleotidase interference when rat brain extracts were used (Table 2). Thirdly, parallel time-courses of PDE and 5'-nucleotidase (^{3}H-cAMP was replaced with ^{3}H-AMP) activities in AtT20 cell extracts indicated that less than 0.3% of ^{3}H-AMP was hydrolysed by 30 min, where up to 30% of ^{3}H-cAMP was hydrolysed. Hence, the further conversion of 5'-AMP to adenosine in AtT20 cytosol was negligible when compared with the PDE activity under the described conditions of PDE assay.

Table 2

Verification of the $ZnSO_4$-$Ba(OH)_2$ precipitation PDE assay

Cytosolic protein (μg)	QAE-Sephadex	$ZnSO_4$-$Ba(OH)_2$	$ZnSO_4$-$Ba(OH)_2$ + 1 mM AMP
	(% of total cAMP hydrolysed)		
2	2 ± 0.3	3 ± 0.3	3 ± 0.1
4	7 ± 0.4	7 ± 0.2	6 ± 0.2
8	11 ± 0.3	14 ± 0.7	11 ± 0.2
16	23 ± 0.7	26 ± 0.5	21 ± 0.4
32	45 ± 2.0	47 ± 0.5	42 ± 1.2
Rat brain cytosol (50 μg)	88 ± 0.6	9 ± 0.3 *	81 ± 1.5

Table 2: PDE activity of AtT20 cytosol (2-32 μg) and rat brain homogenates (50 μg) were measured at 30°C for 10 min using the QAE-Sephadex method and the $BaSO_4$ co-precipitation method with or without 1 mM AMP in the PDE assay buffer (as described in section 2.8). Data are mean±S.E.M. of 3 separate determinations. *, $p<0.001$ when compared with results by QAE-Sephadex method.

2.9 RT-PCR analysis

2.9.1 Design of primers for RT-PCR analysis of PDE1 and PDE4 isozymes

Primers were designed based on the available PDE sequences in the Genbank™ with the aid of GeneJockey II (Biosoft, UK) and Amplify version 1.2ß (University of Wincosin, USA) softwares. The generic antisense primers, pde1r and pde4r, were designed to amplify regions common to all known isozymes/splice variants of the three-gene (PDE1A-C) PDE1 family and the four-gene (PDE4A-D) PDE4 family, respectively (Figure 2). The sense primers, pde1af, pde1bf and pde1cf, and the antisense primers, pde1cr and pde1cr(2), were designed to amplify and distinguish between the PDE1A, PDE1B and PDE1C isozymes (Figure 2). The splice-variant-specific primers were designed based on differences in the 5' (pde1c2, pde1c145, pde4a5 and pde4d3) or 3' (pde1c45r) sequences of the known splice variants (Figure 2). All primers were synthesized by Cruachem, Todd Campus, Glasgow, Scotland, UK. The sequences of the primers are given in Table 3.

Figure 2

Schematic representation showing the regions used for designing RT-PCR primers

Figure 2: A schematic diagram showing the regions of representative PDE1 and PDE4 isozymes used for designing RT-PCR primers. Primers were designed based on the conserved regions within each family (hatched box), or isozyme (gene)-specific regions (solid box), or splice variant-specific regions (arrow). The name and Genbank™ accession number of the PDE isozymes used for this representation are given on the left. The sequences of the primers are shown in Table 3.

Table 3

Sequence information of primers used for RT-PCR analysis

For the analysis of PDE1 mRNA expression
Sense
pde1af = GGGGATGATGAAAAAGAAGCCTGAAG
pde1bf = GCAGTCCACAACTGTCTCAAGAACCTG
pde1cf = CCTCCTTTATAAGACAGGAGTAGCAAAC
pde1c145f = GTGCAGCTATGGAGTCTCCAACCAAG
pde1c2f = GTCATGACGGACACCAGCCACAAGAAG
Anti-sense
pde1r = GTTGGCTCCACWATGAARTCAATGAAAC
pde1cr = GTTTCTCTGTCACCCTGTCTAAAGAACTC
pde1cr(2) = GTTTTCTTTGACTCATTTCCGGTGTTGGAG
pde1c45r = GTTTCTGGATGATGTTTTATCCGTAGTCTCC

For the analysis of PDE4 mRNA expression
Sense
pde4a5f = GACCCCGATCCGCATCCAGCAACG
pde4bf = GTTTATCACAACAGCCTGCACGCTGCTGA
pde4cf = GTTCAAGCGCATGCTCAACCGTGAGTTG
pde4d3f = CATTCCTGGATATGTTTCGATGTGGAC
Anti-sense
pde4r = MCGRTTMAGCATCCTYTTGAAC
pde4br = GTTATGGGAGTACCCAGCCACGTTG
pde4cr = GTACGCCACGTTGGAGTGGTAGTGC
pde4dr = GTTGCCAGACAGCTCCGCTATTCGG

Table 3: Sequences of primers (5'-3') designed to be used in the RT-PCR analysis of PDE isozymes/splice variants expression (as described in section 2.9.1) are tabulated.

2.9.2 RT-PCR protocol

Total RNA was prepared from AtT20 cells and anterior pituitary glands using TRIzol® reagent (GIBCO Life Sciences, Paisley, UK) according to the manufacturer's instructions. First strand cDNA was synthesised from total RNA using SUPERSCRIPT™ preamplification system (GIBCO). Briefly, 5 μg of total RNA was heated with 2.5 μM random hexamers to 70 C for 10 min and quickly chilled on ice. 10 units of SUPERSCRIPT II™ reverse transcriptase were added to start first-strand cDNA synthesis at 42 C for 50 min in a 20-μl reaction volume containing 1X first strand buffer, 10 mM DTT and 0.5 mM dNTP mix. The reaction was terminated by heating at 70 C for 15 min and aliquots of the cDNA were stored at -40 C. PCR was carried out in a 50-μl reaction volume containing 1 μl of cDNA, 0.1-0.5 μM primers, 20 mM Tris-HCl, pH 8.0, 50 mM KCl, 2 mM $MgCl_2$ and 0.2 mM dNTP mix. After heating the mixture to 95 C for 5 min, the PCR was initiated by the addition of 2.5 units *Taq* DNA polymerase (GIBCO) at 80 C, followed by denaturation at 95 C for 1 min, annealing at 60 C for 1 min, extension at 72 C for 3 min, for 35 cycles and a final 10 min of extension at 72 C. PCR primers were tailed at the 3'-end in order to optimise for adenylation [215] and thus facilitate T/A ligation. PCR products that corresponded to the expected size (visualised with ethidium bromide under *uv* light) were purified using the Wizard PCR Prep kit (Promega) or QIAEX II gel extraction kit (Qiagen, West Sussex, UK) before ligation into pGEM®-T or pGEM®-T Easy vectors (Promega) according to the manufacturer's instructions. The ligated plasmid was used to transform JM109 high efficiency competent cells (Promega). Plasmid DNA prepared from antibiotic resistant colonies was extracted using a Plasmid Mini kit (Qiagen), and the insert was

sequenced in both directions using the Applied Biosystems Taq DyeDeoxy™ terminator cycle kit and model 373 DNA sequencer.

2.10 Treatment with PKA catalytic subunit under phosphorylating conditions in cell-free systems.

AtT20 cytosolic fractions or anion-exchange chromatographic fractions were incubated at 30 C in a phosphorylation reaction buffer containing 30 mM Tris-HCl, pH 7.5, 20 mM $MgSO_4$, 0.5 mM ATP with or without PKA catalytic subunit. The final concentration of PKA catalytic subunit in the phosphorylation reaction was kept below 1 μM according to the reported concentrations found in various tissues [216]. The incubation time and the amount of PKA catalytic subunit used are indicated in the relevant figure legends. The phosphorylation reaction was terminated by the addition of 0.1 μM protein kinase A inhibitor peptide [217] and by placing the tubes on ice bath.

2.11 Anion-exchange chromatographic separation of PDE activities

DEAE-cellulose (DE-52 from Whatman) was used to pack a 9 mm × 15 cm column (Pharmacia K9/15 column). The column was equilibrated with the starting buffer containing 50 mM sodium acetate, pH 6.5, 0.1 mM EGTA, 5 mM β-mercaptoethanol, 10 mM NaF, 1 mM EDTA, 0.5 mg/L leupeptin, 0.7 mg/L pepstatin, and 0.2 mM PMSF. Typically, 2 ml of the cytosolic fraction (approximately 2 mg protein) was loaded and the column was washed with 2-column volumes of starting buffer. The column was then eluted with a linear 0.05-1 M sodium acetate gradient. 6 min (about 2 ml) fractions were collected and 10 or 20 μl of each fraction was assayed for PDE activity with 1 μM cAMP as mentioned above in the PDE assay. All chromatographic steps were carried out at 4°C.

2.12 Antibodies selective for PDE4 subfamily

The rabbit polyclonal antibodies, Ab651 (anti-PDE4A) and Ab313 (anti-PDE4D), the anti-VSV monoclonal antibody (anti-VSV), and the expression plasmid, pCI-HSPDE4D3-VSV, were generously supplied by Prof. M. Houslay, University of Glasgow, Scotland, UK. Ab651 was raised to a peptide sequence that corresponds to amino acids 788-886 of human PDE4A5 (a common PDE4A C-terminal region) and recognises all the known PDE4A splice variants [218]. Ab313 was raised to the C-terminal 40 amino acids of PDE4D2 (a common PDE4D C-terminal region) and recognises all the five PDE4D splice variants known [109]. Anti-VSV recognises the five C-terminal amino acids (507-511) of the vesicular stomatitis virus (VSV) glycoprotein [219] that are part of the 11-amino acid VSV epitope tagged to the recombinant human PDE4D3 in the pCI-HSPDE4D3-VSV plasmid [109].

The rabbit polyclonal antibody, AC55 (anti-PDE4A), the monoclonal antibody, M3S1 (anti-PDE4D), and the recombinant rat PDE4D3 purified from baculovirus expression in Sf9 insect cells were generously supplied by Prof. M. Conti, Stanford University, USA. The characterization of these antibodies [220] and the recombinant rat PDE4D3 [221] have been published.

2.13 Immunoprecipitation of PDE4

For each immunoprecipitation reaction, 50 µl of a 20% Protein G-sepharose 4B (Sigma P-3296) suspension (in 20% ethanol) was washed twice (pelleting at 10000g for 15 s between washes) with phosphate-buffered saline (PBS) containing 0.1% BSA (PBS-B) and then incubated with 5 µl of antibody in a final volume of 50 µl (1:10 dilution in PBS-B) for 1h at 4 C with end-on-end mixing. Normal rabbit serum (NRS) at 1:10 dilution and BSA (0.1%) were used as controls in place of polyclonal and monoclonal antibodies respectively. The beads were washed three times with PBS-B and then incubated with the cytosolic extracts (50-500 µl or 0.1-1 mg cytosolic protein) for 1.5 h at 4 C with end-on-end mixing. At the end of the incubation, the immunoprecipitation mixture was centrifuged at 10000g for 1 min to obtain the supernatant and the immunoprecipitate. The supernatant was collected for PDE assay. The immunoprecipitate was washed twice with PBS-B and once with PBS, and then either resuspended in HB (to the same volume as the supernatant) for PDE assay or resuspended to 1× Laemmli's sample buffer (62.5 mM Tris-HCl, pH 6.8, 10% glycerol, 2% SDS, 5% ß-mercaptoethanol, and 0.0025% bromophenol blue [222]) and incubated in a boiling water bath for 3 min before subjected to SDS-PAGE. Complete immunoprecipitation of the PDE4s from the cytosolic extracts was indicated by two observations: 1. No further PDE4 activity was being pulled down with twice the amount of antibodies (10 µl), and 2. The amount of PDE4 activity pulled down was proportional to the amount (up to 1 mg cytosolic protein) of cytosolic extracts used for the immunoprecipitation.

2.14 SDS-PAGE and immunoblot analysis

Immunoprecipitated samples were electrophoresed on 8% SDS-polyacrylamide gel at 30 V for 9 h (model V-16-2 vertical gel system from GIBCO BRL) or 150 V for 1 h (mini-PROTEAN II system from BIO-RAD). The electrophoresis buffer contained 25 mM Tris base, 192 mM glycine and 0.1% SDS (pH 8.3). SDS-electrophoresis calibration kit containing both high (53-212 kDa) and low (14.4-94 kDa) molecular weight markers was used for the calibration of the apparent molecular weights of the separated proteins. 10 ng of recombinant rat PDE4D3 was also included in each run to serve as a positive control for the immunodetection and for comparison with the migration of immunoreactive bands. After electrophoresis, the separated proteins were electroblotted (Trans-Blot cell from BIO-RAD) onto Immobilon membranes overnight at 30 V, 4 C, in a transfer buffer containing 25 mM Tris base, 192 mM glycine and 10% methanol. All subsequent membrane incubations were carried out at room temperature in PBS containing 0.1% BSA and 0.1% Tween-20 (PBS-BT) and the indicated reagents with shaking. After each incubation step, the membranes were rinsed twice and washed three times (10 min per wash) with PBS-BT. The membranes were first blocked in 5% BSA for 1 h, and then incubated with Ab313 (1:1000 dilution) for 1 h. The bound antibody was detected using HRP-conjugated anti-rabbit IgG (1:5000 dilution for 1hr) and the enhanced chemiluminescence (ECL) detection system (Amersham, Little Chalfont, UK). After 1 min incubation in ECL reagents, the membranes were exposed to ECL Hyperfilms for 10-30 s to visualise the immunoreactive signals.

2.15 Transfection of HEK293 cells with recombinant HSPDE4D3

The expression plasmid, pCI-HSPDE4D3-VSV, which contains the cDNA encoding human PDE4D3 fused with a C-terminal VSV epitope tag [109] was transfected into HEK293 cells by the $CaPO_4$ method [223]. Briefly, HEK293 cells were plated at a density of 10^5 cells/cm^2 in 25 cm^2 tissue culture flask 24 h before the transfection. The $CaPO_4$-DNA coprecipitate was prepared by slowly adding 31 µl of 2 M CaCl to a mixture consisted of 220 µl of plasmid DNA (i.e. pCI-HSPDE4D3-VSV, dissolved in 1 mM Tris-HCl, pH 8.0, and 0.1 mM EDTA, to a concentration of 40 µg/ml) and 250 µl of 2X HEPES-buffered saline (50 mM HEPES, pH 7.05, 280 mM NaCl, 10 mM KCl, 1.5 mM Na_2HPO_4 and 12 mM dextrose) with gentle shaking and was further incubated for 30 min at room temperature. The $CaPO_4$-plasmid suspension (500 µl) was then added to the medium above the HEK293 cells monolayer. The next day, the medium containing the $CaPO_4$-plasmid coprecipitate was replaced with fresh medium and the cells were grown for another three days before selecting for neomycin-resistant stably transfected cells with 0.6 mg/ml Geneticin®. The VSV epitope tagged HSPDE4D3 was immunoprecipitated with a monoclonal antibody that recognises the five C-terminal amino acids of VSV glycoprotein [219].

2.16 Data analysis

Data were evaluated by Student's *t*-test or 1-way ANOVA followed by Newman-Keuls or Dunnett two-tailed tests as appropriate. Data of $p<0.05$ were considered statistically significant. The apparent K_m and V_{max} values of the substrate saturation studies were determined either by linear regression analysis of Eadie-Hofstee plot or by one- and two-site models (fitted to the hyperbolic form of Michaelis-Menten equation) with non-linear regression analysis and comparison of fits. The statistical comparisons between one- and two-site fits were made by F-test. The apparent IC_{50} of PDE inhibitors, and the EC_{50} and Hill coefficient of CaM stimulation of PDE1 activity, were determined by fitting to a four-parameter logistic equation, Y=Bottom+(Top-Bottom)/(1+10^((log(IC_{50} or EC_{50})-X)(Hill coefficient)) with non-linear regression analysis, where Y=PDE activity, X=concentration of the modulator. In the case of IC_{50} determination, the Top of the curve (which was the PDE activity incubated with vehicle) was held constant. All curve fitting was carried using GraphPad Prism® version 2.0a.

3 RESULTS

3.1 Biochemical analyses of PDE activities

3.1.1 PDE activities in AtT20 cells

The first attempt was to distinguish cAMP-hydrolysing PDE activities in AtT20 whole cell homogenates by different PDE assay conditions. Using 1 μM cAMP as substrate, PDE activity was found to increase about 2-fold when measured in the presence of excess Ca^{2+} (100 μM) and CaM (100 nM) compared to that in the presence of 0.5 mM EGTA (Figure 3A, WH columns). There was no further increase in PDE activity with up to 500 μM Ca^{2+} and 500 nM CaM. The increased PDE activity in the presence of 100 μM Ca^{2+}/100 nM CaM was defined as the Ca^{2+}/CaM-stimulated PDE1 activity and was calculated from the difference between the total PDE activity (measured with 100μM Ca^{2+}/100 nM CaM) and the Ca^{2+}/CaM-independent PDE activity (measured with 0.5 mM EGTA). Therefore the total PDE activity can be broadly separated into PDE1 activity and Ca^{2+}/CaM-independent PDE activity. To determine the subcellular distribution of the two PDE activities, the whole homogenate was first subjected to centrifugation at 200g for 10 min to obtain the 200g pellet and the resulting supernatant was further centrifuged at 30000g to obtain the 30000g particulate fraction and the cytosolic fraction (i.e. the 30000g supernatant). When PDE activities in these fractions were measured (standardised to the starting whole homogenate volume), more than 90% of PDE1 and about 50% of Ca^{2+}/CaM-independent PDE activity in the whole cell homogenate were recovered in the cytosolic fraction (Figure 3A). Data pooled from several experiments showed that the PDE1 activity constituted 73±2% (mean±S.E.M., n=10) of the total cytosolic PDE activity, and 62±2% (mean±S.E.M., n=13) of the

remaining Ca^{2+}/CaM-independent PDE activity was inhibited by 10 μM rolipram, a PDE4-selective inhibitor (i.e. about 20% of the total cytosolic PDE activity was attributable to PDE4). As treatment of intact cells with a PDE-resistant and cell permeable cAMP analogue, CPT-cAMP, specifically increased Ca^{2+}/CaM-independent PDE activity and reduced PDE1 activity in the cytosolic fraction (Figure 3B), subsequent analyses were focused on the cytosolic PDE activities.

3.1.1.1 Substrate saturation studies of PDE activities in the cytosolic fraction

To assess the properties of the cytosolic PDE1 and Ca^{2+}/CaM-independent PDE activity with respect to cAMP, substrate saturation experiments were performed with 0.25 to 100 μM cAMP (Figure 4). The K_m and V_{max} values were obtained by linear regression of Eadie-Hofstee plots: PDE1 activity, K_m = 0.89±0.29 μM and V_{max} = 0.50±0.05 nmol/min/mg (mean±S.E.M., n=6); Ca^{2+}/CaM-independent PDE activity, K_m = 1.02±0.15 μM and V_{max} = 0.25±0.05 nmol/min/mg (mean±S.E.M., n=5). Therefore, both PDE activities were found to have low K_m values of about 1 μM for cAMP.

Figure 3

Distribution of PDE activities in control and CPT-cAMP-treated AtT20 cells

Figure 3: AtT20 cells were incubated with vehicle (A) or 1 mM CPT-cAMP (B) for 10 min at 37 C. After treatment, cells ($10x10^6$ per group) were lysed by freeze-thawing in 500 µl homogenization buffer to give the whole homogenate (WH). 250 µl of the WH was then centrifuged to obtain the 200g pellet (200g-P), the 30000g particulate fraction (30000g-P) and the 30000g cytosolic fraction (CF). The 200g-P and PF were resuspended to 250 µl with the homogenization buffer and equal volumes (10 µl) of WH, 200g-P, PF, and CF were measured for PDE activities in the presence of 0.5 mM EGTA (empty bar) or 100 µM Ca^{2+} and 100 nM CaM to access the Ca^{2+}/CaM-stimulated PDE1 activity (shaded bar). Data are mean±S.D. of PDE assay triplicates of a representative experiment of 3 performed.

Figure 4

Substrate saturation studies of PDE activities in AtT20 cytosol

Figure 4: (A) PDE1 (empty circles) and Ca^{2+}/CaM-independent PDE (filled circles) activities in AtT20 cytosol were measured in the presence of 0.25-100 μM cAMP. Results of a representative experiment of six are shown (points are means of triplicate PDE assay±S.D.). In this experiment, the apparent K_m and V_{max} values calculated from linear regression of the Eadie-Hofstee plot (insert) are: PDE1 activity (K_m = 0.6 μM, V_{max} = 0.7 nmol/min/mg protein); Ca^{2+}/CaM-independent PDE activity (K_m = 1.4 μM, V_{max} = 0.4 nmol/min/mg). Data from six experiments are summarized in section 3.1.1.1.

3.1.1.2 Pharmacological studies of PDE activities

The inhibition of the two cytosolic PDE activities by various PDE inhibitors were assessed in the presence of 1 μM cAMP as substrate (Figure 5). The non-selective PDE inhibitor, 3-isobutyl-1-methylxanthine (IBMX), was found to inhibit completely both the Ca^{2+}/CaM-independent and -stimulated PDE activities, with similar apparent IC_{50} values of 12±1 and 15±2 μM (mean±S.E.M., n=3) respectively (Figure 5). However, the inhibition profiles of the two PDE activities by more selective PDE inhibitors were very different. Notably, about 60% of the Ca^{2+}/CaM-independent PDE activity was selectively inhibited by rolipram (a specific inhibitor of PDE4) with an apparent IC_{50} value of 0.11±0.03 μM (mean±S.E.M., n = 9), while the Ca^{2+}/CaM-stimulated PDE activity was not inhibited by up to 100 μM rolipram (Figure 5). A derivative of IBMX, 8-methoxymethyl-3-isobutyl-1-methylxanthine (8-MIX), which is known to selectively inhibit PDE1 [224-226] and Zaprinast, a PDE5-selective inhibitor that has also been shown to inhibit PDE1 [226, 227], were considerably more potent inhibitors of the Ca^{2+}/CaM-stimulated PDE activity than of the Ca^{2+}/CaM-independent PDE activity (Figure 5). The apparent IC_{50} values of 8-MIX and Zaprinast for the Ca^{2+}/CaM-stimulated PDE activity, 10±2 and 7±1 μM (mean±S.E.M., n=3) respectively, were similar to those reported for PDE1 isozymes [84]. Vinpocetine, which had been reported to be selective for PDE1 in some studies [49, 226, 228] but not all [229], was observed to inhibit both PDE activities in AtT20 cells with similar potency (Figure 5); apparent IC_{50} values were 62±3 μM for Ca^{2+}/CaM-independent PDE activity and 65±3 μM for PDE1 activity (mean±S.E.M., n=3). Taken together, the pharmacological analysis supported the presence of PDE1 and PDE4 activities in AtT20 cytosol.

Figure 5

Inhibition of PDE activities in AtT20 cytosolic fraction by known PDE inhibitors

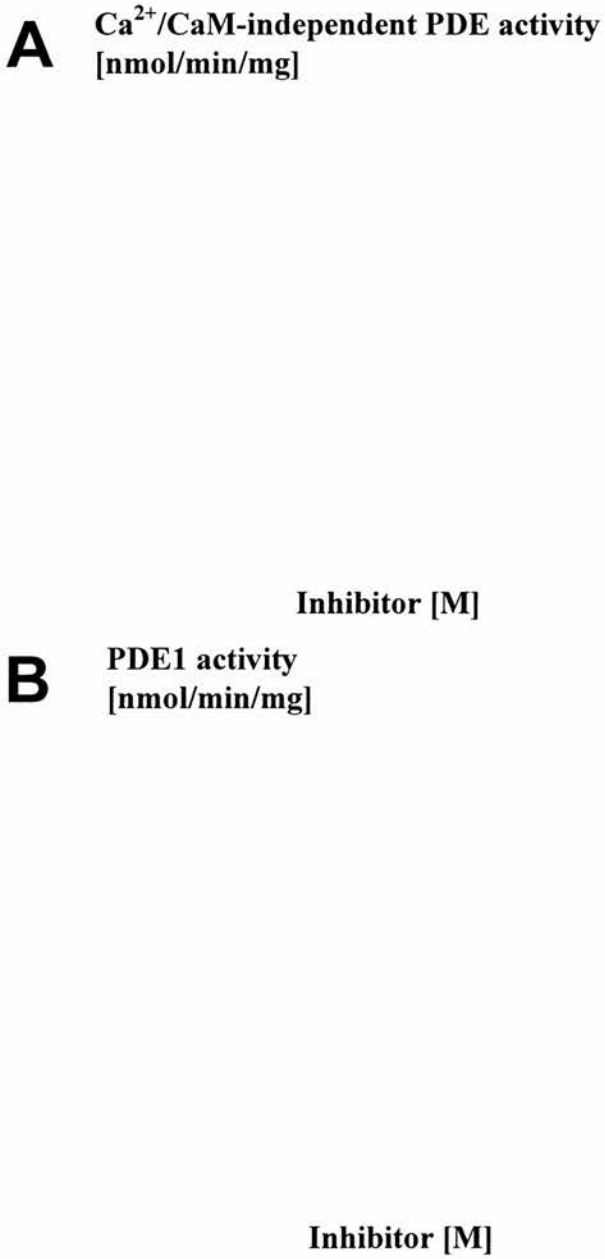

Figure 5: Ca^{2+}/CaM-independent (A) and -dependent (B) PDE activities in the cytosolic fraction of AtT20 cell homogenate were assayed with 1 μM cAMP as substrate and in the presence of vehicle (0.1% DMSO) or PDE inhibitors. Data plotted are mean±S.E.M., n=3 separate determinations. The apparent IC_{50} values obtained using a four-parameter logistic equation model are summarised in section 3.1.1.2.

3.1.1.3 Separation of PDE activities by DEAE-cellulose chromatography

Anion exchange chromatography has been shown to effectively separate PDE1 from PDE4 activity, and from its endogenous activator, CaM [74, 230-232]. As the cAMP-hydrolysing activity in AtT20 cytosolic fraction was mainly contributed by PDE1 and PDE4 isozymes, DEAE cellulose chromatography was used to separate these isozymes for further analysis. Two distinct peaks of PDE activity were obtained when AtT20 cytosolic fraction was eluted with a linear sodium acetate gradient (0.05-1 M) on a DEAE cellulose column (Figure 6A). PDE activity of peak 1 (eluting at 0.1-0.2 M sodium acetate) was Ca^{2+}/CaM-stimulated while that of peak 2 (eluting at 0.4-0.5 M sodium acetate) was Ca^{2+}/CaM-independent and was largely inhibited by 10 μM rolipram. The PDE1 activity in peak 1 was then subjected to substrate saturation analysis (0.25-100μM cAMP) in the presence of 100 μM Ca^{2+} and 100 nM CaM (Figure 6B). Eadie-Hofstee plots from 5 out of 7 experiments suggested a single component of PDE1 activity with an apparent K_m of 0.54±0.06 μM and V_{max} of 2.4±1.1 nmol/min/mg protein (mean±S.E.M., n=5). In the remaining 2 experiments, the data best fitted to two-site model ($F<0.01$) with an additional high K_m component of apparent K_m = 20 and 30 μM, and V_{max} = 4.7 and 1.9 nmol/min/mg protein respectively. In sum, DEAE cellulose chromatographic separation of cAMP-hydrolysing PDE activities in AtT20 cytosolic fraction indicated the prominent presence of low K_m PDE1 and PDE4 activity.

Figure 6

DEAE-cellulose chromatographic separation of PDE activities in AtT20 cell cytosol

Figure 6: (A) Cytosolic fraction prepared from about 10^8 cells was used for each separation. 2 ml fractions were collected over a linear 0.05-1 M sodium acetate (pH 6.5) gradient. 20 µl of each fraction was assayed for PDE activity under 3 conditions: 100 µM Ca^{2+}+100 nM CaM (shaded diamonds), 0.5 mM EGTA (empty triangles) and 0.5 mM EGTA+10 µM rolipram (empty circles). The elution profile shown is representative of 7 similar runs. (B) Eadie-Hofstee plot of peak 1 PDE activity measured with 0.25-100 µM cAMP in the presence of 100 µM Ca^{2+} and 100 nM CaM. The mean K_m and V_{max} values from 7 separate experiments are summarised in section 3.1.1.3.

3.1.2 PDE activities in rat anterior pituitary

Both PDE1 and Ca^{2+}/CaM-independent PDE activities were also detected in rat adenohypophysis crude homogenates with 1 μM cAMP as substrate. The proportion and distribution of the two activities were similar to that found in AtT20 cells: all the PDE1 and about 60% of the remaining Ca^{2+}/CaM-independent PDE activity were recovered in the cytosolic fraction; with PDE1 constituting 71±3% and 81±2% of the total PDE activity in the whole homogenate and the cytosolic fraction respectively (mean±S.E.M, n=3). Of the remaining Ca^{2+}/CaM-independent PDE activity, 67±2% and 56±1% was inhibited by 10 μM rolipram in the whole homogenate and the cytosolic fraction respectively (mean±S.E.M., n=3), i.e. about 10-20% of the total adenohypophysial PDE activity was attributable to PDE4. In two experiments using the cytosolic fractions, the apparent IC_{50} values of rolipram were 0.14 and 0.39 μM.

3.1.2.1 Separation by DEAE-chromatography

When the rat anterior pituitary cytosolic fractions were subjected to DEAE-cellulose chromatography, a sharp peak of PDE activity (peak 1) eluting at 0.05-0.1 M sodium acetate, followed by a broad shoulder (0.1-0.4 M sodium acetate), which were stimulated at least 4- and 2.5-fold, respectively, by 100 μM Ca^{2+}/100 nM CaM were obtained (Figure 7A). Under these conditions, rolipram-sensitive PDE activity was not readily detected. Substrate saturation analysis of peak 1 with 0.25-100 μM cAMP and 100 μM Ca^{2+}/100 nM CaM indicated the presence of low and high K_m PDE1 activities (Figure 7B). The mean K_m values from 3 separate experiments determined by non-linear regression analysis using a two-site model were 0.36±0.11 and 53±12 μM ($p<0.05$, two-tailed unpaired t-test), with V_{max} values of 0.56±0.12

and 20±8 nmol/min/mg respectively (mean±S.E.M, n=3). These kinetic results indicated the presence of low K_m, low capacity as well as high K_m, high capacity PDE1 activities in rat adenohypophysis.

Figure 7

DEAE-cellulose chromatographic separation of PDE activities in rat anterior pituitary cytosol

Figure 7: (A) For each separation, cytosolic fraction prepared from the anterior pituitary glands of 4 Wistar rats was used. Fractions were collected and analysed as in AtT20 cells (Figure 6). The activity profile shown is representative of 3 similar runs. (B) Eadie-Hofstee plot of PDE1 activity in the sharp peak eluting at 0.05-0.1 M sodium acetate. PDE1 activity was assayed in the presence of 100 μM Ca^{2+} and 100 nM CaM with 0.25-100 μM cAMP as substrate. The K_m and V_{max} values were determined by non-linear regression using a 2-site model. In this experiment : K_m^1 = 0.18±0.21 μM and K_m^2 = 34±0.4 μM, with V_{max}^1 = 0.39±0.11 and V_{max}^2 = 7.4±0.2 nmol/min/mg respectively (estimated value±S.E.). The mean K_m and V_{max} values from 3 separate experiments are summarised in section 3.1.2.1.

3.2 RT-PCR analysis of PDE isozyme expression

As the biochemical and pharmacological analyses suggested that the main cAMP-hydrolysing activity in AtT20 cells and rat adenohypophysis was contributed by PDE1 and PDE4 isozymes, the expression of these isozymes was examined by RT-PCR analysis. A list of the primer pairs used and a summary of the results obtained is given in Table 4.

3.2.1 PDE1 mRNAs in AtT20 cells

Three distinct genes code for PDE1A, PDE1B and PDE1C (Figure 2). RT-PCR performed using total RNA extracted from AtT20 cells with gene-specific sense primers, pde1af, pde1bf and pde1cf, and a generic PDE1 antisense primer, pde1r, generated RT-PCR products of the expected size (Table 4 and Figure 8, lane a-c). Although the RT-PCR product corresponding to PDE1A (Figure 8, lane a) could not be subcloned after several attempts, that from the mouse anterior pituitary was subsequently sequenced and identified with mouse PDE1A (see section 3.2.3). The sequence obtained from the RT-PCR product corresponding to PDE1B (Figure 8, lane b) was identified as mouse PDE1B (Table 4). With respect to the identification of PDE1C isozymes, further RT-PCR was carried out to explore the expression of various splice variants, namely PDE1C1, PDE1C2 and PDE1C4/5 (Figure 2). A 2-kb PCR product was obtained using splice variant-specific primers, pde1c145f and pde1c45r (Figure 8, lane c), the nucleotide sequence of which matched the complete coding sequence of mouse PDE1C4/5 (Table 4). Thus the expression of PDE1B and PDE1C4/5 in AtT20 cells at the mRNA level were detected.

3.2.2 PDE4 mRNAs in AtT20 cells

The expression of PDE4 isotypes in AtT20 cells was analysed with a similar approach as for PDE1. Four genes are known to code for PDE4A, PDE4B, PDE4C and PDE4D, each of which is known to give rise to splice variants. As there was limited mouse PDE4 sequences available, the RT-PCR primers were designed based on the rat sequences in the GenBank™ database (Figure 2). RT-PCR analyses using gene- and splice variant-specific sense primers, pde4a5f and pde4d3f, with a generic PDE4-specific anti-sense primer, pde4r, have confirmed the expression of PDE4A5 and PDE4D3 in AtT20 cells (Figure 8, lane d and f, respectively, and Table 4). The expression of PDE4D3 was also demonstrated using the pde4d3f sense primer with a PDE4D-specific anti-sense primer, pde4dr (Figure 8, lane g and Table 4). RT-PCR product amplified using the PDE4B gene-specific primers, pde4bf and pde4br, was sequenced to match the core nucleotide and amino acid sequences of rat PDE4B (Figure 8, lane e and Table 4). No RT-PCR product was obtained using the PDE4C gene-specific primer, pde4cf and pde4cr (Table 4). Thus, RT-PCR analysis have confirmed the expression of multiple PDE4 isozymes in AtT20 cells, specifically mRNAs coding for PDE4A5, PDE4B and PDE4D3 were detected.

3.2.3 PDE1 and PDE4 mRNAs in rat and mouse anterior pituitaries

A similar approach of RT-PCR analysis as described for AtT20 cells was used to examine the expression of PDE1 and PDE4 isozymes in rat anterior pituitary. The expression of PDE1C (Figure 8, lane h, with primers pde1cf and pde1cr), PDE4B (Figure 8, lane i, with primers pde4bf and pde4br) and PDE4D3 (Figure 8, lane j, with primers pde4d3 and pde4dr) were detected and confirmed by sequencing the RT-PCR products (Table 4). As the PCR product corresponding to PDE1A could not be subcloned from the AtT20 cells, RT-PCR was performed using mouse anterior pituitary and with primers, pde1Af and pde1r, for verification (Figure 8, lane k). The RT-PCR product obtained was subcloned and sequenced to match mouse PDE1A (Table 4). RT-PCR product corresponding to PDE1C4/5 was also obtained with mouse anterior pituitary using primers, pde1c145f and pde1c45r (Figure 8, lane l).

In summary, the RT-PCR analysis indicated the expression of multiple isozymes of the PDE1 and PDE4 families in AtT20 cells as well as rat anterior pituitary gland. Specifically, evidence for the expression of low K_m PDE1 variants derived from the PDE1C gene and of the cAMP-specific PDE4s, PDE4B and PDE4D3, was found in both AtT20 cells and rat anterior pituitary gland. In addition, the expression of PDE1B and PDE4A5 was detected in AtT20 cells.

Table 4

RT-PCR Analysis of PDE mRNA expression

Analysis of PDE1 mRNA expression

Sense	Anti-sense	RT-PCR product (bp)	Results
pde1af	pde1r	971	RT-PCR products obtained with AtT20 (Fig. 8a) and mouse AP (Fig. 8k). Sequence of mouse AP RT-PCR product matched the conserved region of mouse PDE1A variants. No RT-PCR product detected with Rat AP.
pde1bf	pde1r	841	Sequence of AtT20 RT-PCR product (Fig. 8b) matched the conserved region mouse PDE1B variants. No RT-PCR product detected with Rat AP.
pde1cf	pde1r	590	RT-PCR product obtained with AtT20.
	pde1cr	494	RT-PCR products obtained with AtT20 and rat AP (Fig. 8h). Sequence of rat AP RT-PCR product matched the conserved region of rat PDE1C variants.
	pde1cr(2)	1154	RT-PCR product obtained with AtT20.
pde1c2f	pde1cr	1402	No RT-PCR product detected with rat AP.
	pde1cr(2)	2068	No RT-PCR product detected with AtT20 and rat AP.
pde1c145f	pde1cr(2)	1887	RT-PCR product obtained with AtT20.
	pde1c45r	1991	RT-PCR product obtained with AtT20 (Fig. 8c) and mouse AP (Fig.8l). Sequence of AtT20 RT-PCR product matched mouse PDE1C4/5 splice variants [L76946/7]. No RT-PCR product detected with rat AP.

Analysis of PDE4 mRNA expression

Sense	Anti-sense	RT-PCR product (bp)	Results
pde4a5f	pde4r	678	Sequence of AtT20 RT-PCR product (Fig. 8d) matched rat PDE4A5 [L27056]. No RT-PCR product detected with rat AP.
pde4bf	pde4br	339	Sequences of AtT20 and rat AP RT-PCR products (Fig. 8e and 8i respectively) matched conserved region of rat PDE4B variants.
pde4cf	pde4cr	453	No RT-PCR product detected with AtT20.
pde4d3f	pde4r	503	Sequence of AtT20 RT-PCR product (Fig. 8f) matched rat PDE4D3 [U09547].
	pde4dr	812	Sequences of AtT20 and rat AP RT-PCR products (Fig. 8g and 8j respectively) matched rat PDE4D3 [U09547].

Table 4: The primer pairs (see Table 3 for sequence information) used to detect the mRNAs of PDE1 and PDE4 isozymes/splice variants in AtT20 cells, rat and mouse anterior pituitary (AP), are tabulated together with the results obtained. The third column indicates the expected size of specific RT-PCR product. Where RT-PCR products were obtained, they were of the expected size and the respective lanes in Figure 8 are shown in brackets. The DNA sequences obtained by subsequent subcloning and sequencing were screened with both the GenBank™ non-redundant nucleotide and protein sequence databases (using blastn and blastx programs respectively). The top matches (93-100% identity with both databases) are shown and where applicable, with the GenBank™ accession number in square brackets.

Figure 8

PDE1 and PDE4 RT-PCR products

Figure 8: RT-PCR were performed using total RNA prepared from AtT20 cells, rat anterior pituitary and mouse anterior pituitary (as described in section 2.9). The primer pairs used to amplify the respective RT-PCR products are: a (pde1af + pde1r); b (pde1bf + pde1r); c (pde1c145f + pde1c45r); d (pde4a5f + pde4r); e (pde4bf + pde4br); f (pde4d3f + pde4r); g (pde4d3f + pde4dr); h (pde1cf + pde1cr); i (pde4bf + pde4br); j (pde4d3f + pde4dr); k (pde1af + pde1r); l (pde1c145f + pde1c45r). 5 µl of each RT-PCR reaction was analysed on a 0.8% agarose gel. All RT-PCR products shown above, except that of lane a and l, have been subsequently subcloned and sequenced to match the PDE isozyme shown below each lane. The sequence of the primers and the results obtained are tabulated in Table 3 and 4 respectively.

3.3 Regulation of PDE1 and PDE4 activities by cAMP-dependent phosphorylation

3.3.1 Studies in intact cells

3.3.1.1 Activation of PDE4 by cAMP-dependent pathway

Incubation of AtT20 cells with 100 nM CRF resulted in a transient stimulation of Ca^{2+}/CaM-independent PDE activity that peaked at around 1 min (Figure 9), which parallels the time-course of the cAMP response to CRF in these cells [180]. In AtT20 cells, the cAMP response to CRF is small and short-lived because of the rapid hydrolysis of cAMP by PDEs. Application of the PDE-resistant cAMP analogue, 8-(4-chlorophenylthio)-cAMP (CPT-cAMP), resulted in a dose-dependent (Figure 10A) and rapid (within 2 min) enhancement of Ca^{2+}/CaM-independent cAMP hydrolysis, which was entirely blocked by 10 μM rolipram, indicating the activation of PDE4 activity (Figure 10B). The effect of CPT-cAMP could be blocked by preincubation of the cells with 30 μM H-89, a protein kinase A (PKA)-selective inhibitor [233] (Figure 12A). This suggested that the activation of PDE4 activity in AtT20 cells by CPT-cAMP is mediated by PKA. Treatment of AtT20 cells with 50 nM calyculin A, a protein phosphatase1/2A inhibitor, was also found to activate PDE4 activity in a time-dependent manner (Figure 11). However, the activation of PDE4 activity by calyculin A, which was usually to a greater extent (more than 2-fold of control) compared to that by CPT-cAMP, was only partially inhibited by preincubation with 30 μM H-89 (Figure 12B). In order to examine the relationship between the effects of CPT-cAMP and calyculin A, time-courses of treatment with CPT-cAMP and calyculin A in isolation and in combination on PDE4 activity were compared (Figure 13). The results indicated significant additive effect of CPT-

cAMP and calyculin A on the activation of PDE4 activity at 5 min, when the effect of calyculin A alone was submaximal. As observed with calyculin A treatment alone, the activation of PDE4 activity by CPT-cAMP and calyculin A in combination was only partially inhibited by preincubation with 30 μM H-89 (Figure 14B).

Figure 9

Time course of CRF activation of Ca^{2+}/CaM-independent PDE activity

Figure 9: AtT20 cells growing on 24-well plates were incubated with 100 nM CRF or vehicle at 24°C for different durations. Total cell extracts prepared from each well by freeze-thawing in homogenisation buffer were assayed for PDE activity in the presence of 0.5 mM EGTA. Data are mean±S.E.M., n = 4. *, $p<0.05$ when compared with the control group in one-way ANOVA followed by Dunnett's two-tailed test.

Figure 10

CPT-cAMP activation of PDE4 activity in AtT20 cells

Figure 10: (A) Concentration dependence of CPT-cAMP activation of Ca^{2+}/CaM-independent PDE activity. AtT20 cells were incubated with 0, 0.1, 1 and 2 mM CPT-cAMP at 37 C for 10 min. Ca^{2+}/CaM-independent PDE activity of the cytosolic fraction was assayed in the presence of 0.5 mM EGTA and expressed as a percentage of control (incubation with vehicle) activity. Data are mean±S.E.M., n = 3. (B) Time-course of 1 mM CPT-cAMP. AtT20 cells were incubated with 1 mM CPT-cAMP at 37°C for 0, 2, 5 and 10 min and the cytosolic fractions were assayed for Ca^{2+}/CaM-independent PDE activity in the presence of 0.5 mM EGTA with (empty circle) or without (shaded circle) 10 μM rolipram. Data are mean±S.E.M., n = 3.

Figure 11

Time-course of Calyculin A activation of PDE4 activity in AtT20 cells

Figure 11: AtT20 cells were treated with 50 nM calyculin A for 0, 2, 5, 10, 30 and 60 min at 37 C. After incubation, the Ca^{2+}/CaM-independent PDE activity of the cytosolic fraction was assayed in the presence of 0.5 mM EGTA with (empty circles) or without (shaded circles) 10 μM rolipram. Data are mean±S.E.M., n=3.

Figure 12

Inhibition of CPT-cAMP and Calyculin A effect by H-89

Figure 12: AtT20 cells were preincubated with vehicle (0.3% DMSO) or 30 μM H-89 at 37 C for 10 min before the addition of (A) 1 mM CPT-cAMP or (B) 50 nM calyculin A for 10 min at 37 C. In (A) the Ca^{2+}/CaM-independent PDE activity of the cytosolic fraction was assayed in the presence of 0.5 mM EGTA and expressed as a percentage of the control (preincubated with vehicle and no CPT-cAMP treatment) PDE activity. In (B) the PDE4 activity was measured as the Ca^{2+}/CaM-independent PDE activity inhibited by 10 μM rolipram. Data are mean±S.E.M., n = 3. *, $p<0.05$ when compared with the control group in one-way ANOVA followed by Dunnett's two-tailed test.

Figure 13

Time course of differential regulation of PDE1 and PDE4 in AtT20 cells by CPT-cAMP and calyculin A

Figure 13: AtT20 cells were incubated with (A) 1 mM CPT-cAMP or (B) 50 nM calyculin A or (C) 1 mM CPT-cAMP and 50 nM calyculin A in combination at 37 C for 5, 10 and 30 min. Data are mean±S.E.M., n=4. *, $p<0.05$, when compared with respective control activity at time 0 in one-way ANOVA followed by Dunnett's two-tailed test.

Figure 14

H-89 inhibition of CPT-cAMP and calyculin A effects in AtT20 cells

Figure 14: AtT20 cells were preincubated with (empty triangles) or without (shaded triangles) 30 μM H-89 at 37 C for 30 min before treatment with 1 mM CPT-cAMP and 50 nM calyculin A in combination at 37 C for 5, 10 and 30 min. Cytosolic extracts from each time points were measured for (A) PDE1 and (B) PDE4 activities. Data are mean±S.E.M., n=3/group. *, $p<0.05$ when compared with control group at time 0. †, $p<0.05$ when compared with corresponding control group at each time point without H-89 treatment.

3.3.1.2 Inhibition of PDE1 by cAMP-dependent pathway

In contrast to PDE4, activation of cAMP-dependent pathway was found to inhibit PDE1 activity. While treatment with CRF produced no consistent alteration of PDE1 activity (data not shown), incubation with CPT-cAMP caused a significant reduction in PDE1 activity (Figure 3 and 13A). Treatment of AtT20 cells with 50 nM calyculin A alone also resulted in a consistent time-dependent inhibition of PDE1 activity (Figure 13B). Notably, treatment with CPT-cAMP and calyculin A in combination synergistically inhibited PDE1 activity at 5 and 10 min ($p<0.05$) and had additive effects at 30 min (Figure 13C). Importantly, treatment with H-89 markedly reduced the inhibition of PDE1 by CPT-cAMP and calyculin A at all time-points examined (Figure 14A).

3.3.1.3 Inhibition of CaM stimulation of PDE1 by cAMP-dependent pathway

The effect of CPT-cAMP and calyculin A on low K_m PDE1 in AtT20 cells was to reduce the maximal activation by Ca^{2+}/CaM (*control* = 0.86±0.03 and *CPT-cAMP+calyculin A* = 0.43±0.05 nmol/min/mg, mean±S.E.M., n=4, $p<0.01$, Student's t-test), and to increase the apparent EC_{50} for CaM by approximately 5-fold (*control* = 6.5±0.7 and *CPT-cAMP+calyculin A* = 36.6±6.9 nM, mean±S.E.M., n=4, $p<0.01$, Student's t-test)(Figure 15). The Hill-coefficient of activation by Ca^{2+}/CaM was unchanged (*control* = 1.2±0.1 and *CPT-cAMP+calyculin A* = 1.6±0.5, mean±S.E.M., n=4).

Figure 15

PDE1 stimulation by CaM was markedly reduced by CPT-cAMP and calyculin A treatment in intact AtT20 cells

Figure 15: Cytosolic fractions of AtT20 cells incubated with vehicles (shaded circles) or 1mM CPT-cAMP and 50 nM calyculin A in combination (empty circles) for 10 min at 37 C were assayed for PDE1 activity in the presence of 100 μM Ca^{2+} and exogenous CaM up to 1 μM. The endogenous CaM content estimated from standard curve using activator-deficient bovine brain PDE1 (Sigma P9529) with heat-inactivated (10 min in boiling water bath) cytosolic fractions was about 0.1 pmol/μg protein, equivalent to about 1-2 nM in the PDE assay reaction mix and was taken into account with the exogenously added CaM. Data shown are mean±S.E.M. of 4 separate cell extracts. The kinetic parameters determined by fitting these data to a 4-parameter logistic equation followed by non-linear regression are summarized in section 3.3.1.3.

3.3.1.4 Immunoprecipitation studies

To investigate further the contribution of specific PDE4 isozymes to the AtT20 cytosolic PDE4 activity, antibodies selective for PDE4A and PDE4D isozymes were used for immunoprecipitation studies. Of the control PDE4 activity, 57±3% (mean±S.E.M., n=6) and 24±1% (mean±S.E.M., n=3) of the activity were immunoprecipitated by a monoclonal PDE4D antibody, M3S1, and a polyclonal PDE4A antibody, AC55, respectively. Importantly, more than 60% of PDE4 activity activated by CPT-cAMP and/or calyculin A was immunoprecipitated by M3S1 (Figure 16), while a much smaller proportion (less than 15%) was immunoprecipitated by AC55 (Figure 17). This indicated that the PDE4 activity activated by CPT-cAMP and/or calyculin A was largely due to the activation of PDE4D isozyme.

Figure 16

Immunoprecipitation of PDE4 in AtT20 cells with M3S1

Figure 16: AtT20 cells were treated with vehicle (0.05% EtOH), 1 mM CPT-cAMP, 50 nM calyculin A, and 1 mM CPT-cAMP plus 50 nM calyculin A in combination, for 10 min at 37 C. Aliquots of cytosolic fractions from each treatment group were incubated with protein G-Sepharose preabsorbed with BSA (0.1%) or M3S1 (5 µl/reaction) at 4 C for 1.5 h (as detailed in section 2.13). After the incubation, the supernatant of the immunoprecipitation with BSA (shaded bar) and M3S1 (hatched bars) was measured for PDE4 activity. The immunoprecipitate (IP) from the BSA (empty bars, BSA-IP) and M3S1 (spotted bars, M3S1-IP) incubation were washed and resuspended to equal volume to the supernatant before measuring for PDE4 activity. Results from a representative experiment of three performed are shown. Data are mean±S.D. of PDE assay triplicates.

Figure 17

Immunoprecipitation of PDE4 in AtT20 cells with AC55

Figure 17: AtT20 cells were treated with vehicle (0.05% EtOH), 1 mM CPT-cAMP, 50 nM calyculin A, and 1 mM CPT-cAMP plus 50 nM calyculin A in combination, for 10 min at 37 C. Aliquots of cytosolic fractions from each treatment group were incubated with protein G-Sepharose preabsorbed with NRS (5 µl/reaction) or AC55 (5 µl/reaction) at 4 C for 1.5 h (as detailed in section 2.13). After the incubation, the supernatant of the immunoprecipitation with NRS (shaded bar) and AC55 (hatched bars) was measured for PDE4 activity. The immunoprecipitate (IP) from the NRS (empty bars, NRS-IP) and AC55 (spotted bars, AC55-IP) incubation were washed and resuspended to equal volume to the supernatant before measuring for PDE4 activity. Results from a representative experiment of three performed are shown. Data are mean±S.D. of PDE assay triplicates.

3.3.1.5 Immunoblot studies

M3S1 immunoprecipitates obtained from control and CPT-cAMP and/or calyculin A-treated AtT20 cells were subjected to immunoblot analysis using the polyclonal PDE4D antibody, Ab313, for detection. Two immunoreactive bands of apparent molecular weight of 93±0.2 and 101±0.2 kDa (mean±S.E.M., n=3) were detected in control AtT20 cytosolic fraction (Figure 18, lane 1). The 93 kDa band appeared to co-migrate with the recombinant rat PDE4D3 (Figure 18, rPDE4D3). Importantly, the migration of both bands in SDS-PAGE appeared to be retarded upon treatment with CPT-cAMP, resulting in two distinct bands of 97±0.1 and 103±0.2 kDa (mean±S.E.M., n=3)(Figure 18, lane 2), while calyculin A treatment (with or without CPT-cAMP) resulted in multiple immunoreactive bands ranging from 93-111 kDa (Figure 18, lane 3 and 4).

Figure 18

Phosphorylation-induced mobility shift of PDE4D splice variants in AtT20 cells

Figure 18: AtT20 cells were treated with vehicle (Lane 1), 1 mM CPT-cAMP (Lane 2), 50 nM calyculin A (Lane 3), or 100 mM CPT-cAMP + 50 nM calyculin A (Lane 4) for 10 min at 37 C. Immunoprecipitates obtained by incubating the respective cytosolic extracts (500 μg protein) with a PDE4D-specific monoclonal antibody, M3S1, were electrophoresed on 8% SDS-PAGE. 10 ng of purified recombinant rat PDE4D3 (rPDE4D3) was included for reference. Subsequent western blot was visualised using a PDE4D-specific polyclonal antibody, Ab313, and the ECL detection reagents (Amersham). Details of SDS-PAGE and western blotting methods are described in Section 2.14. The mean apparent molecular weights of the immunoreactive bands from 3 separate experiments and calculated from the standard curve were: rPDE4D3 (93±0.1 kDa), Lane 1 (93±0.2 and 101±0.2 kDa), Lane 2 (97±0.1 and 103±0.2 kDa), Lane 3 (93-107 kDa) and Lane 4 (100-111 kDa).

3.3.1.6 Regulation of recombinant PDE4D3 expressed in HEK293 cells

The effect of CPT-cAMP and calyculin A on PDE4 activity was also observed in HEK293 cells (Figure 19A), suggesting the presence of mechanisms mediating CPT-cAMP and calyculin A effects similar to that in AtT20 cells. In order to obtain further support for the regulation of AtT20 endogenous PDE4D3 by CPT-cAMP and calyculin A, and to demonstrate if these regulations are common to other cell type, a stably transfected HEK293 cell line (HEK293-4D3-VSV) was established to overexpress a recombinant VSV-tagged human PDE4D3. The expression of VSV-tagged HSPDE4D3 has been characterised in COS-1 cells and shown to be similar in characteristics to its native counterpart [109, 234]. There was a 8-fold increase in basal PDE4 activity of HEK293-4D3-VSV cells compared to that of normal HEK293 cells (*HEK293-4D3-VSV*: 1.0±0.1 nmol/min/mg versus *HEK293*: 0.13±0.1 nmol/min/mg, mean±S.E.M., n=5 and 7, respectively), which was also activated by CPT-cAMP and calyculin A (Figure 19B). The PDE4 activity activated by CPT-cAMP was completely immunoprecipitated by the monoclonal antibody, anti-VSV, which recognises the VSV epitope (Figure 20A). Notably, the PDE4 activity activated by calyculin A treatment was largely but not completely immunoprecipitated by anti-VSV (Figure 20B). Subsequent immunoblot analysis of the anti-VSV immunoprecipitates using the polyclonal PDE4D antibody, Ab313, for detection showed that the recombinant HSPDE4D3-VSV immunoprecipitated by anti-VSV from control HEK293-4D3 cells migrated just behind the rat recombinant 4D3 (Figure 21, rPDE4D3) with an apparent molecular weight of 97±0.4 kDa (mean±S.E.M., n=5) (Figure 21, lane 1), as reported [234]. An additional immunoreactive band of 102±0.6 kDa (mean±S.E.M., n=4) appeared upon treatment

with CPT-cAMP alone (Figure 21, lane 2), while treatment with calyculin A alone or in combination with CPT-cAMP resulted in multiple immunoreactive bands ranging from 99-110 kDa (Figure 21, lane 3 and 4).

Figure 19

Activation of PDE4 activity by CPT-cAMP and Calyculin A in normal and PDE4D3-VSV-transfected HEK293 cells

Figure 19: (A) Normal and (B) HSPDE4D3-VSV-transfected HEK293 cells were incubated with vehicle (0.05% ethanol), 1 mM CPT-cAMP, 50 nM calyculin A, or 1 mM CPT-cAMP and 50 nM calyculin A in combination, for 10 min at 37 C. PDE4 activity in the cytosolic fraction was assayed. Data are mean±S.E.M., n=4 for (A) and 3 for (B).

Figure 20

Immunoprecipitation of PDE4 activity in PDE4D3-VSV-transfected HEK293 cells with anti-VSV monoclonal antibody

Figure 20: HEK293 cells transfected with HSPDE4D3 tagged with VSV epitope were incubated with 1 mM CPT-cAMP (A) or 50 nM calyculin A (B) at 37 C for 10 min. Aliquots of cytosolic fractions from each treatment group were incubated with protein G-Sepharose preabsorbed with BSA (0.1%) or anti-VSV (5 µl/reaction) at 4 C for 1.5 h (as detailed in Section 2.13). After the incubation, the supernatant of the immunoprecipitation with BSA (shaded bar) and anti-VSV (hatched bars) was measured for PDE4 activity. The immunoprecipitate (IP) from the BSA (empty bars, BSA-IP) and anti-VSV (spotted bars, anti-VSV-IP) incubation were washed and resuspended to equal volume to the supernatant before PDE4 activity measurement. Data are mean±S.D. of PDE assay triplicates.

Figure 21

Phosphorylation-induced mobility shift of recombinant HSPDE4D3 in stably transfected HEK293 cells

Figure 21: HEK293 cells transfected with HSPDE4D3 tagged with VSV epitope were treated with vehicle (Lane 1), 1 mM CPT-cAMP (Lane 2), 50 nM calyculin A (Lane 3), or 1 mM CPT-cAMP + 50 nM calyculin A (Lane 4) for 10 min at 37 C. Immunoprecipitates obtained by incubating the respective cytosolic extracts (100 μg protein) with an anti-VSV monoclonal antibody were electrophoresed on 8% SDS-PAGE. 10 ng of purified recombinant rat PDE4D3 (rPDE4D3) was included for reference. Subsequent western blot was visualised using a PDE4D-specific polyclonal antibody, Ab313, and the ECL detection reagents (Amersham). The mean apparent molecular weights of the immunoreactive bands from 3-5 experiments and calculated from the standard curve were: rPDE4D3 (93±0.1 kDa, n=3), Lane 1 (97±0.4 kDa, n=5), Lane 2 (102±0.6 kDa, n=4), Lane 3 (99-110 kDa) and Lane 4 (99-110 kDa).

3.3.2 Studies in cell-free system

3.3.2.1 Differential regulation of PDE1 and PDE4 activity by PKA catalytic subunit

Incubation of AtT20 cytosolic fraction with PKA catalytic subunit under phosphorylating conditions resulted in changes of PDE1 and PDE4 activities similar to those induced by CPT-cAMP and calyculin A in intact cells (Figure 22). The enhancement of Ca^{2+}/CaM-independent PDE activity by PKA was fully inhibited by 10 μM rolipram, indicating selective activation of PDE4 (Figure 23). The specificity of PKA action was indicated by blockade of the activation of PDE4 by adding 10 μM H-89 (not shown) or 0.1 μM PKA inhibitor peptide (PKI) (Figure 23) in the phosphorylation reaction mixture.

The reduction of PDE1 activity by PKA catalytic subunit was further investigated using peak 1 fractions (that contain partially purified PDE1) obtained from the DEAE cellulose chromatographic separation (Figure 6A). As with the cytosolic fraction, incubation of peak 1 fractionates with sub-μM concentration of PKA catalytic subunit resulted in a time-dependent reduction of PDE1 activity (Figure 24A), which was blocked by PKI in the phosphorylation reaction (Figure 24B).

Figure 22

Differential regulation of PDE1 and Ca^{2+}/CaM-independent PDE activities by PKA catalytic subunit

Figure 22: Cytosolic fraction of AtT20 cells was incubated at 30°C with (shaded symbols) or without (empty symbols) 0.2 μM PKA catalytic subunit in a phosphorylation reaction mixture (30 mM Tris-HCl, pH 7.5, 20 mM $MgSO_4$, 0.5 mM ATP). Aliquots were taken from both reaction mixtures at 0, 5, 15 and 30 min for PDE assay. PDE1 activity (squares) was measured in the presence of 100 μM Ca^{2+}/100 nM CaM and 10 μM rolipram, while Ca^{2+}/CaM-independent PDE activity was assayed with 0.5 mM EGTA (diamonds). Data are mean±S.E.M., n = 3.

Figure 23

Selective activation of PDE4 activity by PKA catalytic subunit

Figure 23: Phosphorylation reactions were carried out with 0.2 μM recombinant PKA catalytic subunit in the presence (PKA+PKI) and absence (PKA) of 0.1 μM PKA inhibitor peptide (PKI) at 30 C for 15 min. Control reactions were incubated without added PKA and PKI. Ca^{2+}/CaM-independent PDE activity was measured in the presence of 0.5 mM EGTA with (empty bar) or without (shaded bar) 10 μM rolipram. Data are mean±S.E.M., n=3.

Figure 24

In vitro phosphorylation of PDE1 separated by DEAE chromatography

Figure 24: (A) AtT20 peak 1 fractionates were incubated with 0.8 μM PKA catalytic subunit in a phosphorylation buffer (30 mM Tris-HCl, pH 7.5, 20 mM $MgSO_4$, 0.5 mM ATP) at 30 C for 5, 15, 30 and 60 min. PDE1 activity was expressed as a percentage of control PDE1 activity at each time point incubated without added PKA catalytic subunit. Data are mean±S.E.M., n=3. (B) AtT20 peak 1 fractionate was incubated in a phosphorylation buffer (as (A)) without any added PKA and PKI (control), or with 1 μM PKI alone (PKI), or with 0.8 μM PKA catalytic subunit in the absence (PKA) or presence (PKA+PKI) of 1 μM PKI, for 1 hr at 30 C. Data are mean±S.E.M., n=3. *, $p<0.05$ when compared with control group.

3.3.2.2 Inhibition of CaM stimulation of PDE1 by PKA catalytic subunit

As observed in intact cells studies, the reduction of PDE1 activity by PKA catalytic subunit under phosphorylating conditions was due to a marked reduction to CaM stimulation (Figure 25). Notably, the effect was greater than that observed with CPT-cAMP and calyculin A in intact cells, resulting in a dramatic drop from about 8-fold stimulation in control to less than 1.5-fold in PKA-treated samples (Figure 25). The EC_{50} value for CaM stimulation was also increased more than 3-fold (*control* = 16.5±1.6 and *PKA* = 57.8±8.8 nM, mean±S.E.M., n=3, $P<0.05$, Student's t-test), while the Hill coefficients were not significantly different (*control* = 1.4±0.3 and *PKA*=1.7±0.4, mean±S.E.M., n=3).

Figure 25

PDE1 stimulation by CaM was markedly reduced by cell-free PKA phosphorylation

Figure 25: PDE1 activity of peak 1 fractionate incubated with (empty circles) or without (shaded circles) 0.8 μM PKA catalytic subunit for 1 hr at 30 C was assayed with 0 to 3 μM CaM in the presence of 100 μM Ca^{2+}. Endogenous CaM was negligible as PDE activity measured without added CaM in the presence of 100 μM Ca^{2+} or 0.5 mM EGTA were the same. Data shown are duplicate PDE1 activity determinations at each CaM concentration and are representative of 3 experiments using separate peak 1 fractionates. The mean EC_{50} and Hill-coefficient of CaM stimulation of the PDE1 activity obtained from these experiments are summarized in section 3.3.2.2.

4 DISCUSSION

4.1 Identification of PDE isozymes in rat adenohypophysis

The bulk (about 70%) of PDE activity in the adenohypophysis is Ca^{2+}/CaM-activated i.e. PDE1 ([199, 200] and the present study). Low K_m PDE1 (PDE1C) activity in rat anterior pituitary gland has not been previously reported. The expression of PDE1C mRNA in rat adenohypophysis could be demonstrated by RT-PCR analysis, and is in agreement with the cAMP saturation studies which clearly indicated the presence of both low- and high-K_m PDE1 activities. As primers specific for the high-K_m PDE1A and PDE1B isozymes (but based on the mouse sequence) did not generate any RT-PCR product, the identity of the high-K_m, high-capacity PDE1 in rat adenohypophysis remains to be clarified. Similar RT-PCR analysis with primers specific for various PDE4 isozymes indicated the expression of PDE4B and PDE4D3. As only primers specific for PDE4A5 and PDE4D3 splice variants were used, the expression of other splice variants from these two subfamilies could not be accessed in this study. Although the RT-PCR analysis was not exhaustive, it clearly indicated the potential for differential hydrolysis of cyclic nucleotides in anterior pituitary cells. As corticotrophs constitute only about 10% of the anterior pituitary cells, further analysis employing *in situ* hybridisation and/or immunocytochemistry will be required to clarify the expression of these PDE isotypes within the various types of hormone secreting cells in adenohypophysis.

4.2 Identification of PDE isozymes in AtT20 cells

Similarly to the adenohypophysis, AtT20 cells were found to express substantial PDE1C and PDE4 activities. This conclusion is based on the use of various previously reported family-selective PDE inhibitor compounds (see [31] for a review), the kinetic analysis of cAMP hydrolysis, the chromatographic separation of cAMP-hydrolysing PDE activities, the RT-PCR analysis and the regulation of the PDE activities by activation of cAMP pathway.

RT-PCR analysis clearly indicated the expression of multiple isozymes from the PDE1 and PDE4 families. Sequences obtained from the RT-PCR products confirmed the expression of PDE1B, PDE1C4/5, PDE4A5, PDE4B and PDE4D3 in AtT20 cells. The expression of these PDE isozymes could be correlated with the results obtained from the functional characterisation of cAMP hydrolysis in AtT20 cells. Pharmacological studies using PDE family-selective inhibitors, have indicated the predominance of PDE1 (inhibited by 8-MIX) and PDE4 (inhibited by rolipram) activity in AtT20 cells. This is further supported by the DEAE chromatographic separation of cAMP-hydrolysing PDE activity, which generated two major peaks that correspond to PDE1 (activated by Ca^{2+}/CaM) and PDE4 (rolipram-sensitive). It is of note that 30-40% of the cAMP-hydrolysing activity measured under Ca^{2+}-free conditions in AtT20 cytosol was resistant to rolipram. This PDE activity could be due to basal PDE1 activity and/or other PDEs, as it could be inhibited fully by the non-selective PDE inhibitor, IBMX. The previously published kinetic properties and inhibitor profiles of PDE1C isozymes, such as low K_m values for cAMP of about 1 μM and the relative resistance to vinpocetine inhibition when compared with the

PDE1A and PDE1B isozymes [49, 84], correspond well to the properties of the low K_m PDE1 activity found in AtT20 cells. The high K_m PDE1 activity apparent in two (out of five) substrate saturation experiments using peak 1 of DEAE chromatography could correspond to PDE1A and/or PDE1B. Immunoprecipitation with a PDE4D-specific monoclonal antibody, M3S1, indicated that more than half of the total PDE4 activity in AtT20 cytosolic fraction was attributable to PDE4D isozyme. The remaining PDE4 activity could be due to at least two other PDE4 isozymes, PDE4A5 and PDE4B, which were detected by RT-PCR. In fact, a polyclonal antibody specific for PDE4A, AC55, was found to immunoprecipitate about 24% of the total cytosolic PDE4 activity. Subsequent immunoblotting of the M3S1 immunoprecipitates using a polyclonal PDE4D antibody, Ab313, for detection identified two distinct immunoreactive bands of 93 and 101 kDa, the former co-migrated with the recombinant rat PDE4D3. Furthermore, M3S1 immunoprecipitates from CPT-cAMP-treated cells indicated a mobility shift of the 93 kDa band (to 97 kDa) which is characteristic of the effect of PKA phosphorylation on PDE4D3 [110]. Notably, PDE4D3 is the only PDE4 isozyme that has been shown to be rapidly activated by cAMP-dependent phosphorylation [110]. Thus the 93 kDa band in AtT20 cells corresponds to the mouse PDE4D3 isozyme. Although there is no doubt that the 101 kDa protein is a PDE4D variant (as it was detected by two different PDE4D selective antibodies), its exact identity is less certain as the few reports available currently indicated different apparent molecular weights for the corresponding PDE4D splice variants from human [109] and rat [220]. The observed size of human PDE4D4 and PDE4D5 were 119±2 kDa and 105±2 kDa respectively, while the rat PDE4D4 was observed to migrate at 105 kDa.

However, judging from the relative distance between the 93 kDa and 101 kDa under the conditions of SDS-PAGE used in this study, the 101 kDa is likely to correspond to the mouse PDE4D5. The recent availability of antibodies specific for each of these PDE4D splice variants [156] can be used to confirm the exact identity of these isozymes. Thus, the PDE isozyme that has been shown most conclusively to be expressed in AtT20 cells is PDE4D3, the expression of which was confirmed at both the level of mRNA (by RT-PCR) and protein (by immunoprecipitation and immunoblot). Taken together, these results indicate that multiple PDE1 and PDE4 isozymes may contribute to the degradation of cAMP in AtT20 cells, furthermore, the PDE1C and PDE4D isozymes are likely to be the major cAMP-hydrolysing PDEs in these cells.

4.3 Activation of PDE4 activity by cAMP-dependent phosphorylation in AtT20 cells

Ca^{2+}/CaM-independent PDE activity in AtT20 cells was transiently activated (peak at 1-2 min) upon exposure of the cells to CRF, which parallels the time course of cAMP levels in this system [180]. However, no consistent changes of PDE1 activity by CRF treatment could be detected. This may be due to the high intrinsic PDE activity in these cells, resulting in a relatively small (2-3 folds) and transient CRF-induced cAMP elevation in the absence of PDE inhibitors. According to a recent proposal [39], it would appear that AtT20 cells may fall into the Class II or 'high cycling' category of cells, where basal AC and PDE activities are high in order to keep the cAMP level below the threshold of PKA activation. Accordingly, treatment of AtT20 cells with a PDE-resistant cAMP analogue, CPT-cAMP, resulted in a rapid (as CRF treatment) but sustained activation of Ca^{2+}/CaM-independent PDE activity that was completely inhibited by 10 μM rolipram, indicated selective activation of PDE4 activity by the cAMP pathway. Importantly, the action of CPT-cAMP could be blocked by H-89, indicating the activation of PDE4 activity was mediated by PKA. The selective activation of PDE4 activity in AtT20 cytosolic fraction by PKA catalytic subunit was also demonstrated in a cell-free system. Collectively, these data suggest that cAMP-dependent phosphorylation activates PDE4 activity in AtT20 cells. This conclusion was strengthened by the immunoprecipitation and immunoblot studies using PDE4D-specific antibodies, M3S1 and Ab313, which showed that CPT-cAMP activated PDE4 activity could be largely attributed to the PDE4D subtype and demonstrated the characteristic PKA phosphorylation-induced mobility shift of PDE4D3 in AtT20 cells. Interestingly, the migration of the 101 kDa PDE4D band (pausibly PDE4D5) was also retarded upon CPT-cAMP treatment

(albeit to a lesser extent; a 2 kDa shift compared to that of 4-5 kDa shift in PDE4D3) to 103 kDa. Notably, investigators have been puzzled why only PDE4D3 was observed to be phosphorylated by PKA and not PDE4D4 [114], which similarly to PDE4D5, is a long PDE4D splice variant and contains the PKA phosphorylation site within the RRES motif which corresponds to Ser54 in PDE4D3 [57]. Thus, importantly, the results observed here with the 101 kDa PDE4D band in AtT20 cells suggested that a PDE4D splice variant longer than PDE4D3 could indeed be phosphorylated by PKA in intact cells. In line with this observation, evidence from a recent report has indicated that PDE4D5 is also regulated by PKA phosphorylation [234]. It is of note that several long PDE4 isozymes from the other subfamily, such as PDE4A4, PDE4C1 and PDE4B2, also contain this PKA phosphorylation motif and their regulation by PKA remains to be studied [55].

It is of note that PKA-dependent phosphorylation may not be the only route of activating PDE4 activity in AtT20 cells as the inhibition of protein phosphatases 1/2A by calyculin A also activated cytosolic PDE4 activity ([204] and the present study), but this effect was only partially blocked by H-89 and appeared to be additive with that of CPT-cAMP at submaximal stimulation. The activation of PDE4 activity/isozymes by other protein kinases is known [235-238]. Indeed, PDE4D3 and PDE4D5 have been recently reported to be directly phosphorylated by the extracellular receptor stimulated kinase, ERK2, at a site (Ser579 of HSPDE4D3) towards the C-terminal end of the catalytic domain [239]. Most interestingly, ERK2 phosphorylation resulted in an inhibition of the catalytic activity, indicating that PDE4D3 activity *in vivo* may be a balance between PKA and ERK2 phosphorylation

[239]. The immunoprecipitation studies with M3S1 have shown that PDE4D activity in AtT20 cells was also activated by calyculin A, indicating that the activation of PDE4D by phosphorylation may be reversed through protein phosphatase1/2A. The multiple immunoreactive bands in M3S1 immunoprecipitate obtained with calyculin A treatment could then represent different phosphorylation/hyperphosphorylation species by PKA (where several other potential phosphorylation sites are known to exist [57]) and/or other protein kinases such as ERK2 [239]. The physiological relevance of these phosphorylation events awaits further study. The activation of PDE4D3 activity by another protein phosphatase 1/2A inhibitor, okadaic acid, which potentiated thyroid-stimulating hormone (TSH) stimulation, has also been reported [240]. Importantly, the effect of calyculin A treatment indicated that the phosphorylation and activation of PDE4D3 in the cell is rapidly reversible. Furthermore, the regulation of recombinant HSPDE4D3 expressed in HEK293 cells by CPT-cAMP and calyculin A was similar to that observed with AtT20 endogenous PDE4D3. These results show that PDE4D3 activity may be regulated by multiple kinases in many cell types, and thus function as an important target for integrating signals from other signalling pathways.

4.4 Inhibition of PDE1 activity by cAMP-dependent phosphorylation in AtT20 cells

In contrast to PDE4, PDE1 activity was reduced upon activation of the cAMP cascade in AtT20 cells. Importantly, this is the first demonstration that PDE1 activity could be rapidly regulated in intact cells, pausibly by PKA phosphorylation. The biochemical properties of the PDE1 activity in AtT20 cells were very similar to those previously reported for PDE1C; such as low K_m for cAMP of about 1 μM and relatively resistant to vinpocetine inhibition [83, 84]. Moreover, the expression of PDE1C4/5 mRNA was confirmed by RT-PCR. The reduction of this low K_m PDE1 activity in AtT20 cells by CPT-cAMP/calyculin A could be blocked by H-89, indicating the predominant involvement of PKA. Furthermore, the effects of CPT-cAMP/calyculin A on PDE1 could be reproduced by incubating the cytosolic extracts or the DEAE-cellulose chromatography peak 1 fractions (containing the low K_m PDE1 activity) with PKA catalytic subunit under phosphorylating conditions. Importantly, the reduction of the PDE1 activity by PKA activation in AtT20 cells was more prominent in the presence of calyculin A, suggesting rapid reversal of PKA-mediated inhibition by protein phosphatase 1/2A in intact cells. Thus it is reasonable to propose that PKA activation leads to an inhibition of PDE1C activity and that this can be rapidly reversed by protein phosphatase 1 or 2A in intact cells.

The inhibition of PDE1 activity by PKA in intact cells as well as cell-free extracts was associated with a marked reduction of the maximal stimulation of cAMP hydrolysis by Ca^{2+}/CaM and an increase in the apparent EC_{50} for CaM. Interestingly, the former effect (a marked reduction in V_{max} of CaM-stimulated PDE1 activity) is in contrast to the reported *in vitro* effect of PKA phosphorylation of

PDE1A [69, 92] and of CaM kinase II phosphorylation of PDE1B [93], where the phosphorylated PDE1 activity could be restored to control levels (i.e. V_{max} restorable) by applying high concentrations of Ca^{2+}/CaM which were comparable to those used in the present study. It is of note that there are differences in the amino acid sequence between PDE1A, PDE1B, and PDE1C isozymes at the N-terminal region that contains the putative CaM binding and phosphorylation sites which may account for the different effects of phosphorylation on CaM stimulation of these isozymes (Figure 26). To date, two putative CaM binding sites have been identified in PDE1A using limited proteolysis, deletion mutation and synthetic peptide analyses, and both sites have been shown to be important for maximum stimulation by CaM [56, 64]. While the second (more recently identified) putative CaM binding site (that corresponds to amino-terminal residues 98-121 of PDE1A1 [56]) is highly conserved among members from the three PDE1 gene subfamilies, the first (initially identified) putative CaM binding site (residues 23-41 of PDE1A2 [64]) is highly divergent among PDE1 isozymes, particularly between the PDE1 subfamilies (Figure 26). It is tempting to speculate that variations in the first CaM binding region among PDE1 isozymes may account for the differences in their regulation by CaM and their sensitivities toward CaM stimulation. Indeed, a well established example is the observation that the PDE1A1 isozyme, which differs from PDE1A2 only in the first 18 amino-terminal residues that constitute part of the first putative CaM binding site, has an EC_{50} value for CaM 10-fold less than that of PDE1A2 [56, 67-69]. Amino-terminal sequence comparison among PDE1 isozymes reveals three notable features unique to PDE1C isozymes that are not found in the PDE1A and PDE1B isozymes identified so far (Figure 26). Firstly, there is a 9 amino acid insertion (residues 34-42

of MMPDE1C5) within the first putative CaM binding site. Secondly, there is a consensus PKA phosphorylation site, RLRS (residues 43-46 of MMPDE1C5) within the first putative CaM binding domain. Thirdly, in addition to having the two characterised PKA phosphorylation sites (Ser120 and Ser138 of PDE1A2 [92]) with slight differences, there is an additional PKA phosphorylation site, RRTS (residues 145-148 of MMPDE1C5), at a position right after the "Ser138 of PDE1A2" in PDE1C isozymes. With these unique features of PDE1C in mind, several possible explanations can be put forward to account for the difference in the effect PKA phosphorylation on the V_{max} of CaM-stimulated PDE1A activity [69, 92] and that of CaM-stimulated pausibly PDE1C activity in AtT20 cells reported here. The presence of additional PKA phosphorylation sites at both putative CaM binding sites of PDE1C may result in a complete blockage of CaM binding/stimulation upon PKA phosphorylation, whereas in PDE1A (and possibly PDE1B), the first CaM binding site may still be available for CaM stimulation and thus the observed restoration of V_{max} by increasing CaM concentrations. Alternatively, the 9-amino acid insert in PDE1C within the first putative CaM binding region may alter its property toward CaM stimulation, and in the extreme case of not binding CaM at all, there may be only one functional CaM binding site in PDE1C. On the other hand, the additional PKA phosphorylation at Ser148 of MMPDE1C5 may also result in a complete blockage of CaM binding/stimulation as opposed to PKA phosphorylation at Ser120 and Ser138 of PDE1A2 which decreases its sensitivity to CaM stimulation. Further experiments with recombinantly expressed and purified PDE1C should shed light on this issue. Nevertheless, there are many reports showing mutually exclusive actions of CaM and phosphorylation on CaM-regulated enzymes, where the phosphorylated

enzymes no longer bind to or stimulated by CaM, and vice versa, the CaM-bound enzymes are resistant to phosphorylation [241-244]. In fact, the *in vitro* studies with PDE1A and PDE1B did show that in the presence of excess Ca^{2+}/CaM, phosphorylation was blocked [69]. It is interesting to speculate that the regulation of CaM-stimulated enzymes governed by this antagonistic mechanism will not only depend on the immediate signals (PKA activity versus Ca^{2+}/CaM availability) but also on its pre-existing status (phosphorylated versus Ca^{2+}/CaM-bound).

Figure 26

4.5 Differential regulation of PDE1 and PDE4 by cAMP-dependent phosphorylation: Potential role in the control of ACTH secretion

The induction of cAMP synthesis by CRF produces an increase in intracellular free Ca^{2+}, which on the one hand triggers hormone secretion, and on the other provides a feedback inhibitory signal geared to turn off the cAMP signal and restore the resting state [162]. The Ca^{2+}-dependent reduction of the cellular response to cAMP-generating agonists (such as CRF) by glucocorticoid-induced proteins appears to act through the amplification of this Ca^{2+} feedback [162]. Processes mediating the Ca^{2+} feedback signal includes the inhibition of AC9 and the enhancement of Ca^{2+}-activated K^{+}-currents that repolarise the membrane potential [162]. The characterization of substantial Ca^{2+}/CaM-stimulated PDE activity in rat anterior pituitary and AtT20 cells presented in this thesis, indicated that PDE1 could serve as an additional target for the Ca^{2+} feedback on cAMP pathway. The PDE4D3 isozyme is likely to play a role in the rapid negative feedback of agonist-induced cAMP elevation in corticotrophs, which is supported by *in vitro* and *in vivo* pharmacological studies [202, 203]. In addition, the potential inactivation of PDE4D3 activity by ERK2 phosphorylation [239] may be involved in the potentiation of CRF action by the other ACTH secretagogues, such as AVP and AII, which signal through the IP3/PKC pathway [160], where ERK2 is a potential downstream target. It has been shown that activation of the cAMP cascade by CRF opposes the inhibitory actions of glucocorticoids by blocking glucocorticoid control of gene expression [182] and by reducing the transcription of the Type II glucocorticoid receptor gene [245]. The tendency of cAMP-dependent phosphorylation to shunt cAMP hydrolysis towards the Ca^{2+}/CaM-independent

PDE4 pathway is yet a further aspect of the CRF-induced cAMP signal to by-pass Ca^{2+}-feedback inhibition, and thus reduce the inhibitory action of glucocorticoids [162, 246].

CONCLUSION

This thesis has characterised the expression of multiple PDE isozymes from the PDE1 and PDE4 families in AtT20 cells and the adenohypophysis. In AtT20 cells, evidence were obtained for the expression of PDE1B, PDE1C4/5, PDE4A5, PDE4B, PDE4D3 at the mRNA level, while that of PDE4D3 and a 101 kDa PDE4D splice variant (pausibly PDE4D5) were detected at the protein level with two PDE4D-specific antibodies. Importantly, the PDE1C and PDE4D isozymes were shown to be rapidly and differentially regulated by PKA-dependent phosphorylation *in vitro* and in intact AtT20 cells. This differential regulation by PKA phosphorylation was also shown to be reversible by protein phosphatase 1/2A in intact cells. This regulatory mechanism may function as a switch between Ca^{2+}/CaM-dependent (through PDE1C) and Ca^{2+}/CaM-independent (through PDE4D) mode of cAMP hydrolysis, that contributes to the integration of signals from ACTH secretagogues and glucocorticoids in the regulation of ACTH secretion. In view of the wide occurrence and potential co-existence of these two PDE isozymes in other cell types, this regulatory mechanism may be important in other physiological events.

PERSPECTIVES

1. The unique properties of PDE1C among other PDEs, its high affinity for both cAMP and cGMP, a wide dynamic range of activity stimulated by Ca^{2+}/CaM, and the potential of regulation by PKA phosphorylation demonstrated in this thesis, strongly implicate an important role in the modulation and integration of multiple signal transduction pathways. The regulation by PKA phosphorylation should be verified with both the recombinant enzyme and the endogenous enzymes with PDE1C-specific antibodies. The PDE1C isozymes are expressed in many tissues [49], and the elucidation of its physiological role will prove to be fruitful and important to further our understanding of the interaction between Ca^{2+} and cyclic nucleotide signalling.

2. The cAMP-specific rolipram-sensitive PDE4s are perhaps the most widely expressed phosphodiesterases. Apart from having similar kinetic properties, the multiple isozymes/splice variants of the PDE4 family are distinct in terms of regulation, tissue/cell distribution, subcellular localisation, and function. Indeed, regulation by different phosphorylation events and the subcellular localisation of PDE4s are currently under intense investigation. The functional significance of these phenomenons may be in the contribution to the localisation of cAMP pool/signalling [146-148], and also to the assembly of signal transduction complex [28, 247]. Current observations indicate a complex relationship between PDE4 interaction with other proteins, phosphorylation, and inhibition by selective inhibitors, and the physiological relevance of these regulation is also under intense investigation. The understanding of the regulatory mechanisms

governing the functions of different isozymes is bound to have a major impact both in our understanding of the role of PDE4s in signal transduction and in the development of therapeutics.

3. It would be important to access the functional roles of PDE1 and PDE4 in the regulation of cAMP levels and ACTH secretion in corticotrophs. If PDE1 is a major target of glucocorticoid feedback inhibition of CRF-induced ACTH secretion, its inhibition by a selective inhibitor should markedly attenuate this feedback action. The awaited development of more selective cell permeable PDE1 inhibitor will facilitate such study with intact cells. Alternatively, anti-sense approach to block PDE1 expression could also be used.

4. In recent years, we have accumulated extensive knowledge concerning the regulation of the activity of the different PDE isozymes through indirect (cAMP levels) assessment or *in vitro* (broken cell) system measurement. PDE assay with cell extracts is carried out in an environment that can be very different compared to intracellular conditions. Important factors such as concentrations and spatiotemporal distribution of enzymes, substrates and regulators, within a cell will determine the physiological relevance of potential regulation. A revolution in the field would be the development of technology/technique to assess the activity of PDE in intact cells.

REFERENCES

1. Walsh, D.A., *et al.* (1991) *Motifs of protein phosphorylation and mechanisms of reversible covalent regulation.* Physiol Rev **71**(1): p. 285-304.

2. Schenk, P.W. and B.E. Snaar-Jagalska (1999) *Signal perception and transduction: the role of protein kinases.* Biochim Biophys Acta **1449**(1): p. 1-24.

3. Bouvier, M. (1990) *Cross-talk between second messengers.* Ann N Y Acad Sci **594**: p. 120-9.

4. Selbie, L.A. and S.J. Hill (1998) *G protein-coupled-receptor cross-talk: the fine-tuning of multiple receptor-signalling pathways.* Trends Pharmacol Sci **19**(3): p. 87-93.

5. Bygrave, F.L. and H.R. Roberts (1995) *Regulation of cellular calcium through signaling cross-talk involves an intricate interplay between the actions of receptors, G-proteins, and second messengers.* Faseb J **9**(13): p. 1297-303.

6. Cook, W., D. Lipkin, and R. Markham (1957) *The formation of cyclic dianhydrodiadenylic acid by the alkaline degradation of adenosine-5'-triphosphoric acid.* J Am Chem Soc **79**: p. 3607-3608.

7. Sutherland, E. and T. Rall (1958) *Fractionation and characterization of a cyclic adenine ribonucleotide formed by tissue particles.* Journal of Biological Chemistry **232**: p. 1077-1091.

8. Sutherland, E., T. Rall, and T. Menon (1962) *Adenyl cyclase. I. Distribution, preparation, and properties.* Journal of Biological Chemistry **237**: p. 1220-1227.

9. Butcher, R. and E. Sutherland (1962) *Adenosine 3'-5'-phosphate in biological materials. I. Purification and properties of cyclic 3'-5'-nucleotide phosphodiesterase and the use of this enzyme to characterize adenosine 3'-5'-phosphate in human urine.* Journal of Biological Chemistry **237**: p. 1244-1250.

10. Daniel, P.B., W.H. Walker, and J.F. Habener (1998) *Cyclic AMP signaling and gene regulation.* Annu Rev Nutr **18**: p. 353-83.

11. Wei, J.Y., *et al.* (1998) *Molecular and pharmacological analysis of cyclic nucleotide-gated channel function in the central nervous system [In Process Citation].* Prog Neurobiol **56**(1): p. 37-64.

12. Zagotta, W.N. and S.A. Siegelbaum (1996) *Structure and function of cyclic nucleotide-gated channels.* Annu Rev Neurosci **19**: p. 235-63.

13. Kawasaki, H., *et al.* (1998) *A family of cAMP-binding proteins that directly activate Rap1.* Science **282**(5397): p. 2275-9.

14. Derooij, J., *et al.* (1998) *Epac Is a Rap1 Guanine-Nucleotide-Exchange Factor Directly Activated By Cyclic-Amp.* Nature **396**(6710): p. 474-477.

15. Olsen, S.R. and M.D. Uhler (1991) *Isolation and characterization of cDNA clones for an inhibitor protein of cAMP-dependent protein kinase.* J Biol Chem **266**(17): p. 11158-62.

16. Van Patten, S.M., *et al.* (1991) *Molecular cloning of a rat testis form of the inhibitor protein of cAMP- dependent protein kinase.* Proc Natl Acad Sci U S A **88**(12): p. 5383-7.

17. Collins, S.P. and M.D. Uhler (1997) *Characterization of PKIgamma, a novel isoform of the protein kinase inhibitor of cAMP-dependent protein kinase.* J Biol Chem **272**(29): p. 18169-78.

18. Van Patten, S.M., *et al.* (1992) *The alpha- and beta-isoforms of the inhibitor protein of the 3',5'- cyclic adenosine monophosphate-dependent protein kinase: characteristics and tissue- and developmental-specific expression.* Mol Endocrinol **6**(12): p. 2114-22.

19. Van Patten, S.M., *et al.* (1997) *Specific testicular cellular localization and hormonal regulation of the PKIalpha and PKIbeta isoforms of the inhibitor protein of the cAMP- dependent protein kinase.* J Biol Chem **272**(32): p. 20021-9.

20. de Lecea, L., *et al.* (1998) *Endogenous protein kinase A inhibitor (PKIalpha) modulates synaptic activity.* J Neurosci Res **53**(3): p. 269-78.

21. Wen, W., S.S. Taylor, and J.L. Meinkoth (1995) *The expression and intracellular distribution of the heat-stable protein kinase inhibitor is cell cycle regulated.* J Biol Chem **270**(5): p. 2041-6.

22. Komalavilas, P. and T.M. Lincoln (1996) *Phosphorylation of the inositol 1,4,5-trisphosphate receptor. Cyclic GMP-dependent protein kinase mediates cAMP and cGMP dependent phosphorylation in the intact rat aorta.* J Biol Chem **271**(36): p. 21933-8.

23. Jiang, H., J.B. Shabb, and J.D. Corbin (1992) *Cross-activation: overriding cAMP/cGMP selectivities of protein kinases in tissues.* Biochem Cell Biol **70**(12): p. 1283-9.

24. Barford, D., A.K. Das, and M.P. Egloff (1998) *The structure and mechanism of protein phosphatases: insights into catalysis and regulation.* Annu Rev Biophys Biomol Struct **27**: p. 133-64.

25. Mochly-Rosen, D. (1995) *Localization of protein kinases by anchoring proteins: a theme in signal transduction.* Science **268**(5208): p. 247-51.

26. Tsunoda, S., J. Sierralta, and C.S. Zuker (1998) *Specificity in signaling pathways: assembly into multimolecular signaling complexes.* Curr Opin Genet Dev **8**(4): p. 419-22.

27. Ingber, D. (1998) *In search of cellular control: signal transduction in context [In Process Citation].* J Cell Biochem Suppl **31**: p. 232-7.

28. Schillace, R.V. and J.D. Scott (1999) *Organization of kinases, phosphatases, and receptor signaling complexes.* J Clin Invest **103**(6): p. 761-5.

29. Antoni, F.A., *et al.* (1998) *Calcium control of adenylyl cyclase: the calcineurin connection.* Adv Second Messenger Phosphoprotein Res **32**: p. 153-72.

30. Hurley, J.H. (1998) *The adenylyl and guanylyl cyclase superfamily.* Curr Opin Struct Biol **8**(6): p. 770-7.

31. Beavo, J.A. (1995) *Cyclic-nucleotide phosphodiesterases - functional implications of multiple isoforms.* Physiological reviews **75**: p. 725-748.

32. Manganiello, V.C., *et al.* (1995) *Diversity in cyclic nucleotide phosphodiesterase isoenzyme families.* Arch Biochem Biophys **322**(1): p. 1-13.

33. Nemoz, G., *et al.* (1995) *Activation of cyclic nucleotide phosphodiesterases in FRTL-5 thyroid cells expressing a constitutively active Gs alpha.* Mol Endocrinol **9**(10): p. 1279-87.

34. Lania, A., *et al.* (1998) *Constitutively active Gs alpha is associated with an increased phosphodiesterase activity in human growth hormone-secreting adenomas.* Journal of Clinical Endocrinology and Metabolism **83**(5): p. 1624-1628.

35. Rudolph, U., K. Spicher, and L. Birnbaumer (1996) *Adenylyl cyclase inhibition and altered G protein subunit expression and ADP-ribosylation patterns in tissues and cells from Gi2 alpha-/- mice.* Proc Natl Acad Sci U S A **93**(8): p. 3209-14.

36. Burton, K.A., *et al.* (1997) *Type-Ii Regulatory Subunits Are Not Required For the Anchoring-Dependent Modulation of Ca2+ Channel Activity By Camp-Dependent Protein-Kinase.* Proceedings of the National Academy of Sciences of the United States of America **94**(20): p. 11067-11072.

37. Peppel, K., *et al.* (1997) *G protein-coupled receptor kinase 3 (GRK3) gene disruption leads to loss of odorant receptor desensitization.* J Biol Chem **272**(41): p. 25425-8.

38. Conti, M., *et al.* (1995) *Recent progress in understanding the hormonal-regulation of phosphodiesterases.* Endocrine Reviews **16**: p. 370-389.

39. Houslay, M.D. (1998) *Adaptation in cyclic AMP signalling processes: a central role for cyclic AMP phosphodiesterases.* Semin Cell Dev Biol **9**(2): p. 161-7.

40. Fisher, D.A., *et al.* (1998) *Isolation and characterization of PDE8A, a novel human cAMP-specific phosphodiesterase.* Biochemical and Biophysical Research Communications **246**(3): p. 570-577.

41. Fisher, D.A., *et al.* (1998) *Isolation and characterization of PDE9A, a novel human cGMP-specific phosphodiesterase.* Journal of Biological Chemistry **273**(25): p. 15559-15564.

42. Soderling, S.H., S.J. Bayuga, and J.A. Beavo (1998) *Identification and characterization of a novel family of cyclic nucleotide phosphodiesterases.* Journal of Biological Chemistry **273**(25): p. 15553-15558.

43. Soderling, S.H., S.J. Bayuga, and J.A. Beavo (1998) *Cloning and characterization of a cAMP-specific cyclic nucleotide phosphodiesterase.* Proceedings of the National Academy of Sciences of the United States of America **95**(15): p. 8991-8996.

44. Fujishige, K., *et al.* (1999) *Cloning and characterization of a novel human phosphodiesterase that hydrolyzes both cAMP and cGMP (PDE10A) [In Process Citation].* J Biol Chem **274**(26): p. 18438-45.

45. Soderling, S.H., S.J. Bayuga, and J.A. Beavo (1999) *Isolation and characterization of a dual-substrate phosphodiesterase gene family: PDE10A [In Process Citation].* Proc Natl Acad Sci U S A **96**(12): p. 7071-6.

46. Beavo, J.A., M. Conti, and R.J. Heaslip (1994) *Multiple cyclic nucleotide phosphodiesterases.* Mol Pharmacol **46**(3): p. 399-405.

47. Engels, P., K. Fichtel, and H. Lubbert (1994) *Expression and regulation of human and rat phosphodiesterase type IV isogenes.* FEBS Lett **350**(2-3): p. 291-5.

48. Rybalkin, S.D., *et al.* (1997) *Calmodulin-stimulated cyclic nucleotide phosphodiesterase (PDE1C) is induced in human arterial smooth muscle cells of the synthetic, proliferative phenotype.* J Clin Invest **100**(10): p. 2611-21.

49. Yan, C., *et al.* (1996) *The calmodulin-dependent phosphodiesterase gene pde1c encodes several functionally different splice variants in a tissue-specific manner.* Journal Of Biological Chemistry **271**(41): p. 25699-25706.

50. Jin, S.L., J.V. Swinnen, and M. Conti (1992) *Characterization of the structure of a low Km, rolipram-sensitive cAMP phosphodiesterase. Mapping of the catalytic domain.* J Biol Chem **267**(26): p. 18929-39.

51. Pillai, R., S.F. Staub, and J. Colicelli (1994) *Mutational mapping of kinetic and pharmacological properties of a human cardiac cAMP phosphodiesterase.* J Biol Chem **269**(48): p. 30676-81.

52. Cheung, P.P., *et al.* (1996) *Human platelet cGI-PDE: expression in yeast and localization of the catalytic domain by deletion mutagenesis.* Blood **88**(4): p. 1321-9.

53. Charbonneau, H. (1990) *Structure-function relationships among cyclic nucleotide phosphodiesterases*, in *Cyclic Nucleotide Phosphodiesterases*, J. Beavo and M.D. Houslay, Editors. John Wiley, Chichester. p. 2267-2298.

54. Turko, I.V., S.H. Francis, and J.D. Corbin (1998) *Hydropathic analysis and mutagenesis of the catalytic domain of the cGMP-binding cGMP-specific phosphodiesterase (PDE5). cGMP versus cAMP substrate selectivity.* Biochemistry **37**(12): p. 4200-5.

55. Houslay, M.D., M. Sullivan, and G.B. Bolger (1998) *The multienzyme PDE4 cyclic adenosine monophosphate-specific phosphodiesterase family: intracellular targeting, regulation, and selective inhibition by compounds exerting anti-inflammatory and antidepressant actions.* Adv Pharmacol **44**: p. 225-342.

56. Sonnenburg, W.K., *et al.* (1995) *Identification of inhibitory and calmodulin-binding domains of the PDE1A1 and PDE1A2 calmodulin-stimulated cyclic nucleotide phosphodiesterases.* J Biol Chem **270**(52): p. 30989-1000.

57. Sette, C. and M. Conti (1996) *Phosphorylation and activation of a cAMP-specific phosphodiesterase by the cAMP-dependent protein kinase. Involvement of serine 54 in the enzyme activation.* J Biol Chem **271**(28): p. 16526-34.

58. DiSanto, M.E., K.B. Glaser, and R.J. Heaslip (1995) *Phospholipid regulation of a cyclic AMP-specific phosphodiesterase (PDE4) from U937 cells.* Cell Signal **7**(8): p. 827-35.

59. Nemoz, G., C. Sette, and M. Conti (1997) *Selective activation of rolipram-sensitive, cAMP-specific phosphodiesterase isoforms by phosphatidic acid.* Molecular Pharmacology **51**(2): p. 242-249.

60. Kincaid, R.L., I.E. Stith-Coleman, and M. Vaughan (1985) *Proteolytic activation of calmodulin-dependent cyclic nucleotide phosphodiesterase.* J Biol Chem **260**(15): p. 9009-15.

61. Kakkar, R., R.V. Raju, and R.K. Sharma (1998) *In vitro generation of an active calmodulin-independent phosphodiesterase from brain calmodulin-dependent phosphodiesterase (PDE1A2) by m-calpain.* Arch Biochem Biophys **358**(2): p. 320-8.

62. Kakiuchi, S. and R. Yamazaki (1970) *Calcium dependent phosphodiesterase activity and its activating factor (PAF) from brain studies on cyclic 3',5'-nucleotide phosphodiesterase (3).* Biochem Biophys Res Commun **41**(5): p. 1104-10.

63. Sonnenburg, W.K., *et al.* (1998) *Cyclic Nucleotide Regulation by Calmodulin*, in *Calmodulin and Signal Transduction*, L.J. Van Eldik and D.M. Watterson, Editors. Academic Press. p. 237-278.

64. Charbonneau, H., *et al.* (1991) *Evidence for domain organization within the 61-kDa calmodulin-dependent cyclic nucleotide phosphodiesterase from bovine brain.* Biochemistry **30**(32): p. 7931-40.

65. Sonnenburg, W.K., D. Seger, and J.A. Beavo (1993) *Molecular cloning of a cDNA encoding the "61-kDa" calmodulin-stimulated cyclic nucleotide phosphodiesterase. Tissue-specific expression of structurally related isoforms.* J Biol Chem **268**(1): p. 645-52.

66. Bentley, J.K., *et al.* (1992) *Molecular-Cloning of Cdna-Encoding a 63-Kda Calmodulin-Stimulated Phosphodiesterase From Bovine Brain.* Journal of Biological Chemistry **267**(26): p. 18676-18682.

67. Novack, J.P., *et al.* (1991) *Sequence comparison of the 63-, 61-, and 59-kDa calmodulin-dependent cyclic nucleotide phosphodiesterases.* Biochemistry **30**(32): p. 7940-7.

68. Hansen, R.S. and J.A. Beavo (1986) *Differential Recognition of Calmodulin-Enzyme Complexes By a Conformation-Specific Anticalmodulin Monoclonal-Antibody.* Journal of Biological Chemistry **261**(31): p. 4636-4645.

69. Sharma, R.K. (1991) *Phosphorylation and characterization of bovine heart calmodulin- dependent phosphodiesterase.* Biochemistry **30**(24): p. 5963-8.

70. Cheung, W.Y., *et al.* (1975) *Protein activator of cyclic 3':5'-nucleotide phosphodiesterase of bovine or rat brain also activates its adenylate cyclase.* Biochem Biophys Res Commun **66**(3): p. 1055-62.

71. Kakiuchi, S., *et al.* (1975) *Multiple cyclic nucleotide phosphodiesterase activities from rat tissues and occurrence of a calcium-plus-magnesium-ion-dependent phosphodiesterase and its protein activator.* Biochem J **146**(1): p. 109-20.

72. Wang, J.H., *et al.* (1975) *Bovine heart protein activator of cyclic nucleotide phosphodiesterase.* Adv Cyclic Nucleotide Res **5**: p. 179-94.

73. Rossi, P., *et al.* (1988) *Testis-specific calmodulin-dependent phosphodiesterase. A distinct high affinity cAMP isoenzyme immunologically related to brain calmodulin- dependent cGMP phosphodiesterase.* J Biol Chem **263**(30): p. 15521-7.

74. Torphy, T.J. and L.B. Cieslinski (1990) *Characterization and selective inhibition of cyclic nucleotide phosphodiesterase isozymes in canine tracheal smooth muscle.* Mol Pharmacol **37**(2): p. 206-14.

75. Epstein, P.M., *et al.* (1987) *Ontogenetic changes in adenylate cyclase, cyclic AMP phosphodiesterase and calmodulin in chick ventricular myocardium.* Biochem J **243**(2): p. 525-31.

76. Geremia, R., *et al.* (1984) *Characterization of a calmodulin-dependent high-affinity cyclic AMP and cyclic GMP phosphodiesterase from male mouse germ cells.* Biochem J **217**(3): p. 693-700.

77. Purvis, K., A. Olsen, and V. Hansson (1981) *Calmodulin-dependent cyclic nucleotide phosphodiesterases in the immature rat testis.* J Biol Chem **256**(22): p. 11434-41.

78. Smoake, J.A., L.S. Johnson, and G.T. Peake (1981) *Calmodulin-dependent high-affinity cyclic AMP phosphodiesterase in liver membranes.* Arch Biochem Biophys **206**(2): p. 331-5.

79. Reeves, M.L., B.K. Leigh, and P.J. England (1987) *The identification of a new cyclic nucleotide phosphodiesterase activity in human and guinea-pig cardiac ventricle. Implications for the mechanism of action of selective phosphodiesterase inhibitors.* Biochem J **241**(2): p. 535-41.

80. Weishaar, R.E., *et al.* (1986) *Multiple molecular forms of cyclic nucleotide phosphodiesterase in cardiac and smooth muscle and in platelets. Isolation, characterization, and effects of various reference phosphodiesterase inhibitors and cardiotonic agents.* Biochem Pharmacol **35**(5): p. 787-800.

81. Vandermeers, A., *et al.* (1983) *Purification and kinetic properties of two soluble forms of calmodulin- dependent cyclic nucleotide phosphodiesterase from rat pancreas.* Biochem J **211**(2): p. 341-7.

82. Borisy, F.F., *et al.* (1992) *Calcium/calmodulin-activated phosphodiesterase expressed in olfactory receptor neurons.* J Neurosci **12**(3): p. 915-23.

83. Yan, C., *et al.* (1995) *Molecular-cloning and characterization of a calmodulin-dependent phosphodiesterase enriched in olfactory sensory neurons.*

Proceedings of the National Academy of Sciences of the U.S.A. **92**(21): p. 9677-9681.

84. Loughney, K., *et al.* (1996) *Isolation and characterization of cdnas corresponding to 2 human calcium, calmodulin-regulated, 3',5'-cyclic nucleotide phosphodiesterases.* Journal Of Biological Chemistry **271**(2): p. 796-806.

85. Erneux, C., *et al.* (1985) *A mechanism in the control of intracellular cAMP level: the activation of a calmodulin-sensitive phosphodiesterase by a rise of intracellular free calcium.* Mol Cell Endocrinol **43**(2-3): p. 123-34.

86. Law, P.Y. and H.H. Loh (1993) *delta-Opioid receptor activates cAMP phosphodiesterase activities in neuroblastoma x glioma NG108-15 hybrid cells.* Mol Pharmacol **43**(5): p. 684-93.

87. Smoake, J.A., *et al.* (1995) *Calmodulin-dependent cyclic AMP phosphodiesterase in liver plasma membranes: stimulated by insulin.* Arch Biochem Biophys **323**(2): p. 223-32.

88. Jiang, X., *et al.* (1996) *Inhibition of calmodulin-dependent phosphodiesterase induces apoptosis in human leukemic cells.* Proc Natl Acad Sci U S A **93**(20): p. 11236-41.

89. Spence, S., *et al.* (1995) *Induction of Ca2+/calmodulin-stimulated cyclic AMP phosphodiesterase (PDE1) activity in Chinese hamster ovary cells (CHO) by phorbol 12- myristate 13-acetate and by the selective overexpression of protein kinase C isoforms.* Biochem J **310**(Pt 3): p. 975-82.

90. Hurwitz, R.L., *et al.* (1990) *Induction of a calcium/calmodulin-dependent phosphodiesterase during phytohemagglutinin-stimulated lymphocyte mitogenesis.* J Biol Chem **265**(15): p. 8901-7.

91. Caniglia, C., *et al.* (1997) *Calmodulin-dependent cyclic nucleotide phosphodiesterase in adult and developing chick spinal cord.* J Neurosci Res **49**(2): p. 186-96.

92. Florio, V.A., *et al.* (1994) *Phosphorylation of the 61-kda calmodulin-stimulated cyclic-nucleotide phosphodiesterase at serine-120 reduces its affinity for calmodulin.* Biochemistry **33**(30): p. 8948-8954.

93. Sharma, R.K. and J.H. Wang (1986) *Calmodulin and Ca2+-dependent phosphorylation and dephosphorylation of 63-kDa subunit-containing bovine brain calmodulin-stimulated cyclic nucleotide phosphodiesterase isozyme.* J Biol Chem **261**(3): p. 1322-8.

94. Spence, S., *et al.* (1997) *Receptor-Mediated Stimulation of Lipid Signaling Pathways in Cho Cells Elicits the Rapid Transient Induction of the Pde1b*

Isoform of Ca2+/Calmodulin-Stimulated Camp-Phosphodiesterase. Biochemical Journal **321**(pt.1)): p. 157-163.

95. Byers, D., R.L. Davis, and J.A. Kiger, Jr. (1981) *Defect in cyclic AMP phosphodiesterase due to the dunce mutation of learning in Drosophila melanogaster.* Nature **289**(5793): p. 79-81.

96. Davis, R.L., *et al.* (1989) *Cloning and characterization of mammalian homologs of the Drosophila dunce+ gene.* Proc Natl Acad Sci U S A **86**(10): p. 3604-8.

97. Henkel-Tigges, J. and R.L. Davis (1990) *Rat homologs of the Drosophila dunce gene code for cyclic AMP phosphodiesterases sensitive to rolipram and RO 20-1724.* Mol Pharmacol **37**(1): p. 7-10.

98. Dauwalder, B. and R.L. Davis (1995) *Conditional rescue of the dunce learning/memory and female fertility defects with Drosophila or rat transgenes.* J Neurosci **15**(5 Pt 1): p. 3490-9.

99. Giembycz, M.A. (1996) *Phosphodiesterase-4 and tolerance to beta(2)-adrenoceptor agonists in asthma.* Trends In Pharmacological Sciences **17**(9): p. 331-336.

100. Hulley, P., *et al.* (1995) *Inhibitors of type IV phosphodiesterases reduce the toxicity of MPTP in substantia nigra neurons in vivo.* Eur J Neurosci **7**(12): p. 2431-40.

101. Drees, M., R. Zimmermann, and G. Eisenbrand (1993) *3',5'-Cyclic nucleotide phosphodiesterase in tumor cells as potential target for tumor growth inhibition.* Cancer Res **53**(13): p. 3058-61.

102. Tsafriri, A., *et al.* (1996) *Oocyte maturation involves compartmentalization and opposing changes of cAMP levels in follicular somatic and germ cells: studies using selective phosphodiesterase inhibitors.* Dev Biol **178**(2): p. 393-402.

103. Fisch, J.D., B. Behr, and M. Conti (1998) *Enhancement of motility and acrosome reaction in human spermatozoa: differential activation by type-specific phosphodiesterase inhibitors.* Hum Reprod **13**(5): p. 1248-54.

104. Torphy, T.J. (1998) *Phosphodiesterase isozymes: molecular targets for novel antiasthma agents.* Am J Respir Crit Care Med **157**(2): p. 351-70.

105. Colicelli, J., *et al.* (1989) *Isolation and characterization of a mammalian gene encoding a high- affinity cAMP phosphodiesterase.* Proc Natl Acad Sci U S A **86**(10): p. 3599-603.

106. Swinnen, J.V., D.R. Joseph, and M. Conti (1989) *Molecular cloning of rat homologues of the Drosophila melanogaster dunce cAMP phosphodiesterase: evidence for a family of genes.* Proc Natl Acad Sci U S A **86**(14): p. 5325-9.

107. Milatovich, A., *et al.* (1994) *Chromosome localizations of genes for five cAMP-specific phosphodiesterases in man and mouse.* Somat Cell Mol Genet **20**(2): p. 75-86.

108. Bolger, G., *et al.* (1993) *A family of human phosphodiesterases homologous to the dunce learning and memory gene product of Drosophila melanogaster are potential targets for antidepressant drugs.* Mol Cell Biol **13**(10): p. 6558-71.

109. Bolger, G.B., *et al.* (1997) *Characterization of five different proteins produced by alternatively spliced mRNAs from the human cAMP-specific phosphodiesterase PDE4D gene.* Biochem J **328**(Pt 2): p. 539-48.

110. Sette, C., E. Vicini, and M. Conti (1994) *The ratPDE3/IVd phosphodiesterase gene codes for multiple proteins differentially activated by cAMP-dependent protein kinase [published erratum appears in J Biol Chem 1994 Aug 12;269(32):20806].* J Biol Chem **269**(28): p. 18271-4.

111. Alvarez, R., *et al.* (1995) *Activation and selective inhibition of a cyclic AMP-specific phosphodiesterase, PDE-4D3.* Mol Pharmacol **48**(4): p. 616-22.

112. Torphy, T.J., *et al.* (1995) *Salbutamol up-regulates PDE4 activity and induces a heterologous desensitization of U937 cells to prostaglandin E2. Implications for the therapeutic use of beta-adrenoceptor agoniststst.* J Biol Chem **270**(40): p. 23598-604.

113. Torphy, T.J., H.L. Zhou, and L.B. Cieslinski (1992) *Stimulation of beta adrenoceptors in a human monocyte cell line (U937) up-regulates cyclic AMP-specific phosphodiesterase activity.* J Pharmacol Exp Ther **263**(3): p. 1195-205.

114. Jin, S.L., *et al.* (1998) *Subcellular localization of rolipram-sensitive, cAMP-specific phosphodiesterases. Differential targeting and activation of the splicing variants derived from the PDE4D gene.* J Biol Chem **273**(31): p. 19672-8.

115. Dohlman, H.G., *et al.* (1991) *Model systems for the study of seven-transmembrane-segment receptors.* Annu Rev Biochem **60**: p. 653-88.

116. Hausdorff, W.P., M.G. Caron, and R.J. Lefkowitz (1990) *Turning off the signal: desensitization of beta-adrenergic receptor function [published erratum appears in FASEB J 1990 Sep;4(12):3049].* Faseb J **4**(11): p. 2881-9.

117. Verhoeven, G., J. Cailleau, and P. de Moor (1981) *Hormonal control of phosphodiesterase activity in cultured rat Sertoli cells.* Mol Cell Endocrinol **24**(1): p. 41-51.

118. Tanner, L.I., *et al.* (1986) *Identification of the phosphodiesterase regulated by muscarinic cholinergic receptors of 1321N1 human astrocytoma cells.* Mol Pharmacol **29**(5): p. 455-60.

119. Swinnen, J.V., K.E. Tsikalas, and M. Conti (1991) *Properties and hormonal regulation of two structurally related cAMP phosphodiesterases from the rat Sertoli cell.* J Biol Chem **266**(27): p. 18370-7.

120. Gettys, T.W., *et al.* (1987) *Short-term feedback regulation of cAMP by accelerated degradation in rat tissues.* J Biol Chem **262**(1): p. 333-9.

121. Conti, M., *et al.* (1986) *Effect of phosphodiesterase inhibitors on Sertoli cell refractoriness: reversal of the impaired androgen aromatization.* Endocrinology **118**(3): p. 901-8.

122. Ashby, B. (1989) *Model of prostaglandin-regulated cyclic AMP metabolism in intact platelets: examination of time-dependent effects on adenylate cyclase and phosphodiesterase activities.* Mol Pharmacol **36**(6): p. 866-73.

123. Beltman, J., W.K. Sonnenburg, and J.A. Beavo (1993) *The role of protein phosphorylation in the regulation of cyclic nucleotide phosphodiesterases.* Mol Cell Biochem **127-128**: p. 239-53.

124. Onali, P., *et al.* (1981) *Regulation by a beta-adrenergic receptor of a Ca2+-independent adenosine 3',5'-(cyclic)monophosphate phosphodiesterase in C6 glioma cells.* Biochim Biophys Acta **675**(2): p. 285-92.

125. Pawlson, L.G., *et al.* (1974) *Effects of epinephrine, adrenocorticotrophic hormone, and theophylline on adenosine 3', 5'-monophosphate phosphodiesterase activity in fat cells.* Proc Natl Acad Sci U S A **71**(5): p. 1639-42.

126. Bourne, H.R., G.M. Tomkins, and S. Dion (1973) *Regulation of phosphodiesterase synthesis: requirement for cyclic adenosine monophosphate-dependent protein kinase.* Science **181**(103): p. 952-4.

127. Ball, E.H., P.K. Seth, and B.D. Sanwal (1980) *Regulatory mechanisms involved in the control of cyclic adenosine 3':5'- monophosphate phosphodiesterases in myoblasts.* J Biol Chem **255**(7): p. 2962-8.

128. Loten, E.G., *et al.* (1978) *Stimulation of a low Km phosphodiesterase from liver by insulin and glucagon.* J Biol Chem **253**(3): p. 746-57.

129. Heyworth, C.M., A.V. Wallace, and M.D. Houslay (1983) *Insulin and glucagon regulate the activation of two distinct membrane- bound cyclic AMP phosphodiesterases in hepatocytes.* Biochem J **214**(1): p. 99-110.

130. Takeda, S., *et al.* (1991) *High activity of low-Michaelis-Menten constant 3', 5'-cyclic adenosine monophosphate-phosphodiesterase isozymes in renal inner medulla of mice with hereditary nephrogenic diabetes insipidus.* Endocrinology **129**(1): p. 287-94.

131. Homma, S., *et al.* (1991) *Role of cAMP-phosphodiesterase isozymes in pathogenesis of murine nephrogenic diabetes insipidus.* Am J Physiol **261**(2 Pt 2): p. F345-53.

132. Dousa, T.P. and H. Valtin (1974) *Cellular action of antidiuretic hormone in mice with inherited vasopressin-resistant urinary concentrating defects.* J Clin Invest **54**(3): p. 753-62.

133. Jackson, B.A., *et al.* (1980) *Cellular action of vasopressin in medullary tubules of mice with hereditary nephrogenic diabetes insipidus.* J Clin Invest **66**(1): p. 110-22.

134. Valtin, H., *et al.* (1990) *Causes of the urinary concentrating defect in mice with nephrogenic diabetes insipidus.* Physiol Bohemoslov **39**(1): p. 103-11.

135. Miot, F., J.E. Dumont, and C. Erneux (1983) *The involvement of a calmodulin-dependent phosphodiesterase in the negative control of carbamylcholine on cyclic AMP levels in dog thyroid slices.* FEBS Lett **151**(2): p. 273-6.

136. Buxton, I.L. and L.L. Brunton (1985) *Action of the cardiac alpha 1-adrenergic receptor. Activation of cyclic AMP degradation.* J Biol Chem **260**(11): p. 6733-7.

137. MacFarland, R.T., B.D. Zelus, and J.A. Beavo (1991) *High concentrations of a cGMP-stimulated phosphodiesterase mediate ANP- induced decreases in cAMP and steroidogenesis in adrenal glomerulosa cells.* J Biol Chem **266**(1): p. 136-42.

138. Lee, M.A., R.E. West, Jr., and J. Moss (1988) *Atrial natriuretic factor reduces cyclic adenosine monophosphate content of human fibroblasts by enhancing phosphodiesterase activity.* J Clin Invest **82**(2): p. 388-93.

139. Whalin, M.E., *et al.* (1991) *Phosphodiesterase II, the cGMP-activatable cyclic nucleotide phosphodiesterase, regulates cyclic AMP metabolism in PC12 cells.* Mol Pharmacol **39**(6): p. 711-7.

140. Maurice, D.H. and R.J. Haslam (1990) *Molecular basis of the synergistic inhibition of platelet function by nitrovasodilators and activators of adenylate*

cyclase: inhibition of cyclic AMP breakdown by cyclic GMP. Mol Pharmacol **37**(5): p. 671-81.

141. Grant, P.G. and R.W. Colman (1984) *Purification and characterization of a human platelet cyclic nucleotide phosphodiesterase.* Biochemistry **23**(8): p. 1801-7.

142. Adams, S.R., *et al.* (1991) *Fluorescence ratio imaging of cyclic AMP in single cells.* Nature **349**(6311): p. 694-7.

143. Tank, D.W., *et al.* (1988) *Spatially resolved calcium dynamics of mammalian Purkinje cells in cerebellar slice.* Science **242**(4879): p. 773-7.

144. Tsien, R.W. and R.Y. Tsien (1990) *Calcium channels, stores, and oscillations.* Annu Rev Cell Biol **6**: p. 715-60.

145. Bacskai, B.J., *et al.* (1993) *Spatially resolved dynamics of cAMP and protein kinase A subunits in Aplysia sensory neurons.* Science **260**(5105): p. 222-6.

146. Hempel, C.M., *et al.* (1996) *Spatio-temporal dynamics of cyclic AMP signals in an intact neural circuitm [see comments].* Nature **384**(6605): p. 166-9.

147. Jurevicius, J. and R. Fischmeister (1996) *cAMP compartmentation is responsible for a local activation of cardiac Ca2+ channels by beta-adrenergic agonists.* Proc Natl Acad Sci U S A **93**(1): p. 295-9.

148. Houslay, M.D. and G. Milligan (1997) *Tailoring cAMP-signalling responses through isoform multiplicity.* Trends Biochem Sci **22**(6): p. 217-24.

149. Thompson, W.J. and M.M. Appleman (1971) *Multiple cyclic nucleotide phosphodiesterase activities from rat brain.* Biochemistry **10**(2): p. 311-6.

150. Taira, M., *et al.* (1993) *Molecular cloning of the rat adipocyte hormone-sensitive cyclic GMP- inhibited cyclic nucleotide phosphodiesterase.* J Biol Chem **268**(25): p. 18573-9.

151. Shakur, Y., *et al.* (1995) *Identification and characterization of the type-IVA cyclic AMP-specific phosphodiesterase RD1 as a membrane-bound protein expressed in cerebellum.* Biochem J **306**(Pt 3): p. 801-9.

152. Scotland, G. and M.D. Houslay (1995) *Chimeric constructs show that the unique N-terminal domain of the cyclic AMP phosphodiesterase RD1 (RNPDE4A1A; rPDE-IVA1) can confer membrane association upon the normally cytosolic protein chloramphenicol acetyltransferase.* Biochem J **308**(Pt 2): p. 673-81.

153. Bloom, T.J. and J.A. Beavo (1996) *Identification and tissue-specific expression of PDE7 phosphodiesterase splice variants.* Proc Natl Acad Sci U S A **93**(24): p. 14188-92.

154. O'Connell, J.C., *et al.* (1996) *The SH3 domain of Src tyrosyl protein kinase interacts with the N- terminal splice region of the PDE4A cAMP-specific phosphodiesterase RPDE-6 (RNPDE4A5).* Biochem J **318**(Pt 1): p. 255-61.

155. McPhee, I., *et al.* (1999) *Association with the SRC family tyrosyl kinase LYN triggers a conformational change in the catalytic region of human cAMP-specific phosphodiesterase HSPDE4A4B. Consequences for rolipram inhibition.* J Biol Chem **274**(17): p. 11796-810.

156. Yarwood, S.J., *et al.* (1999) *The RACK1 signaling scaffold protein selectively interacts with the cAMP-specific phosphodiesterase PDE4D5 isoform.* J Biol Chem **274**(21): p. 14909-17.

157. METHODS: A Companion to Methods in Enzymology, ed. M. Conti. Vol. 14 (1). 1998, Academic Press. 1-104.

158. Owens, M.J. and C.B. Nemeroff (1991) *Physiology and pharmacology of corticotropin-releasing factor.* Pharmacol Rev **43**(4): p. 425-73.

159. Antoni, F.A. (1993) *Vasopressinergic control of pituitary adrenocorticotropin secretion comes of age.* Front Neuroendocrinol **14**(2): p. 76-122.

160. Abou-Samra, A.B., *et al.* (1987) *Mechanisms of action of CRF and other regulators of ACTH release in pituitary corticotrophs.* Ann N Y Acad Sci **512**: p. 67-84.

161. Axelrod, J. and T.D. Reisine (1984) *Stress hormones: their interaction and regulation.* Science **224**(4648): p. 452-9.

162. Antoni, F.A. (1996) *Mortyn Jones Memorial Lecture--1995. Calcium checks cyclic AMP-- corticosteroid feedback in adenohypophysial corticotrophs.* J Neuroendocrinol **8**(9): p. 659-72.

163. Abou-Samra, A.B., K.J. Catt, and G. Aguilera (1987) *Calcium-dependent control of corticotropin release in rat anterior pituitary cell cultures.* Endocrinology **121**(3): p. 965-71.

164. Calmodulin and Signal Transduction, ed. L.J. Van Eldik and D.M. Watterson. 1998, Academic Press.

165. Guerineau, N., *et al.* (1991) *Spontaneous and corticotropin-releasing factor-induced cytosolic calcium transients in corticotrophs.* Endocrinology **129**(1): p. 409-20.

166. Antoni, F.A., *et al.* (1992) *Glucocorticoid inhibition of stimulus-evoked adrenocorticotrophin release caused by suppression of intracellular calcium signals.* J Endocrinol **133**(2): p. R13-6.

167. Dayanithi, G. and F.A. Antoni (1989) *Rapid as well as delayed inhibitory effects of glucocorticoid hormones on pituitary adrenocorticotropic hormone release are mediated by type II glucocorticoid receptors and require newly synthesized messenger ribonucleic acid as well as protein.* Endocrinology **125**(1): p. 308-13.

168. Abou-Samra, A.B., *et al.* (1987) *Phorbol 12-myristate 13-acetate and vasopressin potentiate the effect of corticotropin-releasing factor on cyclic AMP production in rat anterior pituitary cells. Mechanisms of action.* J Biol Chem **262**(3): p. 1129-36.

169. Shipston, M.J. and F.A. Antoni (1991) *Early glucocorticoid feedback in anterior pituitary corticotrophs: differential inhibition of hormone release induced by vasopressin and corticotrophin-releasing factor in vitro.* J Endocrinol **129**(2): p. 261-8.

170. von Bardeleben, U., *et al.* (1985) *Combined administration of human corticotropin-releasing factor and lysine vasopressin induces cortisol escape from dexamethasone suppression in healthy subjects.* Life Sci **37**(17): p. 1613-8.

171. Abou-Samra, A.B., K.J. Catt, and G. Aguilera (1986) *Involvement of protein kinase C in the regulation of adrenocorticotropin release from rat anterior pituitary cells.* Endocrinology **118**(1): p. 212-7.

172. Bilezikjian, L.M., A.L. Blount, and W.W. Vale (1987) *The cellular actions of vasopressin on corticotrophs of the anterior pituitary: resistance to glucocorticoid action.* Mol Endocrinol **1**(7): p. 451-8.

173. Schwartz, J., S. Gibson, and A. White (1991) *Regulation of ACTH secretory pathways in cultured pituitary cells.* Am J Physiol **261**(5 Pt 1): p. C793-8.

174. Reisine, T. (1989) *Phorbol esters and corticotropin releasing factor stimulate calcium influx in the anterior pituitary tumor cell line, AtT-20, through different intracellular sites of action.* J Pharmacol Exp Ther **248**(3): p. 984-90.

175. Oki, Y., *et al.* (1991) *Effects of intracellular Ca2+ depletion and glucocorticoid on stimulated adrenocorticotropin release by rat anterior pituitary cells in a microperifusion system.* Endocrinology **128**(3): p. 1589-96.

176. Shipston, M.J. and F.A. Antoni (1992) *Inactivation of early glucocorticoid feedback by corticotropin- releasing factor in vitro.* Endocrinology **130**(4): p. 2213-8.

177. Sabol, S.L. (1980) *Storage and secretion of beta-endorphin and related peptides by mouse pituitary tumor cells: regulation by glucocorticoids.* Arch Biochem Biophys **203**(1): p. 37-48.

178. Clark, T.P. and R.J. Kemppainen (1994) *Glucocorticoid negative feedback in sheep corticotrophs: a comparison with AtT-20 corticotroph tumor cells.* Am J Physiol **267**(2 Pt 2): p. R463-9.

179. Woods, M.D., *et al.* (1992) *Pituitary corticotrope tumor (AtT20) cells as a model system for the study of early inhibition by glucocorticoids.* Endocrinology **131**(6): p. 2873-80.

180. Shipston, M.J., J.S. Kelly, and F.A. Antoni (1996) *Glucocorticoids block protein kinase A inhibition of calcium-activated potassium channels.* J Biol Chem **271**(16): p. 9197-200.

181. Antoni, F.A., *et al.* (1995) *Calcineurin feedback inhibition of agonist-evoked cAMP formation.* J Biol Chem **270**(47): p. 28055-61.

182. Shipston, M.J. and F.A. Antoni (1992) *Early glucocorticoid induction of calmodulin and its suppression by corticotropin-releasing factor in pituitary corticotrope tumor (AtT20) cells.* Biochem Biophys Res Commun **189**(3): p. 1382-8.

183. Bilezikjian, L.M., *et al.* (1991) *Activin-A inhibits proopiomelanocortin messenger RNA accumulation and adrenocorticotropin secretion of AtT20 cells.* Mol Endocrinol **5**(10): p. 1389-95.

184. Boutillier, A.L., *et al.* (1994) *Pituitary adenyl cyclase-activating peptide: a hypophysiotropic factor that stimulates proopiomelanocortin gene transcription, and proopiomelanocortin-derived peptide secretion in corticotropic cells.* Neuroendocrinology **60**(5): p. 493-502.

185. Farrell, W.E., *et al.* (1993) *Glucocorticoid inhibition of ACTH peptides: small cell lung cancer cell lines are more resistant than pituitary corticotroph adenoma cells.* J Mol Endocrinol **10**(1): p. 25-32.

186. Gannon, M.N., *et al.* (1990) *Pharmacological characterization of type II glucocorticoid binding sites in AtT20 pituitary cell culture.* J Steroid Biochem **36**(1-2): p. 83-8.

187. Litvin, Y., *et al.* (1984) *Hormonal activation of the cAMP-dependent protein kinases in AtT20 cells. Preferential activation of protein kinase I by corticotropin releasing factor, isoproterenol, and forskolin.* J Biol Chem **259**(16): p. 10296-302.

188. Litvin, Y., *et al.* (1986) *Somatostatin inhibits corticotropin-releasing factor-stimulated adrenocorticotropin release, adenylate cyclase, and activation of*

adenosine 3',5'-monophosphate-dependent protein kinase isoenzymes in AtT20 cells. Endocrinology **119**(2): p. 737-45.

189. Ray, D.W., S.G. Ren, and S. Melmed (1996) *Leukemia inhibitory factor (LIF) stimulates proopiomelanocortin (POMC) expression in a corticotroph cell line. Role of STAT pathway.* J Clin Invest **97**(8): p. 1852-9.

190. Sheppard, K.E., J.L. Roberts, and M. Blum (1991) *Adrenocorticotropin-releasing factor down-regulates glucocorticoid receptor expression in mouse corticotrope tumor cells via an adenylate cyclase-dependent mechanism.* Endocrinology **129**(2): p. 663-70.

191. Van, L.P., D.H. Spengler, and F. Holsboer (1990) *Glucocorticoid repression of 3',5'-cyclic-adenosine monophosphate- dependent human corticotropin-releasing-hormone gene promoter activity in a transfected mouse anterior pituitary cell line.* Endocrinology **127**(3): p. 1412-8.

192. Westendorf, J.M. and A. Schonbrunn (1985) *Peptide specificity for stimulation of corticotropin secretion: activation of overlapping pathways by the vasoactive intestinal peptide family and corticotropin-releasing factor.* Endocrinology **116**(6): p. 2528-35.

193. Reisine, T.D., *et al.* (1983) *Activation of beta 2-adrenergic receptors on mouse anterior pituitary tumor cells increases cyclic adenosine 3':5'-monophosphate synthesis and adrenocorticotropin release.* J Neurosci **3**(4): p. 725-32.

194. Adler, M., *et al.* (1983) *Action potentials and membrane ion channels in clonal anterior pituitary cells.* Proceedings of the National Academy of Sciences of the U.S.A. **80**: p. 2086-2090.

195. Castellino, F., *et al.* (1992) *Glucocorticoid stabilization of actin filaments: A possible mechanism for inhibition of corticotropin release.* Proceedings of the National Academy of Sciences of the U.S.A. **89**: p. 3775-3779.

196. Luini, A., *et al.* (1985) *Hormone secretagogues increase cytosolic calcium by increasing cAMP in corticotropin secreting cells.* Proceedings of the National Academy of Sciences of the U.S.A. **82**: p. 8034-8038.

197. Guild, S., *et al.* (1986) *Forskolin enhances basal and potassium-evoked hormone release from normal and malignant pituitary tissue: the role of calcium.* Endocrinology **118**: p. 268.

198. Berridge, M.J. (1997) *The AM and FM of calcium signalling.* Nature **386**(6627): p. 759-760.

199. Azhar, S. and K.M.J. Menon (1977) *Cyclic nucleotide phosphodiesterases from rat anterior pituitary.* Eur J Biochem **73**(1): p. 73-82.

200. Nagasaka, A., S. Ohkubo, and H. Hidaka (1983) *3':5'-cyclic-nucleotide phosphodiesterase in the bovine pituitary gland.* Biochim Biophys Acta **755**(3): p. 481-7.

201. Rendon, M.C., *et al.* (1988) *Somatostatin stimulates phosphodiesterase in rat anterior pituitary and brain, and GH4C1 cells.* Second Messengers Phosphoproteins **12**(2-3): p. 75-81.

202. Koch, B. and B. Lutz-Bucher (1989) *Indirect relationship between vasopressin-induced secretion of ACTH and cyclic nucleotides in cultured anterior pituitary cells [published erratum appears in Eur J Pharmacol 1990 Jul 17;182(3):616].* Eur J Pharmacol **159**(1): p. 53-60.

203. Kumari, M., *et al.* (1997) *Stimulation of the hypothalamo-pituitary-adrenal axis in the rat by three selective type-4 phosphodiesterase inhibitors: In vitro and in vivo studies.* British Journal Of Pharmacology **121**(3): p. 459-468.

204. Antaraki, A., K. Ang, and F. Antoni (1997) *Involvement of calyculin A inhibitable protein phosphatases in the cyclic AMP signal transduction pathway of mouse corticotroph tumour (AtT20) cells.* British Journal of Pharmacology **121**: p. 991-999.

205. Slice, L.W. and S.S. Taylor (1989) *Expression of the catalytic subunit of cAMP-dependent protein kinase in Escherichia coli.* J Biol Chem **264**(35): p. 20940-6.

206. Bradford, M.M. (1976) *A rapid and sensitive method for the quantitation of microgram quantities of protein utilizing the principle of protein-dye binding.* Anal Biochem **72**: p. 248-54.

207. Schilling, R.J., D.R. Morgan, and B.F. Kilpatrick (1994) *A high-throughput assay for cyclic nucleotide phosphodiesterases.* Anal Biochem **216**(1): p. 154-8.

208. Krishna, G., B. Weiss, and B.B. Brodie (1968) *A simple, sensitive method for the assay of adenyl cyclase.* J Pharmacol Exp Ther **163**(2): p. 379-85.

209. Bauer, A.C. and U. Schwabe (1980) *An improved assay of cyclic 3',5'-nucleotide phosphodiesterases with QAE-Sephadex columns.* Naunyn Schmiedebergs Arch Pharmacol **311**(2): p. 193-8.

210. Chan, P.S. and M.C. Lin (1974) *Isolation of cyclic AMP by inorganic salt coprecipitation.* Methods Enzymol **38**: p. 38-41.

211. Shimizu, H., J.W. Daly, and C.R. Creveling (1969) *A radioisotopic method for measuring the formation of adenosine 3',5'- cyclic monophosphate in incubated slices of brain.* J Neurochem **16**(12): p. 1609-19.

212. Sinha, A.K. and R.W. Colman (1981) *A new method for separating cyclic AMP from 5'-AMP with application to the assay for cyclic AMP phosphodiesterase.* Anal Biochem **113**(2): p. 239-45.

213. Poch, G. (1971) *Assay of phosphodiesterase with radioactively labeled cyclic 3',5'-AMP as substrate.* Naunyn Schmiedebergs Arch Pharmacol **268**(3): p. 272-99.

214. Carter, J.G., S.J. Berger, and O.H. Lowry (1979) *The measurement of cyclic GMP and cyclic AMP phosphodiesterases.* Anal Biochem **100**(2): p. 244-53.

215. Brownstein, M.J., J.D. Carpten, and J.R. Smith (1996) *Modulation of non-templated nucleotide addition by Taq DNA polymerase: primer modifications that facilitate genotyping.* Biotechniques **20**(6): p. 1004-6, 1008-10.

216. Hofmann, F., P.J. Bechtel, and E.G. Krebs (1977) *Concentrations of cyclic AMP-dependent protein kinase subunits in various tissues.* J Biol Chem **252**(4): p. 1441-7.

217. Walsh, D.A. and D.B. Glass (1991) *Utilization of the inhibitor protein of adenosine cyclic monophosphate- dependent protein kinase, and peptides derived from it, as tools to study adenosine cyclic monophosphate-mediated cellular processes.* Methods Enzymol **201**: p. 304-16.

218. Huston, E., *et al.* (1996) *The human cyclic AMP-specific phosphodiesterase PDE-46 (HSPDE4A4B) expressed in transfected COS7 cells occurs as both particulate and cytosolic species that exhibit distinct kinetics of inhibition by the antidepressant rolipram.* J Biol Chem **271**(49): p. 31334-44.

219. Kreis, T.E. and H.F. Lodish (1986) *Oligomerization is essential for transport of vesicular stomatitis viral glycoprotein to the cell surface.* Cell **46**(6): p. 929-37.

220. Iona, S., *et al.* (1998) *Characterization of the rolipram-sensitive, cyclic AMP-specific phosphodiesterases: identification and differential expression of immunologically distinct forms in the rat brain.* Mol Pharmacol **53**(1): p. 23-32.

221. Salanova, M., S.L. Jin, and M. Conti, eds. *Heterologous expression and purification of recombinant rolipram-sensitive cyclic AMP-specific phosphodiesterase*. METHODS: A Companion to Methods in Enzymology, ed. M. Conti. Vol. 14 (1). 1998, Acedemic Press. 55-64.

222. Laemmli, U.K. (1970) *Cleavage of structural proteins during the assembly of the head of bacteriophage T4.* Nature **227**(259): p. 680-5.

223. Sambrook, J., E.F. Fritsch, and T. Maniatis (1989) *Molecular Cloning: A Laboratory Manual*. Second edition ed: Cold Spring Harbor Laboratory Press

224. Yamaki, M., *et al.* (1992) *Cyclic 3',5'-nucleotide diesterases in dynamics of cAMP and cGMP in rat collecting duct cells.* Am J Physiol **262**(6 Pt 2): p. F957-64.

225. Wells, J.N., J.E. Garst, and G.L. Kramer (1981) *Inhibition of separated forms of cyclic nucleotide phosphodiesterase from pig coronary arteries by 1,3-disubstituted and 1,3,8- trisubstituted xanthines.* J Med Chem **24**(8): p. 954-8.

226. Ahn, H.S., *et al.* (1995) *Cyclic nucleotide phosphodiesterase isozymes in rat mesangial cells.* Eur J Pharmacol **289**(1): p. 49-57.

227. Gantner, F., *et al.* (1997) *In vitro differentiation of human monocytes to macrophages: change of PDE profile and its relationship to suppression of tumour necrosis factor-alpha release by PDE inhibitors.* Br J Pharmacol **121**(2): p. 221-31.

228. Hagiwara, M., T. Endo, and H. Hidaka (1984) *Effects of vinpocetine on cyclic nucleotide metabolism in vascular smooth muscle.* Biochem Pharmacol **33**(3): p. 453-7.

229. Saeki, T. and I. Saito (1993) *Isolation of cyclic nucleotide phosphodiesterase isozymes from pig aorta.* Biochem Pharmacol **46**(5): p. 833-9.

230. Geremia, R., *et al.* (1982) *Cyclic nucleotide phosphodiesterase in developing rat testis. Identification of somatic and germ-cell forms.* Mol Cell Endocrinol **28**(1): p. 37-53.

231. Lin, Y.M., Y.P. Liu, and W.Y. Cheung (1974) *Cyclic 3':5'-nucleotide phosphodiesterase. Purification, characterization, and active form of the protein activator from bovine brain.* J Biol Chem **249**(15): p. 4943-54.

232. Barnette, M.S., *et al.* (1993) *Initial biochemical and functional characterization of cyclic nucleotide phosphodiesterase isozymes in canine colonic smooth muscle.* J Pharmacol Exp Ther **264**(2): p. 801-12.

233. Chijiwa, T., *et al.* (1990) *Inhibition of forskolin-induced neurite outgrowth and protein phosphorylation by a newly synthesized selective inhibitor of cyclic AMP-dependent protein kinase, N-[2-(p-bromocinnamylamino)ethyl]-5-isoquinolinesulfonamide (H-89), of PC12D pheochromocytoma cells.* J Biol Chem **265**(9): p. 5267-72.

234. Hoffmann, R., *et al.* (1998) *cAMP-specific phosphodiesterase HSPDE4D3 mutants which mimic activation and changes in rolipram inhibition triggered by protein kinase A phosphorylation of Ser-54: generation of a molecular model.* Biochem J **333**(Pt 1): p. 139-49.

235. Tetsuka, T., *et al.* (1995) *Activation of protein kinase C stimulates cAMP phosphodiesterase in rat renal collecting tubule.* Am J Physiol **268**(5 Pt 2): p. F808-14.

236. Lenhard, J.M., *et al.* (1996) *Phosphorylation of a camp-specific phosphodiesterase (hspde4b2b) by mitogen-activated protein-kinase.* Biochemical Journal **316**(Pt3): p. 751-758.

237. Michie, A.M., *et al.* (1996) *Rapid regulation of PDE-2 and PDE-4 cyclic AMP phosphodiesterase activity following ligation of the T cell antigen receptor on thymocytes: analysis using the selective inhibitors erythro-9-(2- hydroxy-3-nonyl)-adenine (EHNA) and rolipram.* Cell Signal **8**(2): p. 97-110.

238. MacKenzie, S.J., *et al.* (1998) *Stimulation of p70S6 kinase via a growth hormone-controlled phosphatidylinositol 3-kinase pathway leads to the activation of a PDE4A cyclic AMP-specific phosphodiesterase in 3T3-F442A preadipocytes.* Proc Natl Acad Sci U S A **95**(7): p. 3549-54.

239. Hoffmann, R., *et al.* (1999) *The MAP kinase ERK2 inhibits the cyclic AMP-specific phosphodiesterase HSPDE4D3 by phosphorylating it at ser579 [In Process Citation].* Embo J **18**(4): p. 893-903.

240. Sette, C., S. Iona, and M. Conti (1994) *The short-term activation of a rolipram-sensitive, cAMP-specific phosphodiesterase by thyroid-stimulating hormone in thyroid FRTL-5 cells is mediated by a cAMP-dependent phosphorylation.* J Biol Chem **269**(12): p. 9245-52.

241. Wayman, G.A., H. Tokumitsu, and T.R. Soderling (1997) *Inhibitory cross-talk by cAMP kinase on the calmodulin-dependent protein kinase cascade.* J Biol Chem **272**(26): p. 16073-6.

242. Graff, J.M., *et al.* (1989) *Phosphorylation-regulated calmodulin binding to a prominent cellular substrate for protein kinase C.* J Biol Chem **264**(36): p. 21818-23.

243. Cox, D.E. and R.D. Edstrom (1982) *Inhibition by calmodulin of the cAMP-dependent protein kinase activation of phosphorylase kinase.* J Biol Chem **257**(21): p. 12728-33.

244. Hashimoto, Y., M.M. King, and T.R. Soderling (1988) *Regulatory interactions of calmodulin-binding proteins: phosphorylation of calcineurin by autophosphorylated Ca2+/calmodulin-dependent protein kinase II.* Proc Natl Acad Sci U S A **85**(18): p. 7001-5.

245. Sheppard, K.E., J.L. Roberts, and M. Blum (1991) *Adrenocorticotropin-releasing factor down-regulates glucocorticoid receptor expression in mouse corticotrope tumor cells via an adenylate cyclase-dependent mechanism.* Endocrinology **129**: p. 663-670.

246. Antoni, F.A., *et al.* (1993) *Secretagogue glucocorticoid interactions in the control of anterior pituitary adrenocorticotrophin (ACTH) secretion*, in *Progress in Endocrinology, Proceedings of the Ninth Inernational Congress of Endocrinology, Nice 1992*, R. Mornex, C. Jaffiol, and J. Leclère, Editors. Parthenon Publishers: Carnforth, U.K. p. 530-535.

247. Bray, D. (1998) *Signaling complexes: biophysical constraints on intracellular communication.* Annu Rev Biophys Biomol Struct **27**: p. 59-75.

PUBLISHED PAPER

British Journal of Pharmacology (1997) 121, 991–999

Involvement of calyculin A inhibitable protein phosphatases in the cyclic AMP signal transduction pathway of mouse corticotroph tumour (AtT20) cells

[1]A. Antaraki, K. L. Ang & [2]F. A. Antoni

MRC Brain Metabolism Unit, Department of Pharmacology, University of Edinburgh, 1 George Sq, Edinburgh, EH8 9JZ, Scotland

1 The role of non-calcineurin protein phosphatases in the cyclic AMP signal transduction pathway was examined in mouse pituitary corticotroph tumour (AtT20) cells.

2 Blockers of protein phosphatases, calyculin A and okadaic acid, were applied in AtT20 cells depleted of rapidly mobilizable pools of intracellular calcium and activated by various cyclic AMP generating agonists. Inhibitors of cyclic nucleotide phosphodiesterases were present throughout. The accumulation of cyclic AMP was monitored by radioimmunoassay, phosphodiesterase activity in cell homogenates was measured by radiometric assay.

3 Neither calyculin A nor okadaic acid altered basal cyclic AMP levels but cyclic AMP formation induced by 41 amino acid residue corticotrophin releasing-factor (CRF) was strongly inhibited (up to 80%). 1-Norokadaone was inactive. Similar data were also obtained when isoprenaline or pituitary adenylate cyclase activating $peptide_{1-38}$ were used as agonists.

4 Pertussis toxin did not modify the inhibition of CRF-induced cyclic AMP production by calyculin A.

5 Pretreatment with calyculin A completely prevented the stimulation of cyclic AMP formation by cholera toxin even in the presence of 0.5 mM isobutylmethylxanthine (IBMX) and 0.1 mM rolipram. Cholera toxin mediated ADP-ribosylation of the 45K and 52K molecular weight $G_{s\alpha}$ isoforms in membranes from calyculin A-pretreated cells was enhanced to 150–200% when compared with controls.

6 Cholera toxin-induced cyclic AMP was reduced by calyculin A within 10 min when calyculin A was applied after a 90 min pretreatment with cholera toxin. Under these conditions the effect of calyculin A could be blocked by the combination of 0.5 mM IBMX and 0.1 mM rolipram, but not by 0.5 mM IBMX alone.

7 Phosphodiesterase activity in AtT20 cell homogenates showed a significant, 2.7 fold increase after treatment with calyculin A. In control cells phosphodiesterase activity was blocked by 80% in the presence of IBMX (0.5 mM), or IBMX plus rolipram (0.1 mM). In calyculin A-treated cells phosphodiesterase activity was also strongly inhibited by IBMX, but because of the stimulating effect of calyculin A, the activity remaining was still 55% of that found in control homogenates. This activity was reduced to 5% of control by using IBMX and rolipram in combination. Assay of phosphodiesterase in Ca^{2+} free conditions showed that calyculin A markedly increases the activity of rolipram sensitive (type 4) phosphodiesterase.

8 Taken together, blockers of protein phosphatases (PPases) impaired signal transduction through Gs-mediated pathways and activated cyclic AMP degrading phosphodiesterase(s), indicating that PPases 1 and/or 2A are essential for agonist-mediated regulation of cyclic AMP levels in AtT20 cells, and are thus important in maintaining the secretory phenotype of the cells.

Keywords: Protein phosphatase; calyculin A; okadaic acid; G proteins; corticotrophin releasing factor; pituitary tumour; phosphodiesterase; rolipram; cyclic AMP; FK506

Introduction

Protein phosphatases (PPase) are essential elements of cellular control (Cohen, 1989). However, knowledge about their role in the generation of the cyclic AMP response to agonists is largely limited to the control of cell surface receptor recycling (Sibley *et al.*, 1987; Pitcher *et al.*, 1995). It is generally accepted that in addition to receptors, G proteins (Houslay, 1994), as well as adenylyl cyclases (Jacobowitz & Iyengar, 1994; Kawabe *et al.*, 1994) are substrates for protein kinases. Hence the state of phosphorylation of these signal-transducing proteins is likely to be influenced by protein phosphatases. Previous work in S49 lymphoma cells (Clark *et al.*, 1993) and AtT20 corticotrope tumour cells (Koch & Lutz-Bucher, 1994) has indicated a role for PPases in receptor-stimulated cyclic AMP production, which was apparently distinct from the control of cell-surface receptors.

One of the most prominent PPases, PPase 1, is under the control of inhibitor-1 and DARPP-32 (Klee & Cohen, 1988). These are closely related regulatory phosphoproteins which in the phosphorylated form inhibit PPase 1. The inhibition is relieved upon dephosphorylation of the regulatory protein by the Ca^{2+}/calmodulin-activated protein phosphatase calcineurin (Klee & Cohen, 1988). The latter mechanism provides for a functionally co-ordinated PPase (calcineurin-PPase 1) cascade opposing the actions of protein kinases (Cohen, 1989). Calcineurin-PPase 1 cascades are thought to operate in a number of functionally important systems, such as regulation of glycogenolysis in skeletal muscle (Klee & Cohen, 1988) ion transport in kidney tubule cells (Aperia *et al.*, 1992) and hippocampal long-term depression (Mulkey *et al.*, 1994).

[1]Present address: Department of Experimental Physiology, Medical School, University of Athens, GR 115 27 Athens, Greece.
[2]Author for correspondence.

Previous work (Antoni *et al.*, 1995) in mouse pituitary corticotrope tumour (AtT20) cells has shown that calcineurin inhibits the formation of cyclic AMP induced by the polypeptide hormone 41 amino acid residue corticotrophin releasing-factor (CRF). The present study investigated whether the control of adenosine 3′:5′ cyclic monophosphate (cyclic AMP) accumulation by calcineurin involves the operation of a calcineurin-PPase 1 cascade in this system. The data showed that inhibitors of PPase 1/2A abolish the regulation of cyclic AMP levels by Ca^{2+}/calcineurin. This is nominally consistent with the operation of a PPase cascade. However, there was also a marked reduction of agonist-induced cyclic AMP responses. Furthermore, PPase blockers were also effective in Ca^{2+} depleted cells, where calcineurin is inactive, clearly demonstrating multiple sites of action of PPase 1/2A in the cyclic AMP signal transduction cascade. Overall, the results suggest that PPase 1/2A operate in a functionally co-ordinated manner to maintain the responsiveness of AtT20 cells to receptors coupling to Gs.

A preliminary account of this work has been published (Antaraki & Antoni, 1994).

Methods

Cells

Mouse pituitary corticotroph tumour (AtT20 D16:16) cells (passage 18–35) were maintained as previously described (Woods *et al.*, 1992).

Measurement of cyclic AMP formation

The protocol for experiments with forskolin and agonists of G protein-coupled receptors has been described previously (Antoni *et al.*, 1995). Briefly, cells in 24-well tissue culture plates were washed free of serum and incubated at 37°C in Hank's balanced salt solution without Ca^{2+} and Mg^{2+} (HBSS, Life Technologies, Paisley, U.K.), supplemented with 25 mM HEPES pH 7.4, 2 mM $CaCl_2$, 1 mM $MgSO_4$ and bovine serum albumin (0.25% w/v).

Thirty to forty five minutes later the medium was replaced with fresh medium containing inhibitors of PPases and cyclic nucleotide phosphodiesterases (PDE). Importantly, in all experiments except for those shown in Figure 1b, a Ca^{2+}-depleting medium was applied at this stage (HBSS, supplemented with 25 mM HEPES pH 7.4, 2 mM NaEGTA, 1 mM $MgSO_4$, 5 μM A23187, 5 μM nimodipine and bovine serum albumin (0.25% w/v)), and unless otherwise indicated, this medium was used in the rest of the experiment. These conditions were necessary in order to eliminate Ca^{2+}-dependent regulation of cyclic AMP production (Antoni *et al.*, 1995). In cases where, after preincubation in Ca^{2+}-depleting conditions, $CaCl_2$ was introduced with the CRF-stimulus to reach 2 mM free extracellular $CaCl_2$, the pH of the added CRF containing medium was buffered as required to maintain pH 7.4 during the test stimulation. Because of the intensive degradation of cyclic AMP by cyclic nucleotide phosphodiesterase in AtT20 cells (Woods *et al.*, 1992; Koch & Lutz-Bucher, 1995) 0.5 mM isobutylmethylxanthine (IBMX) was always added to the cells at this stage. In some experiments rolipram, a highly selective blocker of type 4 PDE (Beavo & Reifsnyder, 1990) (courtesy of Schering, A.G., Berlin, F.R.G.), was also included with IBMX as indicated in the figure legends.

The cells were incubated for a further 30 min at 37°C, then cooled to 24°C for 5 min, after which time inducers of cyclic AMP formation were added at 24°C for 10 min (except for time-course studies). This protocol was used because pilot studies had shown calyculin A to be fully effective within 5 min at 37°C, while having no appreciable effect within 30 min at 24°C. Test incubations were carried out at 24°C, because the effects of calcium ions and calcineurin inhibitors were greater under these conditions (Antoni *et al.*, 1995). Note, however, that as cholera toxin action required incubations at 37°C, all experiments with cholera toxin and the analysis of the time-course of calyculin A action in cells pre-activated by CRF (Figures 4 and 6) were carried out at 37°C.

The 10 min test incubation with agonists was terminated by adding HCl to reach a final concentration of 0.1 mM, and cyclic AMP was quantified by direct radioimmunoassay (Brooker *et al.*, 1979). Under the conditions used 90% of the immunoreactive cyclic AMP was intracellular.

Experiments with cholera toxin

Where intact cells were used, all incubations were carried out at 37°C, in order to ensure that ADP-ribosylation proceeded optimally. All other procedures for cyclic AMP determination were the same.

ADP-ribosylation was carried out in cell membranes as previously described (Longbottom & van Heyningen, 1989). Briefly, approximately 2.5×10^7 cells preincubated for 30 min in Ca^{2+} depleting medium with or without 50 nM calyculin A, were homogenized in 20 mM Tris/HCl (pH 7.4), 1 mM EDTA, 250 mM sucrose, 0.1 mM phenyl methyl sulphonyl fluoride (PMSF) and 2 mM benzamidine. Homogenization was carried out by 10 strokes of a glass-Teflon homogenizer and the membrane fraction was separated from the crude homogenate by sequential centrifugations at 300, 2,000, 9,800 and 35,000 x*g*, respectively. Protein content was measured by the Coomassie blue method (Bradford, 1976). The ADP ribosylation assay mixture (final volume 0.1 ml) consisted of 20 μg ml^{-1} pre-activated cholera toxin, 5 μM [adenylate-^{32}P]-NAD^+ (25–35 Ci $mmol^{-1}$), 200 mM K_2HPO_4/NaH_2PO_4 (pH 7.5), 10 mM $MgCl_2$, 2 mM EDTA, 5 mM ATP, 0.5 mM GTP, 10 mM creatine phosphate, 50 u ml^{-1} creatine phosphokinase, 10 mM thymidine and 10 mM isoniazide. The reaction was initiated by the addition of 50 μg membrane protein. The assay mixture was incubated at 30°C for 30 min (maximal incorporation of radioactivity under these conditions) and the reaction was stopped by the addition of 1 ml of 'ice-cold' 10 mM MOPS/0.13 M NaCl (pH 7.5). Subsequently, the mixture was centrifuged at 9,000 x*g*, the pellet solubilized in 60 μl of 0.1% SDS, 50 mM Tris/HCl pH 7.8, 1 mM dithiothreitol (DTT) and 10 μl aliquots of this mixture were applied to a 12% polyacrylamide gel (Pharmacia, Milton Keynes U.K.) and electrophoresed under denaturing conditions. The gel was stained with Coomassie blue, dried and autoradiographed on X-ray film or in Molecular Dynamics phosphorimager cassettes, after which the optical densities of the radioactive bands were quantified with the Imagequant software as supplied by the manufacturer.

Measurement of cyclic nucleotide phosphodiesterase (PDE) activity

Crude homogenates of AtT20 cells were prepared in Teflon/glass homogenizers in homogenizing buffer (20 mM Tris/HCl (pH 8), 1 mM EDTA, 0.2 mM EGTA, 50 mM NaF, 10 mM sodium pyrophosphate, 50 mM benzamidine, 2 mM PMSF, 0.5 μg ml^{-1} leupeptin, 0.7 μg ml^{-1} pepstatin, 4 μg ml^{-1} aprotinin and 10 μg ml^{-1} soybean trypsin inhibitor) 50 μl/10^6 cells, in order to minimize proteolytic cleavage and dephosphorylation (Sette *et al.*, 1994) of PDE. The radiometric assay of PDE activity was by column chromatography (Manganiello & Vaughan, 1973; Kono, 1988) or a co-precipitation/filtration assay (Schilling *et al.*, 1994) which gave comparable results. The PDE assay reaction (250 μl) contained 100 mM TES-HCl pH 7.5, 5 mM $MgSO_4$, 1 or 10 μM substrate cyclic AMP, [^{3}H]-cyclic AMP (NET-275, NEN, Dupont) in tracer amounts, and 50 μl of homogenate. In some experiments, 0.5 mM EGTA was also included to reduce Ca^{2+}-dependent PDE activity to a minimum.

In experiments with PDE inhibitors and calyculin A, the requisite compounds were added to intact cells in order to reproduce the conditions of cyclic AMP experiments as closely as possible. PDE blockers were also added at the requisite concentrations into the PDE assay. The PDE reaction was terminated when it was linear both with respect to time and the amount of homogenate protein added, (5–10 μg or 80–100 μg/assay point, at 1 or 10 μM substrate cyclic AMP, respectively), so that quantitative comparisons between treatment groups could be made.

Reagents

Unless otherwise specified, all reagents were from Sigma Ltd (Poole, Dorset, U.K.). Sources of other materials were as follows: phorbol 12,13 dibutyrate ester (PdBu), calyculin A and okadaic acid, LC-Labs Boston (dissolved at 5 mM in ethanol and stored at −40°C); rat corticotrophin releasing-factor$_{1-41}$ (CRF) Bachem U.K. (Saffron Walden, Essex, U.K.); pituitary adenylate cyclase activating peptide$_{1-38}$ (PACAP) Peninsula Laboratories, (St Helen, Merseyside, U.K.), A23187 (Calbiochem-Novabiochem, Nottingham, U.K.); nimodipine Semat Ltd (St Albans, Herts, U.K.); pertussis toxin (List Laboratories). FK506 (tacrolimus), courtesy of Fujisawa GMBH, München.

Data analysis

Student's *t* test and analysis of variance were used where appropriate and are indicated in the figure legends.

Results

Actions of okadaic acid and calyculin A on receptor-induced cyclic AMP formation

Pilot studies showed that in cells treated with IBMX, both calyculin A (Figure 1a) and okadaic acid (not shown) inhibited CRF-induced cyclic AMP formation irrespective of the calcium status of the cells. Notably, in the presence of maximally effective concentrations of calyculin A, the enhancement of cyclic AMP formation by Ca^{2+}-depletion was no longer apparent. Furthermore, the enhancement of the cyclic AMP response by the calcineurin blocker FK506 (Antoni *et al.*, 1995) could not be observed in the presence of calyculin A (Figure 1b). On the one hand, these data are compatible with the PPase cascade hypothesis, i.e. the serial coupling of calcineurin and PPase1, although the marked reduction of the cyclic AMP response complicates the interpretation of the data. On the other hand, the effects observed in Ca^{2+}-depleted cells clearly indicate that type 1/2A PPases are involved in the control of cyclic AMP accumulation independently of Ca^{2+}calcineurin. In order to examine this problem further, the subsequent studies were carried out in Ca^{2+}-depleted cells.

Under these conditions inhibition of CRF-induced cyclic AMP accumulation by 100 nM calyculin A was evident at all time-points examined after the addition of CRF (Figure 2a). Unless otherwise indicated, all reactions were terminated at 10 min. The reduction of cyclic AMP accumulation by 100 nM calyculin A was observed at all concentrations of CRF that caused a significant enhancement of cyclic AMP production (Figure 2b).

The dose-response curves for okadaic acid and calyculin A revealed that okadaic acid was approximately 80 fold less potent than calyculin A in reducing CRF-induced cyclic AMP formation, moreover 1-norokadaone, an okadaic acid analogue that is not bound by PPases (Nishiwaki *et al.*, 1990), had no effect on cyclic AMP formation (Figure 2c).

Similar data were obtained with the β-adrenoceptor agonist isoprenaline, that activates a β_2 adrenoceptor (Heisler *et al.*, 1983) in AtT20 cells, and PACAP (Figure 2d).

Lack of involvement of pertussis toxin sensitive G-proteins

The half-effective concentration and the maximal effect of calyculin A with respect to CRF-induced cyclic AMP formation was not altered by preincubation of the cells with pertussis toxin (1 μg ml^{-1} 18 h) (Figure 3a).

The same PTX treatment markedly attenuated the inhibitory effect of 10 nM somatostatin (Antoni *et al.*, 1995), a peptide hormone known to reduce cyclic AMP formation through G_i proteins in AtT20 cells (Reisine, 1985).

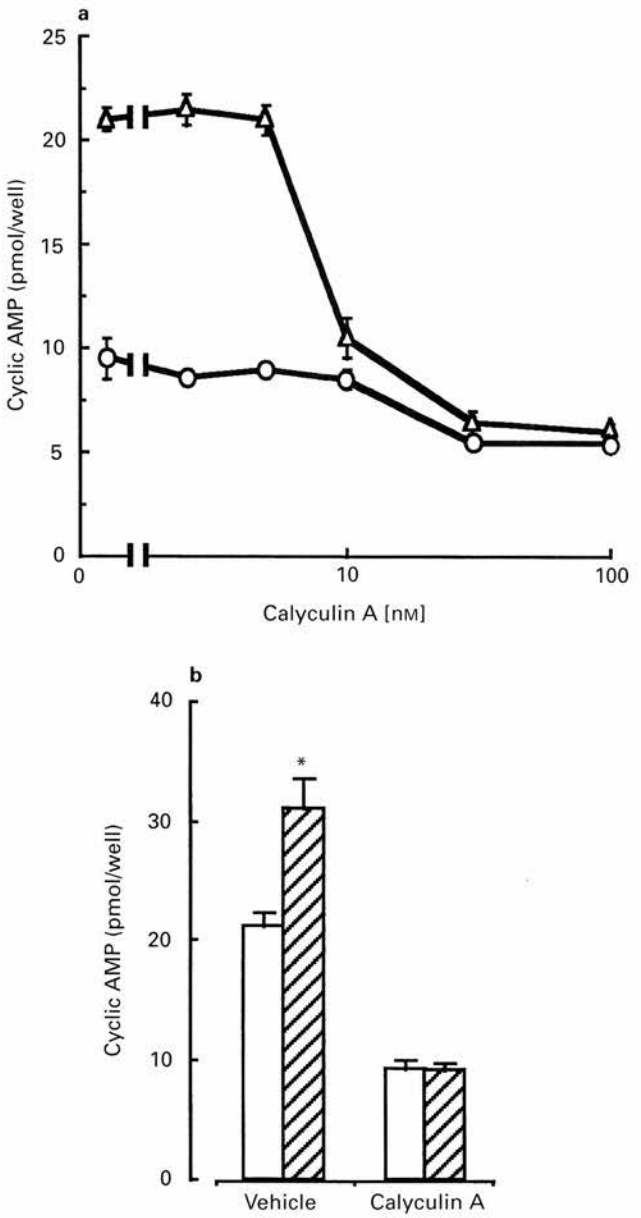

Figure 1 (a) Inhibition of cyclic AMP accumulation in response to 10 nM CRF by 50 nM calyculin A in (△) Ca^{2+}-depleted cells and (○) Ca^{2+}-depleted cells repleted with Ca^{2+} at the time of addition of CRF (see Methods); 0.5 mM IBMX and calyculin A were added 30 min before CRF. Basal levels of cyclic AMP were 0.65±0.002 and 0.54±0.02 pmol/well (mean±s.e.mean) in the Ca^{2+}-depleted and Ca^{2+}-repleted groups, respectively. (b) Blockade of calcineurin modulation of 10 nM CRF-induced cyclic AMP by calyculin A in AtT20 cells incubated in medium containing 2 mM $CaCl_2$ (without ionophore) throughout the course of the experiment. All groups of cells were preincubated with 0.5 mM IBMX, and the indicated combinations of vehicle (0.4% ethanol), 50 nM calyculin A and 2 μM FK506 for 30 min; open columns, control; hatched columns, FK506. Basal cyclic AMP level was 1.6±0.09 pmol/well. Data are means± s.e.mean; $n=4$/group. $^*P<0.05$ vs vehicle, one-way analysis of variance followed by Newman-Keuls test.

Cholera toxin induced cyclic AMP synthesis was blocked by calyculin A

Pretreatment with 50 nM calyculin A completely blocked the formation of cyclic AMP induced by cholera toxin despite the presence of IBMX (not shown and (Koch & Lutz-Bucher, 1994)) or IBMX as well as rolipram (Figure 4).

In view of the complete block of the effect of cholera toxin by preincubation with calyculin A, the effects of calyculin A pretreatment on ADP-ribosylation were examined. In membranes prepared from calyculin A-pretreated cells (Figure 5), there was a clear increase (50% and 100% expressed in arbitrary optical density units in experiment 1 and 2, respectively) of [^{32}P]-ADP ribose incorporation into two major radiolabelled bands corresponding to the two commonly occurring 45K and 52K molecular weight splice variants (Robishaw *et al.*, 1986) of $G_{s\alpha}$. No differential changes in the intensity of radiolabelling of these bands were discernible.

In order to circumvent the apparent blockade of the activation of G_s by calyculin A, the cells were activated by cholera toxin for 90 min, after which PDE blockers and calyculin A were added in sequence. Under these conditions (Figure 6a) when only 0.5 mM IBMX was present, a marked inhibition of cyclic AMP accumulation developed within 10 min after the addition of 50 nM calyculin A. However, 0.5 mM IBMX and 0.1 mM rolipram in combination blocked the effect of calyculin A at all time points, except at 30 min when a small (20%), but statistically significant ($P<0.05$, one-way ANOVA followed by Newman Keuls test) inhibition developed.

As IBMX and rolipram in combination also markedly (close to 150%) enhanced the cyclic AMP response to cholera toxin when compared with IBMX alone, the response to 10 nM CRF was re-examined. This was also increased upon the addition of 0.1 mM rolipram and 0.5 mM IBMX, but only by 20% when compared with the response observed in the presence of 0.5 mM IBMX alone (not shown). However, the profound inhibition by calyculin A either as preincubation (not shown), or when given 1.5 min after the addition of CRF (Figure 6b) prevailed even in the presence of 0.1 mM rolipram and 0.5 mM IBMX.

Effect of calyculin A on phosphodiesterase activity

Analysis of the time-course of calyculin A action on cholera toxin-induced cyclic AMP formation (see Figure 6a) indicated that calyculin A may enhance phosphodiesterase activity in

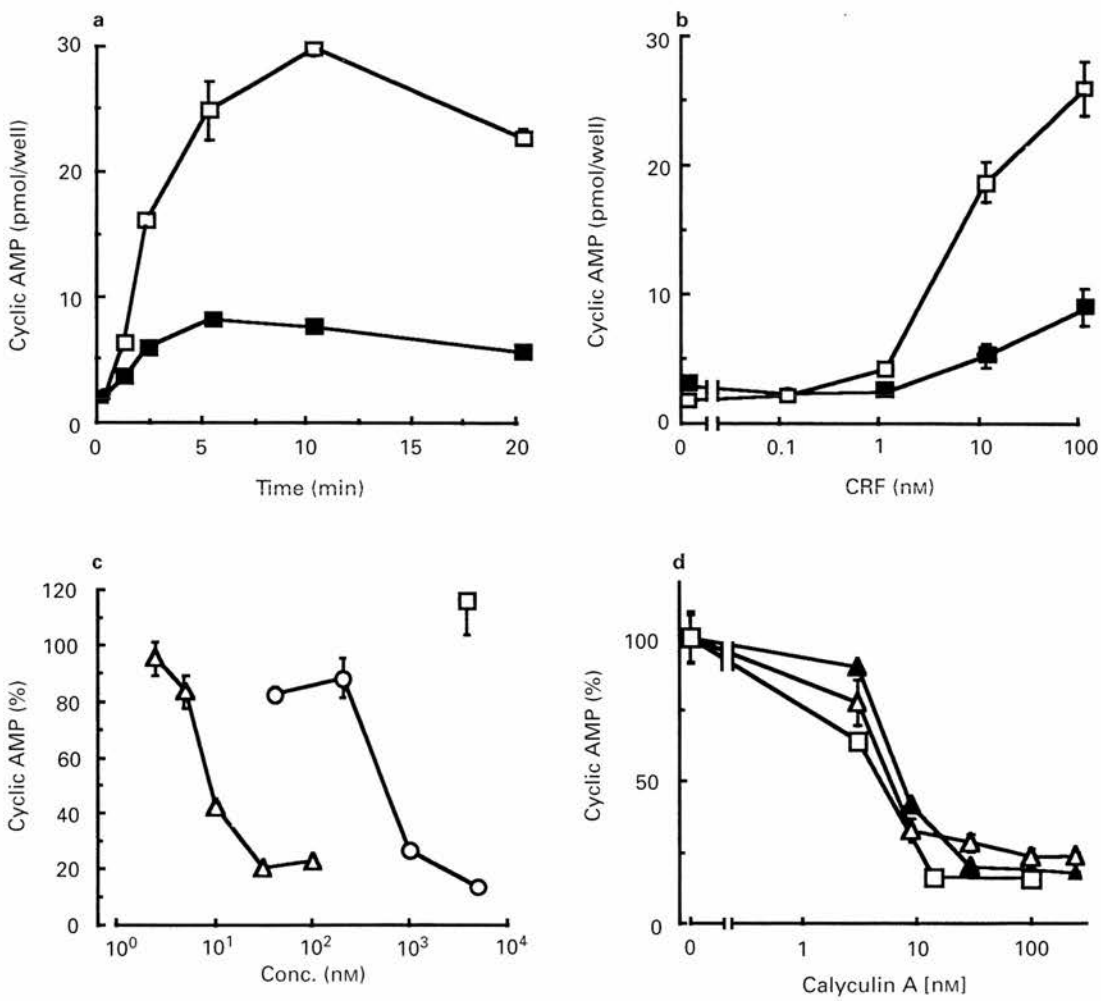

Figure 2 Inhibition of CRF-induced cyclic AMP production by protein phosphatase (PPase) blockers in Ca^{2+}-depleted AtT20 cells in the presence of 0.5 mM IBMX. PPase blockers and IBMX were applied 30 min before the addition of CRF. Data are means and vertical lines show s.e.mean; $n=4-6$/group, and representative of at least two identical experiments. (a) Time-course of cyclic AMP formation induced by 10 nM CRF in cells treated with (□) vehicle or (■) 100 nM calyculin A. (b) Effect of (■) 100 nM calyculin A and (□) vehicle on cyclic AMP production in response to various concentrations of CRF, the reaction was terminated 10 min after the addition of CRF. (c) Specificity of PPAse blocker action on cyclic AMP production evoked by 10 nM CRF. Data are expressed as percentage of the cyclic AMP response to 10 nM CRF. Basal levels of cyclic AMP were 0.79 ± 0.05 pmol/well, CRF-induced cyclic AMP taken as 100% was 11.3 ± 0.4 pmol/well. Effects (△) calyculin A, (○) okadaic acid and (□) 1-nor-okadone are shown. (d) Concentration-dependent effect of calyculin A on cyclic AMP accumulation induced by (▲) 10 nM CRF, (△) PACAP or (□) isoprenaline. All stimuli caused comparable increases (10–20 fold basal) of total cyclic AMP.

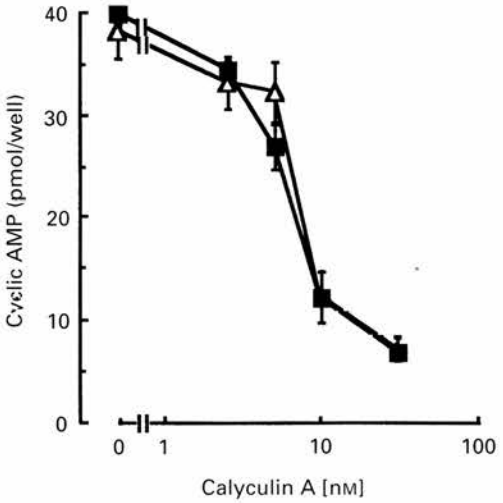

Figure 3 Effect of various concentrations of calyculin A on cyclic AMP production induced by 10 nM CRF in calcium-depleted AtT20 cells after 18 h of treatment with (■) vehicle or (△) 1 μg ml^{-1} pertussis toxin. Calyculin A was applied 30 min before stimulation by CRF. IBMX (0.5 mM) was present during the addition of calyculin A and CRF. Data are means and vertical lines show s.e.mean; $n = 4$, representative of two experiments.

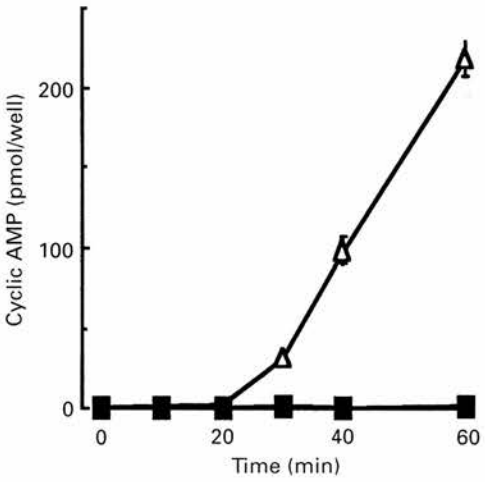

Figure 4 Interaction of calyculin A with cholera toxin in calcium depleted AtT20 cells. Levels of cyclic AMP in AtT20 cells pretreated with 0.5 mM IBMX and 0.1 mM rolipram plus vehicle (△) or 50 nM calyculin A (■) for 30 min. Cholera toxin (125 ng ml^{-1}) was added at 0 min. Means ± s.e.mean (vertical lines) $n = 4$/group, representative of two experiments.

AtT20 cells. Measurement of PDE activity in Ca^{2+}-depleted cells revealed a clear stimulation of cyclic AMP hydrolysis upon 30 min of pretreatment with 50 nM calyculin A (Figure 7a and b). Treatment with PDE blockers by use of the same protocol as in the experiments for cyclic AMP accumulation and also including the blockers in the PDE assay (10 μM substrate) showed (Figure 7b) that IBMX inhibited PDE activity up to 80%. However, because of the marked enhancement of PDE activity in calyculin A treated cells, the activity remaining in the presence of IBMX was 55% of that found in control cells. Combination of rolipram with IBMX reduced this activity to 5% of control.

The time-course of the onset of the effect of calyculin A on PDE activity was assayed under Ca^{2+} free conditions at 1 μM substrate thus favouring detection of PDE4. A significant increase of activity was evident within 5 min of addition to the cells (Figure 7c) and was completely blocked by addition of 10 μM rolipram in the PDE assay (Figure 7c). Addition of 30 nM calyculin A into the PDE assay did not mimic this effect,

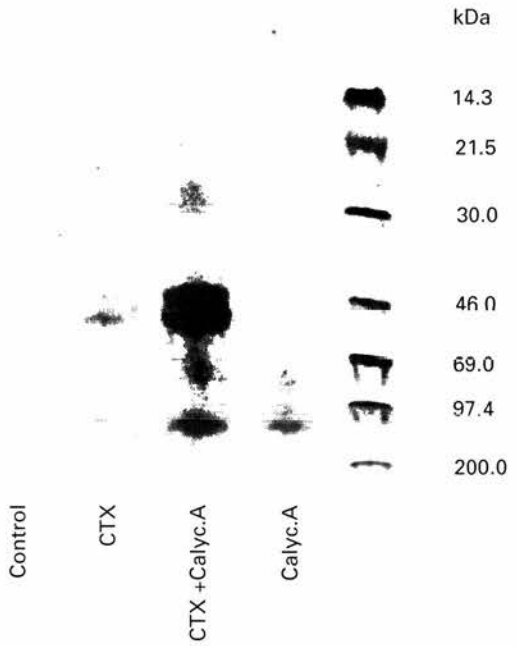

Figure 5 Effect of pretreatment with calyculin A on cholera toxin induced ADP-ribosylation in AtT20 cell membranes. Cells were incubated with 0.4% (v/v) ethanol or 50 nM calyculin A in Ca^{2+}-depleting medium for 30 min and membranes were reacted with cholera toxin (CTX) in ADP-ribosylation buffer or ADP-ribosylation buffer alone for 30 min, after which the proteins were resolved by gel electrophoresis under denaturing conditions. Autoradiography was carried out with X-ray film as well as phosphorimager cassettes. Data shown are representative of two identical experiments. Control: vehicle treated cells, membranes in ADP ribosylation buffer only, CTX: vehicle treated cells, membranes treated with CTX; CTX + Calyc. A: cells treated with calyculin A membranes reacted with CTX and ADP ribosylation buffer; Calyc.A: cells treated with calyculin A, membranes in ADP ribosylation buffer only. Quantification of the optical densities by image analysis indicated a 2 fold increase of incorporation into the two bands migrating approximately at 45K and 52K molecular weight. The high molecular weight band at 97K may be a dimer of the lower molecular weight forms.

furthermore, assays in the presence of 100 μM Ca^{2+}, 100 nM calmodulin and 10 μM rolipram showed no increase of PDE activity after treatment with calyculin A (results not shown). Collectively, these data indicate selective activation of a type 4 PDE by calyculin A.

Effects of calyculin A are not mimicked by activation of protein kinase C

In view of the possible activation of protein kinase C by calyculin A (Gopalakrishna *et al.*, 1992) the effects of phorbol dibutyrate ester (PdBu) on CRF-induced cyclic AMP accumulation were also examined. In calcium-depleted cells pretreated with 0.5 mM IBMX, 10 nM PdBu produced a significant ($P < 0.0001$, two-way ANOVA) 30% inhibition of CRF-evoked cyclic AMP, which was also apparent in the presence of a maximally effective concentration (50 nM) of calyculin A (Figure 8). The actions of PdBu and calyculin A on CRF-induced cyclic AMP were not additive, PdBu produced a smaller decrement in the presence of calyculin A ($P < 0.01$ for interaction between PdBu and calyculin A in a linear ANOVA model). Finally, treatment of Ca^{2+}-depleted cells with 10 nM PdBu for 30 min failed to alter PDE activity (not shown).

Discussion

Previous work has indicated a prominent role of PPases in cellular responsiveness through the dephosphorylation of G-protein coupled membrane receptors (Sibley *et al.*, 1987;

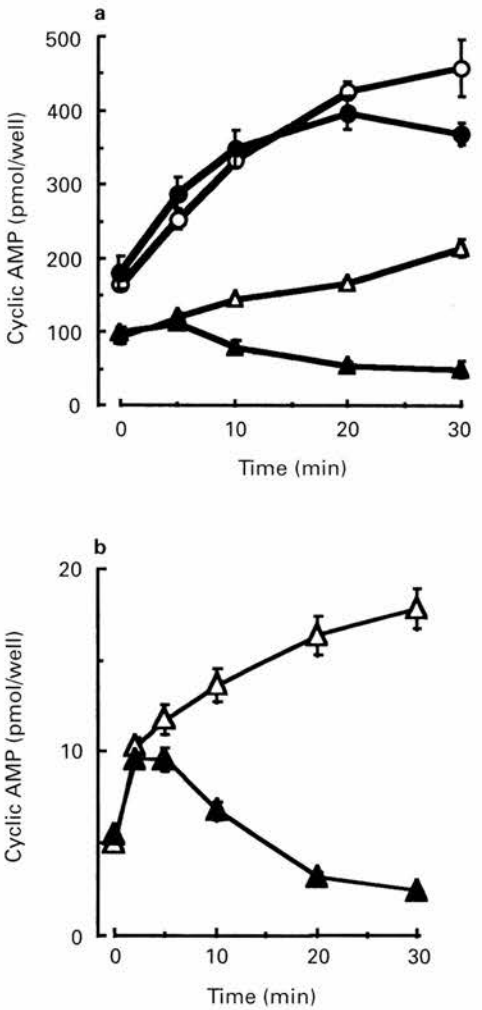

Figure 6 (a) Levels of cyclic AMP in AtT20 cells pretreated for 90 min with (125 ng ml^{-1}) cholera toxin; 0.5 mM IBMX (△, ▲) or 0.5 mM IBMX and 0.1 mM rolipram (○, ●) were added 5 min before vehicle (△, ○) or 50 nM calyculin A (▲, ●) was introduced at 0 min. Data are representative of two identical experiments. (b) Levels of cyclic AMP in AtT20 cells pretreated with 0.5 mM IBMX and 0.1 mM rolipram for 30 min; 10 nM CRF was added 1.5 min before the addition of vehicle (△) or 50 nM calyculin A (▲) at 0 min.

Pitcher *et al.*, 1995). While it is possible that some of the effects observed in the present study are due to the depletion of cell surface receptor pools required for a sustained response to agonist stimulation, the data clearly show effects of PPase blockers downstream of membrane receptors. The reduction of agonist as well as cholera toxin-stimulated cyclic AMP synthesis indicates impairment of the activation of adenylyl cyclase by G_s. Moreover, a marked stimulation of cyclic AMP phosphodiesterase activity was demonstrated which was functionally relevant with respect to cyclic AMP accumulation.

Specificity of PPase inhibitors

The relative potencies of calyculin A and okadaic acid to inhibit receptor-induced cyclic AMP formation respectively, conform with the pharmacology of these compounds to inhibit PPase1 activity (Cohen *et al.*, 1990). Similarly, a previous study (Koch & Lutz-Bucher, 1994) found a 100 fold difference in the potencies of calyculin A and okadaic acid to block CRF- and PACAP-induced cyclic AMP production in AtT20 cells. A close structural analogue of okadaic acid, 1-norokadaone, that does not bind to protein phosphatases (Nishiwaki *et al.*, 1990) was inactive in our system. The cyclic AMP response to forskolin, a direct activator of adenylyl cyclase, is unchanged

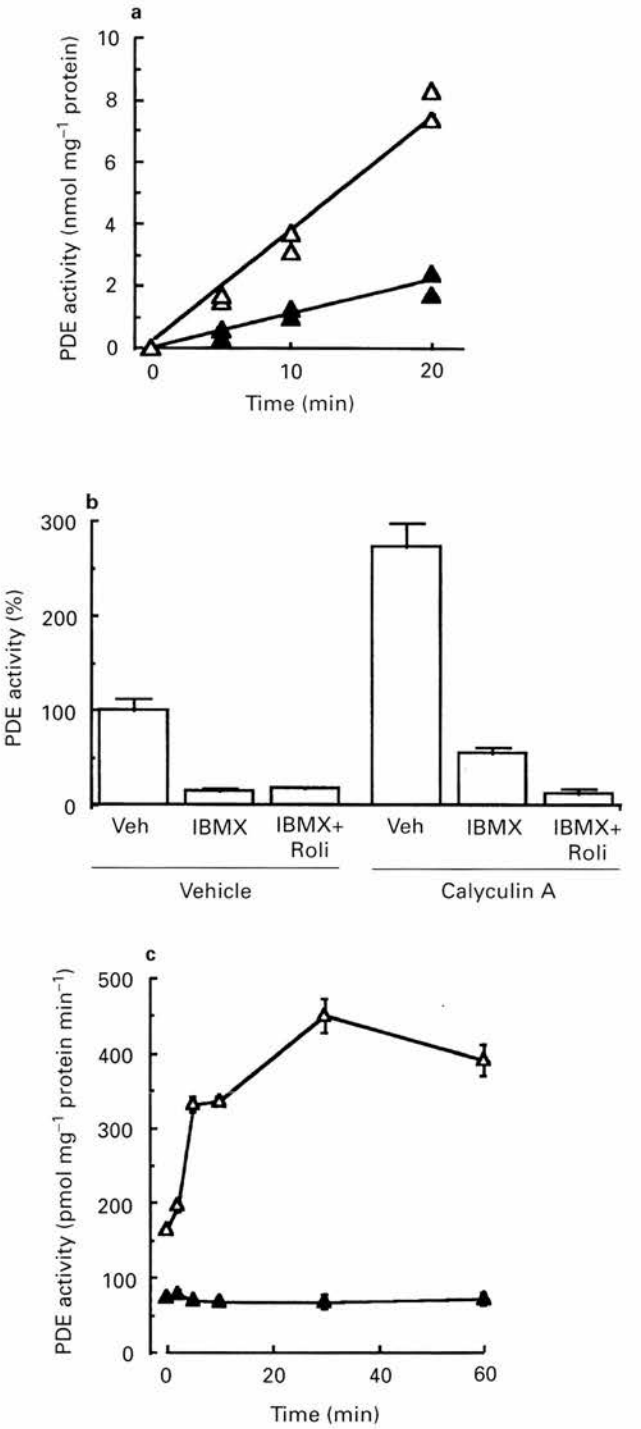

Figure 7 Effect of calyculin A and phosphodiesterase (PDE) blockers on cyclic AMP phosphodiesterase activity in calcium-depleted AtT20 cells. (a) Time-course of PDE activity in homogenates prepared from (▲) vehicle (Veh) or (△) 50 nM calyculin A-treated AtT20 cells with 10 μM cyclic AMP as substrate. Individual points from a representative experiment. (b) Cyclic AMP PDE activity in homogenates prepared from AtT20 cells pretreated with vehicle or 50 nM calyculin A plus 0.5 mM IBMX or 0.5 mM IBMX and 0.1 mM rolipram (Roli) PDE blockers were also added to the assay reaction mixture (substrate 10 μM cyclic AMP), the reactions were terminated at 10 min. Data are means ± s.e.mean, $n = 4$/group, pooled from 3 separate experiments, the basal activity taken as 100% ranged between 60 and 100 pmol mg^{-1} protein min^{-1} in these experiments. (c) Cyclic AMP PDE activity of homogenates prepared from AtT20 cells pretreated with 50 nM calyculin A for the indicated time intervals. The PDE activity was assayed in the presence of (△) 0.1% (v/v) DMSO (Veh) or (▲) 10 μM rolipram the assay buffer contained 0.5 mM EGTA and 1 μM cyclic AMP substrate.

(Koch & Lutz-Bucher, 1994) or even enhanced (A. Antaraki, & F.A. Antoni, unpublished data), upon treatment with PPase blockers, which argues against an impairment of adenylyl cyclase catalytic activity or a generalized toxic damage to cellular metabolism. Finally, activation of protein kinase C with phorbol ester did not mimic the effects of calyculin A. It is therefore reasonable to suggest that the effects observed here are due mainly to blockade of PPase activity, primarily types 1 and 2A, and not to non-specific interferences with other mechanisms of cellular control.

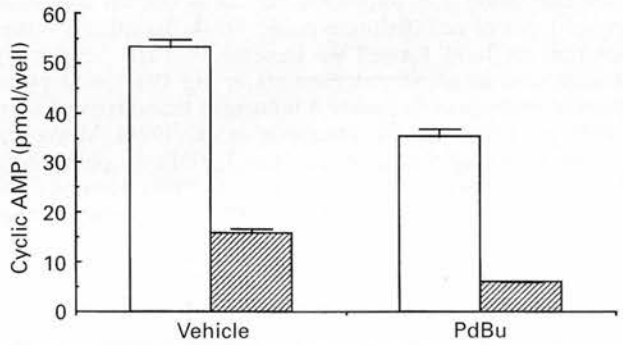

Figure 8 Effect of 10 nM phorbol 12, 13 dibutyrate ester (PdBu) on cyclic AMP accumulation induced by 10 nM CRF in Ca^{2+}-depleted AtT20 cells in the presence (hatched columns) or absence (open columns) of a maximally effective (50 nM) concentration of calyculin A. Cells were preincubated for 30 min with 0.5 mM IBMX and the indicated combinations of vehicle (0.4% ethanol), calyculin A and PdBu. Data are means ± s.e.mean, $n=4$/group, representative of two experiments. Two-way ANOVA $P<0.0001$ for the effects of calyculin A and PdBu, there was also a significant interaction $P<0.01$ between the two treatments.

Blockade of modulation of cyclic AMP by Ca^{2+} in the presence of calyculin A

Calcium ions exert a powerful and functionally relevant negative feedback effect on cyclic AMP formation in AtT20 cells (Shipston *et al.*, 1994; Antoni *et al.*, 1995) which is interrupted by blockers of calcineurin such as FK506. In the present study calyculin A blocked the effects of calcium depletion and repletion previously (Antoni *et al.*, 1995) shown to enhance and inhibit the CRF-induced cyclic AMP response, respectively. Accordingly, the effect of FK506 was also abolished. Nominally, these data are consonant with the calcineurin-PPase1 cascade hypothesis (Figure 9). However, calyculin A caused a strong net inhibition of the cyclic AMP response to activation by G_s-coupled receptors, whereas blockers of calcineurin enhanced it. Furthermore, the suppression of the cyclic AMP response by calyculin A was also observed in Ca^{2+}-depleted cells. Thus, while these findings favour that calcineurin operates through PPase1 in AtT20 cells as proposed previously for other systems (Klee & Cohen, 1988), it is clear that further sites of PPase action are involved that are readily demonstrable in cells depleted of rapidly mobilizable Ca^{2+}.

Effects of PPase blockade on G_s mediated responses

Overall, the consequence of PPase inhibition was a marked reduction of the rate of receptor- as well as cholera toxin-stimulated cyclic AMP formation. Pertussis toxin sensitive G-proteins have no apparent role in this effect of PPase blockers.

Surprisingly, despite the complete blockade of cholera toxin-induced cyclic AMP formation by calyculin A, the ADP-ribosylation of $G_{s\alpha}$ by cholera toxin was enhanced. As recent work suggests that $G_{s\alpha}$ in the heterotrimeric complex with β and γ subunits is a much better substrate for cholera toxin than the dissociated α-subunit (Toyoshige *et al.*, 1994), these data

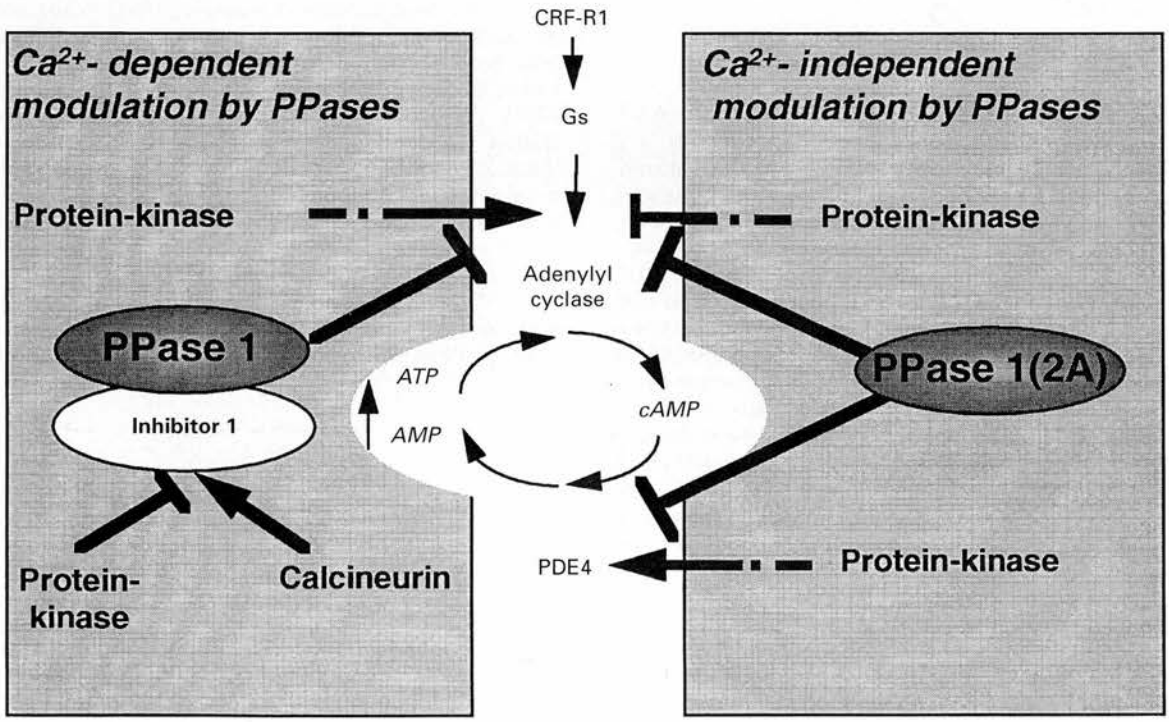

Figure 9 Schematic summary of multiple sites of PPase modulation of the cyclic AMP (cAMP) signal transduction cascade in AtT20 cells. Arrows and T-s represent stimulation and inhibition, respectively. The broken effector lines indicate that multiple enzymatic steps may be involved. Ca^{2+}-dependent modulation by PPases: the operation of a calcineurin-PPase1 cascade is suggested by the loss of Ca^{2+}/calcineurin modulation of agonist-induced cyclic AMP synthesis by calyculin A. The respective protein kinase(s) that appear to be facilitatory to G_S-cyclase coupling remain to be identified. The site of PPase1 action is not known. Ca^{2+}-independent modulation by PPases: a calyculin A-sensitive mechanism is required for efficient coupling of G_S and adenylyl cyclase implying the existence of inhibitory phosphorylation. The site(s) of this modulation and the protein kinases are not known. Calyculin A enhanced the activity of a rolipram-sensitive PDE, indicating constitutive stimulant phosphorylation of a PDE 4 isotype.

could be interpreted to suggest that the probability of G_s subunit dissociation, which is a prerequisite for the activation of adenylyl cyclase (Gilman, 1987), is reduced by calyculin A. This hypothesis is also compatible with the observation that after irreversible activation of $G_{s\alpha}$ by cholera toxin, the principal mediator of calyculin A action appeared to be a rolipram/IBMX sensitive PDE, whereas this was clearly not the case when calyculin A was applied before cholera toxin. Blockade of PDE with rolipram/IBMX also failed to prevent the inhibition of CRF-induced activation of adenylyl cyclase by calyculin A, where cycling of $G_{s\alpha}$ from the activated (dissociated) to the deactivated (heterotrimeric) state is likely to be essential for the stimulating effect of the agonist (Gilman, 1987). In addition, other workers have shown a drastic reduction of the cyclic AMP response to CRF in membranes of AtT20 cells pretreated with calyculin A (Koch & Lutz-Bucher, 1994). Thus calyculin A interferes with the activation of adenylyl cyclase by G_s. This implies that in AtT20 cells constitutive phosphorylation/dephosphorylation reactions regulate the coupling of G_s to adenylyl cyclase.

Phosphorylation of $G_{s\alpha}$ by a variety of protein kinase cascades, particularly epidermal growth factor-induced kinase cascades, has been observed previously (see Houslay, 1994; Liebman *et al.*, 1996 for reviews). One apparent outcome of $G_{s\alpha}$ phosphorylation by epidermal growth factor-induced mechanisms is the inhibition of the activation of adenylyl cyclase by G_s-coupled receptors, which conforms with the findings presented here. Another potential mechanism that could underlie the reduction in the stimulation of adenylyl cyclase by receptor-activated G_s is the phosphorylation of adenylyl cyclase by protein kinases (Premont *et al.*, 1992). Adenylyl cyclase type 9 is the predominant cyclase isotype expressed in AtT20 cells (Antoni *et al.*, 1995; Paterson *et al.*, 1995), which, like other mammalian cyclase isoforms, is potentially phosphorylated by several protein kinases (Antoni, 1997). However, the functional relevance of specified phosphorylation sites in adenylyl cyclases remains to be investigated.

Effects on PDE

Calyculin A substantially (2–3 fold) enhanced cyclic AMP hydrolysis in homogenates from calcium-depleted cells, and this was also evident in cells incubated in normal, calcium-containing medium (A. Antaraki, K.L. Ang & F.A. Antoni, unpublished data) showing that the effects are not due to depletion of intracellular calcium stores.

The aim of the preliminary analysis of AtT20 cell PDE activity presented here was to clarify the results obtained with cholera toxin. AtT20 cells contain both Type 1 and Type 4 PDE activity (Ang & Antoni, 1996) and calyculin A specifically increased the latter. Moreover, at 10 μM of substrate cyclic AMP, IBMX blocked 80% of total PDE activity while rolipram caused a 40% inhibition. As PDE activity rose almost 3 fold in response to calyculin A, PDE activity was substantial, 55% of that in vehicle-treated cells, in the presence of 0.5 mM IBMX. Combination of rolipram and IBMX in calyculin A-treated cells produced close to complete (95%) inhibition of PDE activity. These results can be correlated with the observation that when cyclic AMP formation was stimulated by cholera toxin i.e. irreversibly activated $G_{s\alpha}$ the combination of rolipram and IBMX but not IBMX alone blocked the inhibitory effect of calyculin A on cyclic AMP accumulation. Thus under these conditions the effect of calyculin A on cyclic AMP accumulation was largely due to activation of PDE.

These findings indicate that a large proportion of PDE activity in AtT20 cells is under stimulant control by constitutively active protein kinase(s) and is inhibited by calyculin A sensitive dephosphorylation. Regulation of various PDEs by phosphorylation is an important element of cellular control in several types of cell (Beltman *et al.*, 1993). Specifically, other investigators have formed an increase of PDE activity by okadaic acid in adipocytes (Shibata *et al.*, 1991), and phosphorylation by protein kinase A influences the activity of Type 4 PDE in a thyroid cell line (Sette *et al.*, 1994). Moreover, control of calmodulin activated Type 1 PDEs by phosphorylation has been also shown (Sharma *et al.*, 1988). However, the impact of these changes on cyclic AMP signals awaits further analysis.

Functional implications

A diagrammatic summary of the results presented in this paper is shown in Figure 9. Taken together, the present observations suggest that in AtT20 cells multiple phosphorylations by constitutively active protein kinases block cellular responses to cyclic AMP generating agonists. PPases inhibited by calyculin A and okadaic acid (primarily PPase 1 with possible requirement for concomitant blockade PPase 2A) have essential and functionally consonant actions in opposing constitutive phosphorylations and thus maintaining the transduction of extracellular signals operating through heterotrimeric G protein activation. AtT20 cells have been cultured as a relatively well-differentiated secretory cell line for almost three decades (Yasumura, 1968), while normal rat pituitary corticotrophs and human corticotroph adenoma cells generally dedifferentiate in similar culture conditions within a few weeks (Westphal *et al.*, 1986; Childs *et al.*, 1989). As cyclic AMP may provide the signal for proliferation of a differentiated phenotype of endocrine cell (Dumont *et al.*, 1989) the constitutively active protein kinases are likely to promote non-differentiated growth, which is suppressed by PPases. Evidence specifically showing unique patterns of constitutional Ser/Thr phosphorylation and a resultant increase in the activity of pp60 (c-*src*) in AtT20 cells has been obtained (Gould *et al.*, 1989). Thus the present findings may help to explain the tumour promoter actions of PPase blockers, i.e. the facilitation of proliferation without differentiation.

We thank the MRC and the British Council for financial support. A.A. is a Fellow of the British Council.

References

ANG, K.L. & ANTONI, F.A. (1996). Rolipram-inhibitable cyclic nucleotide phosphodiesterase (PDE) in rat adenohypophysis: Potential functional role in corticotrophs and somatotrophs. *Br. J. Pharmacol.*, **116,** P361.

ANTONI, F.A. (1997). Calcium regulation of adenylyl cyclase–relevance for endocrine control. *Trends Endocrinol. Metab.*, **8,** 7–14.

ANTONI, F.A., BARNARD, R.J.O., SHIPSTON, M.J., SMITH, S.M., SIMPSON, J. & PATERSON, J.M. (1995). Calcineurin feedback inhibition of agonist-evoked cAMP formation. *J. Biol. Chem.*, **270,** 28055–28061.

APERIA, A., IBARRA, F., SVENSSON, L.-B., KLEE, C.B. & GREENGARD, P. (1992). Calcineurin mediates α-adrenergic stimulation of Na,K-ATPase activity in renal tubule cells. *Proc. Natl. Acad. Sci. U.S.A.*, **89,** 7394–7397.

BEAVO, J.A. & REIFSNYDER, D.H. (1990). Primary sequence of cyclic nucleotide phosphodiesterease isozymes and the design of selective inhibitors. *Trends Pharmacol. Sci.*, **11,** 150–155.

BELTMAN, J., SONNENBURG, W.K. & BEAVO, J.A. (1993). The role of protein phosphorylation in the regulation of cyclic nucleotide phosphodiesterases. *Mol. Cell. Biochem.*, **127/128,** 239–253.

BRADFORD, M.M. (1976). A rapid and sensitive method for the quantitation of microgram quantities of protein utilising the principle of dye-binding. *Anal. Biochem.*, **72,** 248–254.

BROOKER, G., HARPER, J.F., TERASAKI, W.L. & MOYLAN, R.D. (1979). Radioimmunoassay of cyclic AMP and cyclic GMP. In *Advances in Cyclic Nucleotide Research*. ed. Brooker, G., Greengard, P. & Robison, G.A., pp. 2–34. New York: Raven Press.

CHILDS, G.V., LLOYD, J., UNABIA, G. & ROUGEAU, D. (1989). Growth and secretory responses of enriched populations of corticotropes. *Endocrinology*, **125,** 2540–2549.

CLARK, R.B., FRIEDMAN, J., KUNKEL, M.W., JANUARY, B.G. & SHENOLIKAR, S. (1993). Okadaic acid induces both augmentation and inhibition of β_2-adrenergic stimulation of cAMP accumulation in S49 lymphoma cells. *J. Biol. Chem.*, **268,** 3245–3250.

COHEN, P. (1989). Structure and regulation of protein phosphatases. *Ann. Rev. Biochem.*, **58,** 453–508.

COHEN, P., HOLMES, C.F.B. & TSUKITANI, Y. (1990). Okadaic acid: a new probe for the study of cellular regulation. *Trends Biochem. Sci.*, **15,** 98–102.

DUMONT, J.E., JAUNIAUX, J.-C. & ROGER, P.P. (1989). The cyclic AMP-mediated stimulation of cell proliferation. *Trends Biochem. Sci.*, **14,** 67–71.

GILMAN, A.G. (1987). G-proteins -transducers of receptor-generated signals. *Ann. Rev. Biochem.*, **56,** 615–649.

GOPALAKRISHNA, R., CHEN, Z.H. & GUNDIMEDA, U. (1992). Nonphorbol tumor promoters okadaic acid and calyculin A induce membrane translocation of protein kinase C. *Biochem. Biophys. Res. Commun.*, **189,** 950–957.

GOULD, K.L., BILEZIKJIAN, L.M. & HUNTER, T. (1989). AtT20 cells express modified forms of PP60c-src. *Mol. Endocrinol.*, **3,** 70–88.

HEISLER, S., REISINE, T. & AXELROD, J. (1983). Densensitization of β_2-adrenergic receptors and adrenocorticotropin release. *Biochem. Biophys. Res. Commun.*, **111,** 112–119.

HOUSLAY, M.D. (1994). Phosphorylation of heterotrimeric G proteins, In *GTPases in Biology*. ed. Dickey, B.F. & Birnbaumer, L., pp. 147–165. Berlin:Springer Verlag.

JACOBOWITZ, O. & IYENGAR, R. (1994). Phorbol ester-induced stimulation and phosphorylation of adenylyl cyclase 2. *Proc. Natl. Acad. Sci. U.S.A.*, **91,** 10630–10634.

KAWABE, J.I., IWAMI, G., EBINE, T., OHNO, S., KATADA, T., UEDA, Y., HOMCY, C.J. & ISHIKAWA, Y. (1994). Differential activation of adenylyl cyclase by protein kinase C isozymes. *J. Biol. Chem.*, **269,** 16554–16558.

KLEE, C.B. & COHEN, P. (1988). The calmodulin regulated protein phosphatase, In *Calmodulin*. ed. Cohen, P. & Klee, C.B., pp. 225–245. Amsterdam:Elsevier.

KOCH, B. & LUTZ-BUCHER, B. (1994). Inhibition of protein phosphatases by okadaic acid and calyculin-A differentially modulates hormonal- and forskolin-stimulated formation of cyclic AMP in AtT20 corticotrophs: effect of pituitary adenylate cyclase activating polypeptide and corticotropin-releasing factor. *Cell. Signal.*, **6,** 467–473.

KOCH, B. & LUTZ-BUCHER, B. (1995). Multifactorial regulation of pituitary adenylate cyclase-activating polypeptide (PACAP)-induced production of cyclic AMP in AtT-20 corticotrophs: major involvement of rolipram-sensitive and insensitive phosphodiesterases. *Mol. Cell. Endocrinol.*, **112,** 27–34.

KONO, T. (1988). Insulin-sensitive cAMP phosphodiesterase in rat adipose tissue. *Methods Enzymol.*, **159,** 745–751.

LIEBMAN, C., GRANEß, A., BOEHMER, A., KOVALENKO, M., ADOMEIT, A., STEINMETZER, T., NÜRNBERG, B., WETZKER, R. & BOEHMER, F.-D. (1996). Tyrosine phosphorylation of $G_{s\alpha}$ and inhibition of bradykinin-induced activation of the cyclic AMP pathway in A431 cells by epidermal growth factor receptor. *J. Biol. Chem.*, **271,** 31089–31105.

LONGBOTTOM, D. & VAN HEYNINGEN, S. (1989). The activation of rabbit intestinal adenylate cyclase by cholera toxin, *Biochim. Biophys. Acta*, **1014,** 289–297.

MANGANIELLO, V. & VAUGHAN, M. (1973). An effect of insulin on cyclic adenosine 3′:5′-monophosphate phosphodiesterase activity in fat cells. *J. Biol. Chem.*, **248,** 7164–7170.

MULKEY, R.M., ENDO, S., SHENOLIKAR, S. & MALENKA, R.C. (1994). Involvement of a calcineurin/inhibitor-1 phosphatase cascade in hippocampal long-term depression. *Nature*, **369,** 486–488.

NISHIWAKI, S., FUJIKI, H., SUGANUMA, M., FURUYA-SUGURI, H., MATSUSHIMA, R., IIDA, Y., OJIKA, M., YAMADA, K., UEMURA, T., YASUMOTO, T., SCHMITZ, F. & SUGIMURA, T. (1990). Structure-activity relationship within a series of okadaic acid derivatives. *Carcinogenesis*, **11,** 1837–1841.

PATERSON, J.M., SMITH, S.M., HARMAR, A.J. & ANTONI, F.A. (1995). Control of a novel adenylyl cyclase by calcineurin. *Biochem. Biophys. Res. Commun.*, **214,** 1000–1008.

PITCHER, J.A., STURGIS PAYNE, E., CSORTOS, C., DEPAOLI-ROACH, A.A. & LEFKOWITZ, R.J. (1995). The G-protein-coupled receptor phosphatase: A protein phosphatase type 2A with a distinct subcellular distribution and substrate specificity. *Proc. Natl. Acad. Sci. U.S.A.*, **92,** 8343–8347.

PREMONT, R.T., JACOBOWITZ, O. & IYENGAR, R. (1992). Lowered responsiveness of the catalyst of adenylyl cyclase to stimulation by G_s in heterologous desensitization: a role for adenosine 3′,5′-monophosphate-dependent phosphorylation. *Endocrinology*, **131,** 2774–2784.

REISINE, T. (1985). Multiple mechanisms of somatostatin inhibition of adrenocorticotropin release from mouse anterior pituitary tumor cells. *Endocrinology*, **116,** 2259–2266.

ROBISHAW, J.D., SMIGEL, M.D. & GILMAN, A.G. (1986). Molecular basis for two forms of the G protein that stimulate adenylate cyclase. *J. Biol. Chem.*, **261,** 9587–9590.

SCHILLING, R.J., MORGAN, D.R. & KILPATRICK, B.F. (1994). A high-throughput assay for cyclic nucleotide phosphodiesterase. *Anal. Biochem.*, **216,** 154–158.

SETTE, C., IONA, S. & CONTI, M. (1994). The short-term activation of a rolipram-sensitive, cAMP-specific phosphodiesterase by thyroid-stimulating hormone in thyroid FRTL-5 cells is mediated by a cAMP-dependent phosphorylation. *J. Biol. Chem.*, **269,** 9245–9252.

SHARMA, R.K., MOOIBROEK, M. & WANG, J.H. (1988). Calmodulin-stimulated cyclic nucleotide phosphodiesterase isozymes, In *Calmodulin*. ed. Cohen, P. & Klee, C.B., pp. 265–295. Amsterdam:Elsevier.

SHIBATA, H., ROBINSON, F.W.R.S.T. & KONO, T. (1991). Effects of okadaic acid on insulin-sensitive cAMP phosphodiesterase in rat adipocytes–evidence that insulin may stimulate the enzyme by phosphorylation. *J. Biol. Chem.*, **266,** 17948 17953.

SHIPSTON, M.J., HERNANDO, F., BARNARD, R.J.O. & ANTONI, F.A. (1994). Glucocorticoid negative feedback in pituitary corticotropes: pivotal role for calcineurin inhibition of adenylyl cyclase. *Ann. New York Acad. Sci.*, **746,** 453–456.

SIBLEY, D.R., BENOVIC, J.L., CARON, M.G. & LEFKOWITZ, R.J. (1987). Regulation of transmembrane signaling by receptor phosphorylation. *Cell*, **48,** 913–922.

TOYOSHIGE, M., OKUYA, S. & REBOIS, R.V. (1994). Choleragen catalyzes ADP-ribosylation of the stimulatory G protein heterotrimer but not its free α-subunit. *Biochemistry (U.S.A.)*, **33,** 4865–4871.

WESTPHAL, M., JAQUET, P. & WILSON, C.B. (1986). Long-term culture of human corticotropin-secreting adenomas on extracellular matrix and evaluation of serum-free conditions. *Acta Neuropathol. (Berl.)*, **71,** 142–149.

WOODS, M.D., SHIPSTON, M.J., MULLENS, E.L. & ANTONI, F.A. (1992). Pituitary corticotrope tumor (AtT20) cells as a model system for the study of early inhibition by glucocorticoids. *Endocrinology*, **131,** 2873–2880.

YASUMURA, Y. (1968). Retention of differentiated function in clonal animal cell lines particularly hormone-secreting cultures. *Am. Zool.*, **8,** 285–305.

(Received December 23, 1996
Revised March 24, 1997
Accepted April 4, 1997)